**FINAL PROJECT**

# ANALYSIS OF ROAD EMBANKMENT STABILITY USING GEOTEXTILE REINFORCEMENT

**(Study Case at STA 5+325 of Tawang-Ngalang Segment IV Road and Bridge Construction)**

**Submitted to Universitas Islam Indonesia Yogyakarta to Fulfil the Requirement to obtain Bachelor of Civil Engineering Degree**


**FARIZAL SYAFE'IE**
**19511074**



**CIVIL ENGINEERING STUDY PROGRAM**
**FACULTY OF CIVIL ENGINEERING AND PLANNING**
**UNIVERSITAS ISLAM INDONESIA**

**2024**

**FINAL PROJECT**

# ANALYSIS OF ROAD EMBANKMENT STABILITY USING GEOTEXTILE REINFORCEMENT

**(Study Case at STA 5+325 of Tawang-Ngalang Segment IV Road and Bridge Construction)**

Arranged by:

**Farizal Syafe'ie**
**19511074**

Accepted as one of the requirements to obtain the degree of Bachelor of Civil Engineering

Defended on November 24th,2024

By the board of examiners

| Supervisor | Examiner I | Examiner II |
|---|---|---|
| **Dr. Hanindya Kusuma A, S.T., M.T** | **Dr. Ir. Lalu Makrup, M.T.** | **Anisa Nur A, S.T., M.Eng.** |
| **NIK : 045110407** | **NIK : 885110106** | **NIK : 215111305** |

Authorizing,
Head of Civil Engineering Program

**Ir. Yunalia Muntafi S.T., M.T., Ph.D.(Eng).,IPM.**
**NIK : 095110101**

# FREE PLAGIARISM STATEMENT

I hereby declare in all conscience that Final Project report that I made to fulfill one of the requirements of Civil Engineering Study Program of Universitas Islam Indonesia is my own work. As for parts of my research that quoted from somebody else's work has been written in the source very clearly based on norm, rules, and ethics of scientific writing. If in the future, it is found that all or partial part of this Final Project report is not my own work or there is plagiarism in certain parts, I am willing to accept sanctions, including the revocation of my academic title in accordance with applicable laws.

Yogyakarta, 10th October 2024

Statement maker,

Farizal Syafe'ie

(19511074)

# PREFACE

Alhamdulillahirabbil'alamin, praise to Allah SWT who has bestowed His grace, Taufiq and guidance, so that the authors can complete the Final Project with the title of "Analysis of Road Embankment Stability Using Geotextile Reinforcement (Study Case at STA 5+325 of Tawang-Ngalang Segment IV Road and Bridge Construction". This Final Project is one of the academic requirements in completing the Final Project of undergraduate studies at the Civil Engineering Study Program, Faculty of Civil Engineering and Planning, Universitas Islam Indonesia, Yogyakarta.

In the preparation of this Final Project, there are many obstacles faced by the author, but thanks to the advice, criticism, and encouragement from various parties, this Final Project can be completed. In this regard, the author would like to express his deepest gratitude to:

1. Dr. Hanindya Kusuma Artati, S.T., M.T., as the Final Project Supervisor, for the guidance, advice, counsel, and support given to the author in the preparation of this Final Project and during the author's study period.
2. Dr. Ir. Lalu Makrup, M.T., as Examiner I for the thesis defense.
3. Anisa Nur Amalina, S.T., M.Eng., as Examiner II for thesis defense.
4. Ir. Yunalia Muntafi, S.T., M.T., Ph.D.(Eng)., IPM. As the head of Civil Engineering Study Program Faculty of Civil Engineering and Planning, Universitas Islam Indonesia.
5. PT. Aneka Dharma Persada and PT. Geomine Bara Studio for giving me chances and opportunities to sharpen my engineering skills and knowledge. Also, for allowing and providing me technical data and guidance for my research.
6. My family especially my parents, Surahman and Siti Nafsiyah, who have showered me with love and countless prayers, also my siblings, Hendra Yoga Pratama S.T., and Aulia Rachman S.E., have provide me with their never-ending support in all aspects of my life.

7. My friends Roy, Si Ed, Bose, Item, Vero, Pil, Zee, Cc, Bianca, and Dea.

Yogyakarta, 10th October 2024
Author,

Farizal Syafe'ie

19511074

# TABLE OF CONTENT


Title Page i

Validation Sheet ii

FREE PLAGIARISM STATEMENT iii

PREFACE iv

TABLE OF CONTENT vi

LIST OF FIGURES x

LIST OF TABLES xv

APPENDIX LIST xvi

NOTATION LIST AND ABBREVIATION xx

ABSTRACT xxii

CHAPTER I PRELIMINARY 1

1.1 Background 1

1.2 Problem Formulation 3

1.3 Purpose 3

1.4 Advantage 4

1.5 Limit 4

CHAPTER II LITERATURE REVIEW 6

2.1 General Review 6

2.2 Embankment Stability 6

2.3 Embankment stability with Geotextile 8

CHAPTER III BASIC THEORIES 16

3.1 Soil 16

3.1.1 Soil Properties 16

3.1.2 Soil Classification 21
3.2 Soil Investigation 24
3.3 Soil Embankment Load 25
3.3.1 Pavement Load 25
3.3.2 Traffic load 26
3.3.3 Earthquake load 26
3.4 Slope Stability 27
3.4.1 Safety Factor 29
3.4.2 Fellenius Method 30
3.5 Slope Reinforcement Using Geotextile 32
3.5.1 Geotextile type 33
3.5.2 Working Mechanism of Geotextile on field 34
3.5.3 Slope Stability Analysis Using Geotextile 35
3.6 Settlement 40
3.6.1 Consolidation Settlement 40
3.6.2 Settlement Calculation Parameter 41
3.7 PLAXIS 43
CHAPTER IV METHODOLOGY 47
4.1 Research Method 47
4.2 Research Location 47
4.3 Data Collection 48
4.4 Research Procedure 49
4.5 Variation of Models 50
4.6 Research Flowchart 51
CHAPTER V ANALYSIS AND RESULT 53

5.1 Embankment Stability 53
5.2 Parameter data 53
5.2.1 Soil parameter 53
5.2.2 Load parameter 54
5.2.3 Geotextile data 55
5.3 Analysis of Existing Embankment Stability Without Reinforcement 56
5.3.1 Analysis of Construction Phase Existing Embankment 57
5.3.2 Analysis of Post-Construction Existing Embankment 67
5.3.3 Fellenius method 71
5.4 Primary Consolidation Calculation 74
5.5 Geotextile calculation 76
5.5.1 Parameter Data 77
5.5.2 External stability calculation 78
5.5.3 Internal stability calculation 86
5.5.4 Control of Tensile Strength between Soil and Geotextile 89
5.6 Embankment of Existing Condition Using Geotextile Reinforcement 90
5.6.1 Analysis of Construction Phase Existing Embankment Using Geotextile Reinforcement 90
5.6.2 Analysis of Post-Construction Existing Embankment Using Geotextile Reinforcement 100
5.7 Discussion 105
5.7.1 Factor of safety 106
5.7.2 Consolidation Settlement 109
CHAPTER VI CONCLUSION AND SUGGESTION 111
6.1 Conclusion 111

6.2 Suggestion 112

References 113

Appendix 115

# LIST OF FIGURES


Figure 3. 1 Soil Conditions 17
Figure 3. 2 Diagram of Soil Phase 17
Figure 3. 3 Earthquake Zoning Map 27
Figure 3. 4 Flat Failure 28
Figure 3. 5 Rotation Failure 28
Figure 3. 6 Irregular failure 29
Figure 3. 7 Modelling of Fellenius Method 31
Figure 3. 8 Woven Geotextile 33
Figure 3. 9 Non-Woven Geotextile 34
Figure 3. 10 Working Mechanism of Geotextile on Field 35
Figure 3. 11 Failure Body and Length of Geotextile 36
Figure 3. 12 Soil Compression Index ($C_c$) 42
Figure 3. 13 Influential Factor (Osterberg,1957) 43
Figure 3. 14 PLAXIS Input 44
Figure 3. 15 PLAXIS Calculation 45
Figure 3. 16 PLAXIS Calculation 45
Figure 3. 17 PLAXIS Curve 46
Figure 4. 1 Research Location 47
Figure 4. 2 Existing Elevation 49
Figure 4. 3 The Flowchart of Research 52
Figure 5. 1 Graph of Relationship between Acceleration and Earthquake Time 55
Figure 5. 2 Cross Section of STA 5+325 Of Tawang-Ngalang Segment IV Road with Angle Of 25 º 56
Figure 5. 3 Cross Section of Embankment Variation with Angle Of 20º 56
Figure 5. 4 Construction Phase 57
Figure 5. 5 Deformed Mesh of Existing Embankment Phase 1 Without Reinforcement 58

Figure 5. 6 Displacement of Existing Embankment Phase 1 Without Reinforcement Due to Embankment Load 58
Figure 5. 7 Effective Stress of Existing Embankment Phase 1 Without Reinforcement Due to Embankment Load 59
Figure 5. 8 Potential Failure Area on Existing Embankment Phase 1 With Angle Of 25º Without Reinforcement Due To Embankment Load 59
Figure 5. 9 Deformed Mesh Existing Embankment Phase 2 Without Reinforcement Due to Embankment Load 60
Figure 5. 10 Displacement Value of Existing Embankment Phase 2 Without Reinforcement Due to Embankment Load 61
Figure 5. 11 Effective Stress of Existing Embankment Phase 2 Without Reinforcement Due to Embankment Load 61
Figure 5. 12 Potential Failure Area on Existing Embankment Phase 2 With Angle Of 25º Without Reinforcement Due to Embankment Load 62
Figure 5. 13 Deformed Mesh for Existing Embankment with Angle Of 25º By Adding Pavement Load Without Reinforcement 63
Figure 5. 14 Deformed Mesh for Existing Embankment with Angle Of 25º By Adding Pavement and Earthquake Loads Without Reinforcement 63
Figure 5. 15 Displacement Value of Existing Embankment Phase 3 With Angle Of 25º By Adding Pavement Load Without Reinforcement 64
Figure 5. 16 Displacement Value of Existing Embankment Phase 3 With Angle Of 25º By Adding Pavement and Earthquake Loads Without Reinforcement 64
Figure 5. 17 Effective Stress of Existing Embankment Phase 3 With Angle Of 25º By Adding Pavement Load Without Reinforcement 65
Figure 5. 18 Effective Stress of Existing Embankment Phase 3 With Angle Of 25º By Adding Pavement And Earthquake Loads Without Reinforcement 65
Figure 5. 19 Potential Failure Area on Existing Embankment Phase 3 With Angle of 25º By Adding Pavement Load Without Reinforcement 66

Figure 5. 20 Potential Failure Area on Existing Embankment Phase 3 With Angle of 25º By Adding Pavement and Earthquake Loads Without Reinforcement 66
Figure 5. 21 Consolidation Settlement of Existing Embankment Phase 3 With Angle Of 25º 67
Figure 5. 22 Deformed Mesh for Existing Embankment with Angle of 25º By Adding Road Structure and Traffic Loads Without Reinforcement 68
Figure 5. 23 Displacement Value of Existing Embankment with Angle of 25º By Adding Road Structure and Traffic Loads Without Reinforcement 69
Figure 5. 24 Effective Stress of Existing Embankment with Angle Of 25º By Adding Road Structure Load Without Reinforcement 69
Figure 5. 25 Potential Failure Area on Existing Embankment with Angle of 25º By Adding Road Structure Load Without Reinforcement 70
Figure 5. 26 Consolidation Settlement of Existing Embankment Post-Construction with Angle of 25º 71
Figure 5. 27 The Method of Slice 71
Figure 5. 28 Division of The Zone 76
Figure 5. 29 Deformed Mesh Existing Embankment Phase 1 Using Geotextile Due to Embankment Load 91
Figure 5. 30 Displacement Value of Existing Embankment Phase 1 Using Geotextile Due to Embankment Load 92
Figure 5. 31 Effective Stress of Existing Embankment Phase 1 Using Geotextile Due to Embankment 92
Figure 5. 32 Potential Failure Area on Existing Embankment Phase 1 With Angle Of 25º Using Geotextile Due to Embankment Load 93
Figure 5. 33 Deformed Mesh of Existing Embankment Phase 2 Using Geotextile Reinforcement Due to Embankment Load 93
Figure 5. 34 Displacement Value of Existing Embankment Phase 2 Using Geotextile Due to Embankment Load 94

Figure 5. 35 Effective Stress of Existing Embankment Phase 2 Using Geotextile Due to Embankment Load 95
Figure 5. 36 Potential Failure Area on Existing Embankment Phase 2 with Angle of 25º Using Geotextile Due to Embankment Load 95
Figure 5. 37 Deformed Mesh for Existing Embankment with Angle of 25º By Adding Pavement Load Using Geotextile 96
Figure 5. 38 Deformed Mesh for Existing Embankment Angle of 25º By Adding Pavement and Earthquake Loads Using Geotextile 96
Figure 5. 39 Displacement Value of Existing Embankment with Angle of 25º By Adding Pavement Load Using Geotextile 97
Figure 5. 40 Displacement Value of Existing Embankment with Angle of 25º By Adding Pavement and Earthquake Loads Using Geotextile 97
Figure 5. 41 Effective Stress of Existing Embankment Phase 3 Using Geotextile By Adding Road Structure Load 98
Figure 5. 42 Effective Stress of Existing Embankment Phase 3 Using Geotextile By Adding Road Structure and Earthquake Load 98
Figure 5. 43 Potential Failure Area on Existing Embankment with Angle of 25º By Adding Pavement Load Using Geotextile 99
Figure 5. 44 Potential Failure Area on Existing Embankment with Angle of 25º By Adding Pavement and Earthquake Loads Using Geotextile 99
Figure 5. 45 Consolidation Settlement of Existing Embankment Phase 3 Using Geotextile with Angle of 25º 100
Figure 5. 46 Deformed Mesh for Existing Embankment with Angle Of 25º By Adding Road Structure Load Using Reinforcement 101
Figure 5. 47 Deformed Mesh for Existing Embankment with Angle Of 25º By Adding Road Structure and Earthquake Loads Using Reinforcement 101
Figure 5. 48 Displacement Value of Existing Embankment with Angle Of 25º By Adding Road Structure Load Using Geotextile 102

Figure 5. 49 Displacement Value of Existing Embankment with Angle Of 25º By Adding Road Structure and Earthquake Load Using Geotextile 102
Figure 5. 50 Effective Stress of Existing Embankment with Angle Of 25º By Adding Road Structure Using Geotextile 103
Figure 5. 51 Effective Stress of Existing Embankment with Angle Of 25º By Adding Road Structure and Earthquake Load Using Geotextile 103
Figure 5. 52 Potential Failure Area on Existing Embankment with Angle Of 25º By Road Structure Load Using Geotextile 104
Figure 5. 53 Potential Failure Area on Existing Embankment with Angle of 25º By Road Structure and Earthquake Load Using Geotextile 104
Figure 5. 54 Consolidation Settlement of Reinforced Existing Embankment Post-Construction with Angle Of 25º 105
Figure 5. 55 Safety Factor for Construction Phase 107
Figure 5. 56 Safety Factor for Post-construction Phase 108
Figure 5. 57 Consolidation Settlement 109

# LIST OF TABLES


Table 2. 1 Comparison Past and Present Research 12
Table 3. 1 Unit Weight of Soil Value 18
Table 3. 2 Elastic Modulus of Different Soil Type 19
Table 3. 3 Poisson Ratio 20
Table 3. 4 Cohesion 20
Table 3. 5 Internal Friction Angle 21
Table 3. 6 Permeability 21
Table 3. 7 Unified Soil Classification System 23
Table 3. 8 AASHTO classification 24
Table 3. 9 Traffic Load 26
Table 3. 10 Recommendation for safety factor of slope 30
Table 3. 11 Safety Factor of Slope 30
Table 4. 1 N-SPT Result 48
Table 5. 1 Soil Parameter Data 53
Table 5. 2 Geotextile Data 55
Table 5. 3 Recapitulation of Calculation Steps Using Fellenius Method 73
Table 5. 4 Recapitulation of Consolidation Settlement 76
Table 5. 5 Soil Bearing Capacity Coefficient 77
Table 5. 6 Recapitulation of Geotextile Overlapping Length 87
Table 5. 7 Recapitulation of Geotextile Effective Length 87
Table 5. 8 Recapitulation of Geotextile Length on Active Zone 88
Table 5. 9 Recapitulation of Geotextile Total Length 89
Table 5. 10 Factor of Safety Recapitulation for Construction Phase 106
Table 5. 11 Factor of Safety Recapitulation for Post-Construction 108
Table 5. 12 Recapitulation of Consolidation Settlement 109

# APPENDIX LIST


Appendix 1 Cross Section of STA 5+325 116

Appendix 2 SPT Value 117

Appendix 3 Recapitulation of Laboratory Result 118

Appendix 4 Geotextile Specification 119

Appendix 5 Deformed Mesh of Alternative Internal Angle Of 20° For Phase 1 Without Reinforcement Due to Embankment Load 120

Appendix 6 Displacement Value of Alternative Internal Angle Of 20° For Phase 1 Without Reinforcement Due to Embankment Load 120

Appendix 7 Effective Stress of Alternative Internal Angle Of 20° Phase 1 Without Reinforcement Due to Embankment Load 121

Appendix 8 Potential Failure Area on Alternative Internal Angle Of 20° Phase 1 Without Reinforcement Due to Embankment Load 121

Appendix 9 Deformed Mesh of Alternative Internal Angle Of 20° For Phase 2 Without Reinforcement Due to Embankment Load 122

Appendix 10 Displacement Value of The Alternative Internal Angle Of 20° For Phase 2 Without Reinforcement Due to Embankment Load 122

Appendix 11 Effective Stress of Alternative Internal Angle Of 20° Phase 2 Without Reinforcement Due to Embankment Load 123

Appendix 12 Potential Failure Area on Alternative Internal Angle Of 20° Phase 2 Without Reinforcement Due to Embankment Load 123

Appendix 13 Deformed Mesh of Alternative Internal Angle Of 20° For Phase 3 Without Reinforcement by Adding Pavement Load 124

Appendix 14 Deformed Mesh of Alternative Internal Angle Of 20° For Phase 3 Without Reinforcement by Adding Pavement and Earthquake Load 124

Appendix 15 Displacement Value of The Alternative Internal Angle Of 20° For Phase 3 Without Reinforcement by Adding Pavement Load 125

Appendix 16 Displacement Value of The Alternative Internal Angle Of 20° For Phase 3 Without Reinforcement by Adding Pavement and Earthquake Load 125
Appendix 17 Effective Stress of Alternative Internal Angle Of 20° Phase 3 Without Reinforcement by Adding Pavement Load 126
Appendix 18 Effective Stress of Alternative Internal Angle Of 20° Phase 3 Without Reinforcement by Adding Pavement and Earthquake Load 126
Appendix 19 Potential Failure Area on Alternative Internal Angle Of 20° Phase 3 Without Reinforcement by Adding Pavement Load 127
Appendix 20 Potential Failure Area on Alternative Internal Angle Of 20° Phase 3 Without Reinforcement by Adding Pavement and Earthquake Load 127
Appendix 21 Consolidation Settlement of Alternative Internal Angle Of 20° Phase 3 For Construction Phase 128
Appendix 22 Deformed Mesh for On Alternative Internal Angle Of 20° By Adding Road Structure Load Without Reinforcement 128
Appendix 23 Displacement Value of The Alternative Internal Angle Of 20° By Adding Road Structure Load Without Reinforcement 129
Appendix 24 Effective Stress of Alternative Internal Angle Of 20° By Adding Road Structure Load Without Reinforcement 129
Appendix 25 Potential Failure Area on The Alternative Internal Angle Of 20° By Road Structure Load Without Reinforcement 130
Appendix 26 Consolidation Settlement of Alternative Internal Angle Of 20° For Post-Construction 130
Appendix 27 Deformed Mesh of Reinforced Alternative Internal Angle Of 20° For Phase 1 Using Geotextile Due to Embankment Load 131
Appendix 28 Displacement Value of The Reinforced Alternative Internal Angle Of 20° For Phase 1 Using Geotextile Due to Embankment Load 131
Appendix 29 Effective Stress of Reinforced Alternative Internal Angle Of 20° Phase 1 Using Geotextile Due to Embankment Load 132

Appendix 30 Potential Failure Area on Reinforced Alternative Internal Angle Of 20° Phase 1 Using Geotextile Due to Embankment Load 132
Appendix 31 Deformed Mesh of Reinforced Alternative Internal Angle Of 20° For Phase 2 Using Geotextile Due to Embankment Load 133
Appendix 32 Displacement Value of The Reinforced Alternative Internal Angle Of 20° For Phase 2 Using Geotextile Due to Embankment Load 133
Appendix 33 Effective Stress of Reinforced Alternative Internal Angle Of 20° Phase 2 Using Geotextile Due to Embankment Load 134
Appendix 34 Potential Failure Area on Reinforced Alternative Internal Angle Of 20° Phase 2 Using Geotextile Due to Embankment Load 134
Appendix 35 Deformed Mesh of Reinforced Alternative Internal Angle Of 20° For Phase 3 Using Geotextile by Adding Pavement Load 135
Appendix 36 Deformed Mesh of Reinforced Alternative Internal Angle Of 20° For Phase 3 Using Geotextile by Adding Pavement and Earthquake Loads 135
Appendix 37 Displacement Value of Reinforced Alternative Internal Angle Of 20° For Phase 3 Using Geotextile by Adding Pavement Load 136
Appendix 38 Displacement Value of Reinforced Alternative Internal Angle Of 20° For Phase 3 Using Geotextile by Adding Pavement And Earthquake Loads 136
Appendix 39 Effective Stress of Reinforced Alternative Internal Angle Of 20° Phase 3 Using Geotextile by Adding Pavement Load 137
Appendix 40 Effective Stress of Reinforced Alternative Internal Angle Of 20° Phase 3 Using Geotextile by Adding Pavement And Earthquake Loads 137
Appendix 41 Potential Failure Area on Reinforced Alternative Internal Angle of 20° For Phase 3 Using Geotextile by Adding Pavement Load 138
Appendix 42 Potential Failure Area on Reinforced Alternative Internal Angle Of 20° For Phase 3 Using Geotextile by Adding Pavement and Earthquake Loads 138

Appendix 43 Consolidation Settlement on Reinforced Alternative Internal Angle Of 20° For Construction Phase 139
Appendix 44 Deformed Mesh for Reinforced Alternative Angle Of 20º By Adding Road Structure Load Using Reinforcement 139
Appendix 45 Deformed Mesh for The Reinforced Alternative Angle Of 20º By Adding Road Structure and Earthquake Loads Using Reinforcement 140
Appendix 46 Displacement Value of Reinforced Alternative Internal Angle of 20° Using Geotextile by Adding Road Structure Load 140
Appendix 47 Displacement Value of Reinforced Alternative Internal Angle Of 20° Using Geotextile by Adding Road Structure and Earthquake Loads 141
Appendix 48 Effective Stress of Reinforced Alternative Internal Angle Of 20° By Adding Road Structure Load Using Geotextile 141
Appendix 49 Effective Stress of Reinforced Alternative Internal Angle Of 20° By Adding Road Structure and Earthquake Loads Using Geotextile 142
Appendix 50 Potential Failure Area on The Reinforced Alternative Internal Angle Of 20° By Road Structure Load Using Geotextile 142
Appendix 51 Potential Failure Area on The Reinforced Alternative Internal Angle Of 20° By Road Structure and Earthquake Loads Using Geotextile 143
Appendix 52 Consolidation Settlement of Reinforced Alternative Internal Angle Of 20° Using Geotextile for Post-Construction 143

# NOTATION LIST AND ABBREVIATION

$\gamma_{sat}$ = Saturated unit weight ($kN/m^3$)

$\gamma_d$ = Dry unit weight ($kN/m^3$)

$\gamma_b$ = Bulk unit weight ela($kN/m^3$)

v = Poisson Ratio

c = Cohesion ($kN/m^2$)

k = Permeability (m/day)

$E_s$ = Elastic modulus ($kN/m^2$)

R = radius of failing body (m)

n = total of intersection

$K_a$ = coefficient of active soil

SF = safety factor

$\varphi$ = friction angle (degree)

$a_i$ = length of curve circle on-i intersection ( m)

$W_i$ = weight of intersection soil on-i (kN)

$U_i$ = pore water pressure of intersection on-I (kN/m)

$\theta_i$ = define angle (degree)

$\sigma_{hc}$ = horizontal stress of soil ($kN/m^2$)

$q$ = uniform load (kN/m)

Sv = thickness of reinforcement layer (m)

$T_{all}$ = allowable tensile strength of reinforcement material ($kN/m^2$)

$\sigma_v$ = vertical soil stress ($kN/m^2$)

$H_i$ = height of observed land referring to soil surface (m)

$Z_i$ = height of observed land referring to soil surface (m)

$\beta$ = coefficient of soil interface to geotextile

$L_o$ = geotextile overlapping length (m)

$L_i$ = geotextile effective length (m)

$L_z$ = geotextile length on active zone (m)

$L_{total}$ = total length of geotextile (m)

q = uniform load (kN/m)

$\sigma_{ult}$ = allowable soil bearing capacity ($kN/m^2$)

$\sigma_{occurs}$ = bearing capacity ($kN/m^2$)

c = soil cohession ($kN/m^2$)

Sc = primary settlement (m)

Cc = soil compression index

$E_o$ = pore number

$P_o$ = effective overburden stress ($kN/m^2$)

$\Delta_p$ = vertical stress change ($kN/m^2$)

*I* = influential factor

# ABSTRACT

Tawang-Ngalang Segment IV Road and Bridge Construction in Gunungkidul Regency, Yogyakarta, is constructed to connect the city and suburban areas in southern Yogyakarta for a more effective way of travel. Gunungkidul regency is mountainous area, which means uneven area for construction. Therefore, excavation and embankment are necessary to provide little to no difference for the road elevation. This research will be focused on the safety of embankments structure.

The study case taken is embankment on STA 5 + 325 with 6.75 in height. Using secondary type of data taken from PT. Geomine Bara Studio also laboratory and detailed engineering drawing data from PT. Aneka Dharma Persada. The objective of this research is to calculate the safety of embankment structure and to provide an alternative for the embankment angle for a safer road construction afterwards. Therefore, the embankment will be reinforced with geotextile with internal angle variations, and analysed with Fellenius method for static calculation, and PLAXIS as the instrument of Finite Element Method (FEM).

The result shows that the safety factor for internal angle 25° and 20° with no reinforcement using static calculation are both collapses. After geotextile in installed on the location, the safety factors are 1.402 and 1.483 respectively. As for the consolidation settlement occur on the site for internal angle 25° with no reinforcement and after being reinforced are 0.1905 m and 0.1813 m. While for internal angle 20° with no reinforcement and after being reinforced are 0.1845 m and 0.1764 m.

**Key words**: Embankment, Geotextile, Consolidation

# CHAPTER I
# PRELIMINARY

## 1.1 Background

D.I Yogyakarta is one of the most well-known province for its touristy destinations. There are various types of entertainment that attract domestic, as well as internatioanal tourist. One of the factors affecting this is the various contour of the province. There are higher areas such as mountains and hills for hiking, or just chilling out at the cafes viewing the citylights. Also, lower areas such as beaches to enjoy the sunsets. Higher lands are located in the Northern Yogyakarta. While the lower lands are in the southern part of Yogyakarta. There are already transportation access to connect the centre of Yogyakarta for both southern and northern parts of Yogyakarta to accommodate the local people also for the tourists.

By the time, the existing transportation access to the southern part of Yogyakarta which there's only one main access, no longer fulfilling the demand of road capacity of the vehicles passing and also still not accessible to many potential touristy places. Because not only the local and tourist, heavy vehicles also passing through this access road.

Therefore the government of D.I. Yogyakarta made a decision to build new access road that connect the centre of Yogyakarta to the southern parts of Yogyakarta located in Gunungkidul Regency. This project is called Tawang-Ngalang Road and Bridge Construction. The aim of this project is to provide alternative access that connects Yogyakarta to Gunungkidul through Piyungan-Patuk.

The project works are divided to five different segment for the construction . But the writer will specifically takes segment 4 for obtaining the research data. Tawang Ngalang Segment IV Road and Bridge Construction has a total of 3,4 km road and 80 m long bridge.

The construction of new access road oftenly done on various condition of soil contour. This means that the original contour is not even yet and remain uncapable if the surface is not even out. Therefore, the even soil contour will be needed in order to execute the design plan for the road and bridge construction. In order to obtain the even contour, areas that are too shallow will have to be filled with embankment. The materials for embankment can be taken from some sources, such as quarries, or excavation materials from different sources.

The embankment construction will create different elevation of two different soil surfaces which will produce compression forces. So the higher soil surface will move to to lower surface due to the gravitional forces. This event will disturb the soil stability and can lead to the collapse of the embankment strcuture that not only will damage the embankment structure itself, but also can endanger construction or people nearby. Therefore the analysis of slope stability of embankment must be done in order to make sure that the construction is safe and strong. The tern “slope” here means a tilted soil surfaced and create particular angle towards a horizontal body.

For the location of the research, it specifically takes the embankment on STA 5 + 325 as the object of the research. In this location the embankment height is 6.75 m from the original soil with the site classification of intermediate soil and clay type of soil.

Reinforcement remains required in order to fulfill the safety factor of 1.2. The type of reinforcement used is geotextile reinforcement. Geotextile itself is a reinforcement in geotechnical field that uses sythetic polimer. It will be used as the protection from landslide or even the land collapse.

This research analysis calculation will be divided into some stages. The first stage will be structural modelling and calculation of embankment on original soil without geotextile reinforcement to obtain safety factor and settlement of the soil. As for the second stage, the structure that collapse on this stages will be recalculated using manual calculations that will use Fellenius method in order to obtain the safety factor, but this time, the calculation will be added with the calculation of the number of required geotextile layer. After that the structure using geotextile will be

remodelled and recalculated using the need of geotextile layer as the reference. This will be done in order to get the embankment structure that can function optimally and effectively.

### 1.2 Problem Formulation

Based on the explanation of the background above, the problem formulation of this research

1. How much is the factor of safety value of existing slope with internal angle of 25° using PLAXIS V20 based on finite element method for construction and post construction phase without reinforcement?
2. How much is the factor of safety value of existing slope with internal angle of 25° with reinforcement using PLAXIS V20 based on finite element method for construction phase and post construction phase?
3. How much is the consolidation settlement value occurring on existing slope with internal angle of 25° with and without reinforcement using PLAXIS V20 based on finite element method for construction and post construction phase?
4. How much is the factor of safety value of alternative internal angle of 20° using PLAXIS V20 based on finite element method for construction phase and post construction without reinforcement?
5. How much is the factor of safety value of alternative internal angle of 20° with reinforcement using PLAXIS V20 based on finite element method for construction and post construction phase?
6. How much is the consolidation settlement value occurring on alternative internal angle of 20° with and without reinforcement using PLAXIS V20 based on finite element method for construction and post construction phase?

### 1.3 Purpose

Based on the problem formulation that have been mentioned before, the purposes of the research are:

1. Obtaining the factor of safety value of existing slope with internal angle of 25° using PLAXIS V20 based on finite element method for construction and post construction phase.

2. Obtaining the factor of safety value of existing slope with internal angle of 25° with reinforcement using PLAXIS V20 based on finite element method for construction and post construction phase.
3. Obtaining the consolidation settlement value occurring on existing slope with internal angle of 25° with and without reinforcement using PLAXIS V20 based on finite element method for construction and post construction phase.
4. Obtaining the factor of safety value of alternative internal angle of 20° using PLAXIS V20 based on finite element method for construction and post construction phase.
5. Obtaining the factor of safety value of reinforced alternative internal angle of 20° with geotextile reinforcement using PLAXIS V20 based on finite element method for construction and post construction phase.
6. Obtaining the consolidation settlement value occurring on the alternative internal angle of 20° with and without geotextile reinforcement using PLAXIS V20 based on finite element method for construction and post construction phase.

### 1.4 Advantage

The advantages of this final project are as follows.

1. To increase the knowledge of the readers regarding road embankment stability using geotextile reinforcement with fellenius method.
2. To provide knowledge in the operation of the PLAXIS program.
3. To be used as a reference for the future research on the same case.

### 1.5 Limit

For the writing of the final project to be structured, the following observation limits are made.

1. The location of the research is on STA 5+325 of Tawang-Ngalang Segment IV Road and Bridge Construction in Gunungkidul districts, D.I. Yogyakarta.
2. The data that will be used by the writer is the SPT value obtained by PT. Goemine Bara Studio.
3. Drainage work is not analyzed.

4. The geotextile used is a woven UW-250 produced by PT.Teknindo Geosistem type with a tensile strength = 52 kN/m.
5. Calculation is using Fellenius method to determine the safety factor of original soil embankment without geotextile reinforcement.
6. Stability analysis of soil embankment using PLAXIS V20.
7. The traffic load is 15 kN/m$^2$ based on "Departemen Pekerjaan Umum tahun 2009 about Requirement and Design Criteria of Road Techniques.
8. The earthquake load 0,367 g based on earthquake zoning map.
9. Ground water surface is considered based on data obtained on field.
10. Time and cost analyses is not calculated.

# CHAPTER II
# LITERATURE REVIEW

## 2.1 General Review

In the world of civil engineering, an embankment is an artificial structure built by filling and compacting soil or other materials above the original ground surface. Its functions vary, it can be to elevate the surface of an area, form a road embankment or dam, or even flatten uneven land contours. According to Braja M. Das (1988), embankment is a mass of soil artificially placed and compacted above the original ground surface, with a specific purpose such as increasing elevation, improving subgrade conditions, or creating a supporting structure.

## 2.2 Embankment Stability

Arsy & Artati (2018) conducted research on "Embankment Stability Analysis on the Road Construction Using Geotextile Reinforcement with Fellenius Method". This research aims to increase soil bearing capacity. The results of this study before use reinforcement obtained of three variations, such as variations in geotextile length are 10 m, 13 m and 15 m, variations in vertical distance between geotextiles are 0,3 m, 0,4 m and 0,6 m and slope angle variations are 19°, 25° and 29°. Safety factor from analysis result without reinforcement with Fellenius method manually is 1,786, while using Geoslope without earthquake is 1,947 and with earthquake is 1,030.

Budiasto & Purwanto (2018) conducted research on "Analysis of Road Embankment Stability with Geotextile Reinforcement Using PLAXIS Program". This research aims to determine the cause of landslides slope before retrofitting and damage to the existing soil anchoring. The results of this study before use reinforcement obtained safe number and decrease for 200 days of road embankment at 2m, 4m, 6m, and 8m embankment height with a variation in modeling. Analysis of the stability of road embankment using the PLAXIS V.8.5 program at 2 m, 4 m, 6 m, 8 m embankment with variations in modeling, original embankment

conditions, original replacement embankment, original embankment with geotextile, original replacement embankment with geotextile and original replacement embankment with geotextile and counterweight. On the original embankment condition 1,074 during construction, 1,002 after construction and a decrease of 0,009 m

Isadono (2020) conducted research on "Analysis of Slope Stability Using Geotextile Reinforcement with PLAXIS 8.6 And Fellenius Method". This research aims to determine the safety factor toward failure and Marshland decrease number. The results of this study are in two steps, namely the first analysis is carried out at a variation of the water level of 20 m with variations in embankment height. The results of the analysis on the embankment with a height of 2,1 meters obtained a SF of 2,379 and a soil reduction by 0,986 meters. Embankment with a height of 4,2 meters obtained a safety factor of 2,009 and a soil reduction of 0,127 meters. In the embankment with a height of 6,3 meters, a safety factor of 1,6919 and a soil reduction of 0,237 meters were obtained. Embankment with a height of 8,4 meters obtained a safety factor of 1,514 and a soil reduction of 0,20834 meters. embankment with a height of 10,5 meters collapsed. To be able to find out the safety factor of 10,5 meters embankment, the calculation was carried out using the fellenius method. The results of the fellenius calculation obtained a safety factor of 0,946. The next step is to carry out the same analysis of 18m water level variations and analysis of the geotextile- reinforced.

Afdhal (2018) conducted research on “Stability Analysis of Slope Road Embankments with Geotextile Reinforcement Using Geoslope 2018 Program in Tawang - Ngalang Segmen IV Highway Construction Project”. This research aims to determine Knowing the value of the existing slope safety factor with geotextile reinforcement using the Geoslope program. The result of the analysis using the 2018 Geoslope program on the original slope embankment at an angle of 350 obtained the safe number (SF) without earthquake loads during the first phase construction period of 3.638 > 1.5; the second phase of 1.759 > 1.5; the third phase was 1.396 < 1.5 and during post-construction it was 1.303 < 1.5. Meanwhile, on the original slope embankment at an angle of 350, the safe number (SF) with earthquake

loads during the first phase of construction gained 1.251 > 1.1; the second phase of 0.729 <1.1; the third phase reached 0.674 < 1.1 and during post-construction 0.644 < 1.1.

Maulida (2023) conducted research on “Stability Analysis of Slope Road Embankment with Geotextile Reinforcement Using the Finite Element Method”. This research aims to determine Knowing the value of safety number (SF) and the amount of consolidation settlement on the original embankment slope, new corner embankment slope without reinforcement and with geotextile reinforcement using finite element method. The result of the analysis is Safety number value (SF) for the original embankment slope with an angle of 39° of the embankment construction periods up to 2,5 m 2,5265; embankment up to 5 m 1,8616; embankment up to 7 m 1,5425; and embankment up to 9 m 1,2846, during post-construction the safety number (SF) of the original embankment slope win an angle 39° was 1,1517 with a consolidation settlement of 0,1865 m. On the embankment slope with an angle of 34° during the construction period of the embankment up to 2,5 m 2,7294; embankment up to 5 m 1,1978; embankment up to 7 m 1,6733; and embankment up to 9 m 1,3998; during post-construction, the safety number (SF) of the slope of the 34° corner embankment was 1,2340 with a consolidation settlement of 0,1645 m.

### 2.3 Embankment stability with Geotextile

Arsy (2018) conducted research under the theme of “Embankment Stability Analysis on the Road Construction Using Geotextile Reinforcement with Fellenius Method”. The safety factor of this research after using reinforcement from analysis result with Fellenius method manually on length variation with geotextile length of 10 m, 13 m and 15 m obtained 2,339, 2,347 and 2,375, while using Geoslope without earthquake 2,497, 2,855 and 2,947, and with earthquake 1,304, 1,422 and 1,448. Safety factors from analysis result using reinforcement with Fellenius method manually on vertical distance between geotextile variaton with number of Sv 0.3 m, 0.4 m and 0.6 m are 2,646, 2,347 and 2,059, using Geoslope without the earthquake 2,869, 2,855 and 2,758, while with earthquake 1,436, 1,422 and 1,405.

Safety factors from analysis result using reinforcement with Fellenius method manually on slope angle variation with angle of 19°, 25° and 29° are 2,440, 2,347 and 2,355, using Geoslope without earthquake 2,930, 2,855 and 2,696, and with earthquake 1,423, 1,422 and 1,409.

Budiasto (2018) conducted research on “Analysis of Road Embankment Stability with Geotextile Reinforcement Using PLAXIS Program”. From the analysis of the PLAXIS program, a safe number greater than the safe number required by 1,4 and a decrease of 2 m of original embankment conditions with geotextile 1,785 during construction, 1,452 after construction and a decrease of -0,038 m, an original embankment replacement 0,5 m with geotextile 1,859 during construction, 1,529 after construction and a decrease of -0,038 m. The original embankment replacement 1 m with geotextile 2,065 during construction, 1,716 after construction and a decrease of -0,043 m. On the 4 m embankment of original embankment replacement 1 m condition with geotextile 1,645 during construction, 1,512 after construction and a decrease of -0,005 m. On the 6 m embankment of original embankment replacement 1 m condition with geotextile 1,457 during construction, 1,410 after construction and a decrease of 0,045 m. On the 8 m embankment of original embankment replacement 1 m condition with geotextile and counterweight 1,504 during construction, 1.501 after construction and a decrease of 0.471 m.

Isadono (2020) conducted research on "Analysis of Slope Stability Using Geotextile Reinforcement with PLAXIS 8.6 And Fellenius Method". The safety factors of this research in the analysis of the geotextile reinforced embankment, there is an increase in SF and a decrease in the number of soil settlement. For example, in the 20 m water Table embankment, the embankment with a height of 2,1 meters obtained an SF of 3,2248 and a soil settlement of 0,0964 meters. The embankment with the height of 4,2 meters obtained a SF of 3,0511 and a soil settlement of 0,1609 meters. Embankment with a height of 6,3 meters obtained a SF of 2,5303 and a settlement. The results of the analysis on the embankment variation also improved the quality in terms of SF and soil settlement after being reinforced with geotextile. of 0,2308 meters. Embankment with a height of 8,4

meters obtained SF of 2,0385 and a decrease in soil by 0,32 meters. Meanwhile, the embankment with a height of 10,5 meters obtained a safety factor of 1,7528 and a soil settlement obtained of 0,423 meters. The results of the analysis on the embankment variation also improved the quality in terms of SF and soil settlement after being reinforced with geotextile.

Afdhal (2018) conducted research on "Stability Analysis of Slope Road Embankments with Geotextile Reinforcement Using Geoslope 2018 Program in Tawang - Ngalang Segmen IV Highway Construction Project". This research aims to determine Knowing the value of the existing slope safety factor with geotextile reinforcement using the Geoslope program. The result of the analysis The output of manual calculations using the Fellenius method without an earthquake load, the safe number (SF) without an earthquake load recovered 1.335 <1.5. For embankments with a 320-angle slope with geotextile, the safe number (SF) without earthquake loads during the first phase of construction realized 4.094 > 1.5; the second phase of 2.797 > 1.5; the third phase attained 2.602 > 1.5 and during post-construction it was 2.566 > 1.5. Whereas on the 320-slope embankment with geotextile, the value of the safe number (SF) with earthquake loads during the first phase of construction attained 1.635 > 1.1; the second phase of 1.231 > 1.1; the third phase was 1.192 > 1.1 and during post-construction it had 1.187 > 1.1. The yield of land subsidence that occurred on the original slope embankment at an angle of 350 achieved 0.0847 m while slope embankment at an angle of 350 was 0.03 m.

Maulida (2023) conducted research on "Stability Analysis of Slope Road Embankment with Geotextile Reinforcement Using the Finite Element Method". This research aims to determine Knowing the value of safety number (SF) and the amount of consolidation settlement on the original embankment slope, new corner embankment slope without reinforcement and with geotextile reinforcement using finite element method. The result of the analysis is On the embankment slope with an angle of 34° with geoxtextile reinforcement during the construction period of the embankment up to 2,5 m 2,6458; embankment up to 5 m 2,4334; embankment up to 7 m 2,0975; and embankment up to 9 m 1,5981; during post-construction the safety number (SF) slope of the 34° corner embankment with geotextile

reinforcement was 1,3283 so that it was more than required by 1,3; and the resulting consolidated settlement of 0,1632 m. These results show that changing the slope angle of the embankment and geotextile reinforcement can increase the slope embankment safety number (SF).

**Table 2. 1 Comparison Past and Present Research**

| **RESEARCHER** | Arsy (2018) | Budiasto (2018) | Isadono (2020) | Afdal (2023) | Maulida (2023) | Syafe ie (2024) |
|---|---|---|---|---|---|---|
| **TITLE** | Embankment Stability Analysis on the Road Construction Using Geotextile Reinforcement with Fellenius Method | Analysis of Slope Stability Using Geotextile Reinforcement with PLAXIS 8.6 And Fellenius Method | Analysis of Slope Stability Using Geotextile Reinforcement with PLAXIS 8.6 And Fellenius Method | Stability Analysis of Slope Road Embankments with Geotextile Reinforcement Using Geoslope 2018 Program in Tawang - Ngalang Segmen IV Highway Construction Project | Stability Analysis of Slope Road Embankment with Geotextile Reinforcement Using the Finite Element Method | Analysis of Slope Stability Using Geotextile Reinforcement with PLAXIS and Fellenius Method |
| **PURPOSE** | Increasing soil bearing capacity | Determining the safety factor toward failure and Marshland decrease number | Determining the safety factor toward failure | Knowing the value of the existing slope safety factor with geotextile reinforcement using the Geoslope program. | Knowing the value of safety number (SF) and the amount of consolidation settlement on the original embankment slope, new corner embankment slope without reinforcement and with geotextile reinforcement using finite element method. | Determining the safety factor and the amount of settlement on road embankment with alternative embankment. Also, the variation of geotextile used. |

Source: Arsy & Artati (2018), Budiasto & Purwanto (2018), Isadono (2020), Afdhal (2023), Maulida (2023), Syafei'e (2024)

**Continuation of Table 2.1 Comparison Past and Present Research**

| | | | | | | |
|---|---|---|---|---|---|---|
| **METHOD** | Geotextile Reinforcement with Fellenius Method | PLAXIS 8.6 And Fellenius Method | Geotextile Reinforcement with PLAXIS 8.6 And Fellenius Method | Analysis using Geoslope program for the stability of the safe number of existing slopes with geotextile reinforcement. | The analysis used the finite element method with the help of the PLAXIS 8.6 program to find the safe number (SF) of the embankment slope and the consolidation settlement that will occur. | PLAXIS program And Fellenius Method |
| **RESULT** | The safety factor of this research after using reinforcement from analysis result with Fellenius method manually on length variation with geotextile length of 10 m, 13 m and 15 m obtained 2,339, 2,347 and 2,375, while using Geoslope without earthquake 2,497, 2,855 and 2,947, and with earthquake 1,304, 1,422 and 1,448. Safety factors from analysis result using reinforcement with Fellenius method manually on vertical distance between geotextile variaton with number of Sv 0.3 m, 0.4 m and 0.6 m are 2,646, 2,347 and 2,059, | a safe number greater than the safe number required by 1,4 and a decrease of 2 m of original embankment conditions with geotextile 1,785 during construction, 1,452 after construction and a decrease of -0,038 m, an original embankment replacement 0,5 m with geotextile 1,859 during construction, 1,529 after construction and a decrease of -0,038 m. The original embankment replacement 1 m with geotextile 2,065 during construction, 1,716 after construction and a decrease of -0,043 m. On the 4 m embankment of original embankment | The safety factors of this research in the analysis of the geotextile reinforced embankment, there is an increase in SF and a decrease in the number of soil settlement. For example, in the 20 m water Table embankment, the embankment with a height of 2,1 meters obtained an SF of 3,2248 and a soil settlement of 0,0964 meters. The embankment with the height of 4,2 meters obtained a SF of 3,0511 and a soil settlement of 0,1609 meters. Embankment with a | The results of the analysis using the 2018 Geoslope program on the original slope embankment at an angle of 350 obtained the safe number (SF) without earthquake loads during the first phase construction period of 3.638 > 1.5; the second phase of 1.759 > 1.5; the third phase was 1.396 < 1.5 and during post-construction it was 1.303 < 1.5. Meanwhile, on the original slope embankment at an on | Safety number value (SF) for the original embankment slope with an angle of 39° of the embankment construction periods up to 2,5 m 2,5265; embankment up to 5 m 1,8616; embankment up to 7 m 1,5425; and embankment up to 9 m 1,2846, during post-construction the safety number (SF) of the original embankment slope win an angle 39° was 1,1517 with a consolidation settlement of 0,1865 | |

Source: Arsy & Artati (2018), Budiasto & Purwanto (2018), Isadono (2020), Afdhal (2023), Maulida (2023), Syafei'e (2024)

**Continuation of Table 2.1 Comparison Past and Present Research**

| | | | | | | |
|---|---|---|---|---|---|---|
| **RESULT** | using Geoslope without the earthquake 2,869, 2,855 and 2,758, while with earthquake 1,436, 1,422 and 1,405. Safety factors from analysis result using reinforcement with Fellenius method manually on slope angle variaton with angle of 19°, 25° and 29° are 2,440, 2,347 and 2,355, using Geoslope without earthquake 2,930, 2,855 and 2,696, and with earthquake 1,423, 1,422 and 1,409. | replacement 1 m condition with geotextile 1,645 during construction, 1,512 after construction and a decrease of -0,005 m. On the 6 m embankment of original embankment replacement 1 m condition with geotextile 1,457 during construction, 1,410 after construction and a decrease of 0,045 m. On the 8 m embankment of original embankment replacement 1 m condition with geotextile and counterweight 1,504 during construction, 1.501 after construction and a decrease of 0.471 m. | height of 6,3 meters obtained a SF of 2,5303 and a settlement. The results of the analysis on the embankment variation also improved the quality in terms of SF and soil settlement after being reinforced with geotextile. of 0,2308 meters. Embankment with a height of 8,4 meters obtained SF of 2,0385 and a decrease in soil by 0,32 meters. Meanwhile, the embankment with a height of 10,5 meters obtained a safety factor of 1,7528 and a soil settlement obtained of 0,423 meters. The results of the analysis on the embankment variation also improved the quality in terms of SF and soil settlement after being reinforced with geotextile. | angle of 350, the safe number (SF) with earthquake loads during the first phase of construction gained 1.251 > 1.1; the second phase of 0.729 <1.1; the third phase reached 0.674 < 1.1 and during post-construction 0.644 < 1.1. The output of manual calculations using the Fellenius method without an earthquake load, the safe number (SF) without an earthquake load recovered 1.335 <1.5.For embankments with a 320-angle slope with geotextile, the safe number (SF) without earthquake loads during the first phase of construction realized 4.094 > 1.5; the second phase of 2.797 > 1.5; the third | m. On the embankment slope with an angle of 34° during the construction period of the embankment up to 2,5 m 2,7294; embankment up to 5 m 1,1978; embankment up to 7 m 1,6733; and embankment up to 9 m 1,3998; during post-construction, the safety number (SF) of the slope of the 34° corner embankment was 1,2340 with a consolidation settlement of 0,1645 m. On the embankment slope with an angle of 34° with geoxtextile reinforcement during the construction period of the embankment up to 2,5 m 2,6458; embankment up to 5 | |

Source: Arsy & Artati (2018), Budiasto & Purwanto (2018), Isadono (2020), Afdhal (2023), Maulida (2023), Syafei'e (2024)

**Continuation of Table 2.1 Comparison Past and Present Research**

| | | | | | | |
|---|---|---|---|---|---|---|
| **RESULT** | | | | phase attained 2.602 > 1.5 and during post-construction it was 2.566 > 1.5. Whereas the 320-slope embankment with geotextile, the value of the safe number (SF) with earthquake loads during the first phase of construction attained 1.635 > 1.1; the second phase of 1.231 > 1.1; the third phase was 1.192 > 1.1 and during post-construction it had 1.187 > 1.1. The yield of land subsidence that occurred on the original slope embankment at an angle of 350 achieved 0.0847 m while slope embankment at an angle of 350 was 0.03 m. | m 2,4334; embankment up to 7 m 2,0975; and embankment up to 9m 1,5981; during post-construction the safety number (SF) slope of the 34° corner embankment with geotextile reinforcement was 1,3283 so that it was more than required by 1,3; and the resulting consolidated settlement of 0,1632 m. These results show that changing the slope angle of the embankment and geotextile reinforcement can increase the slope embankment safety number (SF). | |

Source: Arsy & Artati (2018), Budiasto & Purwanto (2018), Isadono (2020), Afdhal (2023), Maulida (2023), Syafei'e (2024)

# CHAPTER III
# BASIC THEORIES

## 3.1 Soil

From the perspective of civil engineering, the soil consists of a loose combination of organic matter, minerals, and sediments on top of bedrock. Carbonates, organic debris, or oxides that settle in between the particles can be the reason for the relatively weak connections between grains. Either water, air, or both may be present in the voids between the particles. Soil is created by weathering rocks and other geological processes close to the earth's surface. Soil can originate from its parent rock by either a physical or chemical process. The processes of erosion, wind, water, ice, human beings, and weather-related changes that destroy soil particles are the causes of physical soil formation, which breaks down rocks into smaller pieces. Particles may be in rounded, jagged or any forms in between those two. In general, oxygen, carbon dioxide, water (especially that which contains acids or alkalis), and other chemical processes can all affect chemical weathering. Soil that has weathered and is still in its original location is referred to as residual soil, and soil that has moved is referred to as transported soil (Hardiyatmo, 2002).

### 3.1.1 Soil Properties

Based on the volume weight of soil, soil types are divided into three conditions, dry soil, saturated soil, and unsaturated soil. Those type are differentiate by the materials inside it. Dry soil consist of two materials which are grain and air (Hardiyatmo, 2002). Saturated soil also consist of two materials, grain and water. While unsaturated soil consist of three materials, grain, water, and ait. The illustration of each condition can be seen in Figure 3.1 below.

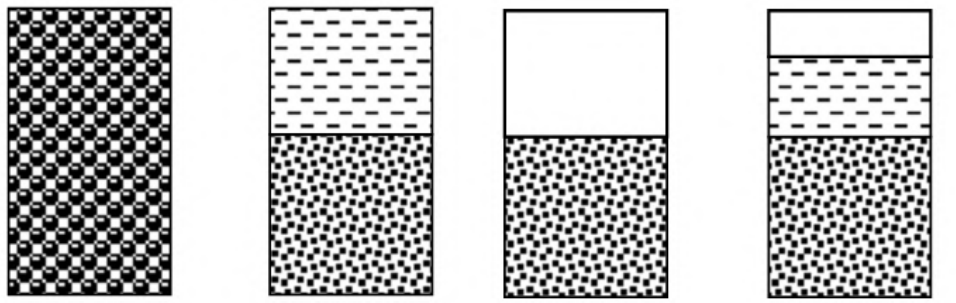

(a)Soil (grain+pore) | (b)Saturated Soil (grain+water) | (c)Dry Soil (grain+air) | (d)Unsaturated Soil (grain+water+air)

**Figure 3. 1 Soil Conditions**

(Source: Panguriseng, 2018)

Each soil elements (Grain, water, air), has its own volume and weight. The description of the soil parameter can be seen in Figure 3.2 below.

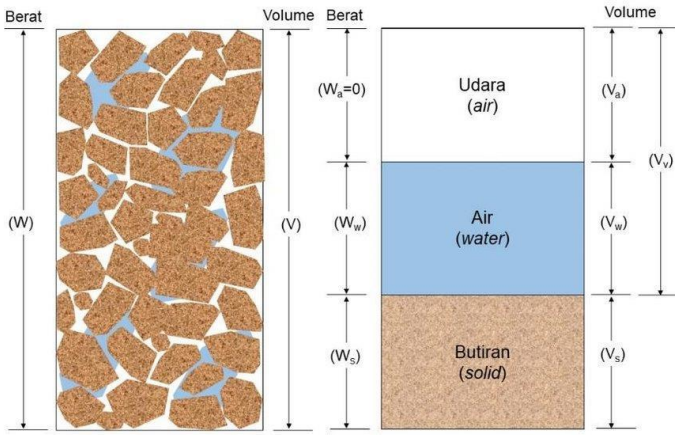


**Figure 3. 2 Diagram of Soil Phase**

(Source: Hardiyatmo, 2002)

Based on the soil phase diagram above, some relations can be formulated in Equation 3.1, Equation 3.2, Equation 3.3, and Equation 3.4 below:

a. Weight of soil $(W) = W_s + W_w$ (3.1)

b. Volume of pore $(V_v) = V_w + V_a$ (3.2)

c. Volume of soil $(V) = V_s + V_w + V_a$ (3.3)

$(V) = V_s + V_v$ (3.4)

Description:

W = total weight of soil

$W_a$ = weight of air = 0 (ignored)

$W_w$ = weight of water

V = total volume of soil

$V_a$ = volume of air

$V_w$ = volume of water

$V_v$ = volume of pore

$V_s$ = volume of grain

Other than those parameters mentioned above, some soil parameters below, will be used for slope stability analysis both static as well as Finite Element Method (FEM).

1. Bulk unit weight ($\gamma_b$)

   Bulk unit weight is the ratio of the total weight of soil grain (W) to the total volume of soil (V). It can be formulated as follows:

   $$\gamma_b = \frac{W}{V} \quad (3.5)$$

2. Dry unit weight ($\gamma_d$)

   Dry unit weight is the ratio of solid grain weight (Ws) to the total volume of soil (V). It can be formulated in Equation 3.6 as follows:

   $$\gamma_d = \frac{Ws}{V} \quad (3.6)$$

3. Saturated unit weight ($\gamma_{sat}$)

   Saturated unit weight is the ratio of solid grain weight ($W_s$) to the volume of solid grain (Vs). It can be formulated in Equation 3.7 as follows:

   $$\gamma_{sat} = \frac{Ws}{Vs} \quad (3.7)$$

   Determining the unit weight of soil ($\gamma$) and the saturated unit weight ($\gamma_{sat}$), can be seen in the Table 3.1.

**Table 3. 1 Unit Weight of Soil Value**

| No | Soil type | $\gamma_{sat}$ (kN/m$^3$) | $\gamma_d$ (kN/m$^3$) |
|---|---|---|---|
| 1 | Gravel | 20 - 22 | 15 – 17 |
| 2 | Sand | 18 – 20 | 13 – 16 |

**Continuation Table 3.1 Unit Weight of Soil Value**

| | | | |
|---|---|---|---|
| 3 | Silt | 18 – 20 | 14 – 18 |
| 4 | Clay | 16 - 22 | 14 – 21 |

(Source: Budhu, 2015)

4. Elastic modulus

   Elastic modulus or also known as Young's modulus generally represents the material stiffness of certain materials from the ratio of stress to strain. In geotechnical engineering, elastic modulus is used to determine the behaviour of various soil types. This value can be obtained through undrained triaxial test on the laboratory or empirically through boring data as can be seen on the Table 3.2 below.

**Table 3. 2 Elastic Modulus of Different Soil Type**

| **Soil type** | **$E_s$ (kN/m$^2$)** |
|---|---|
| **Clay** | |
| Very soft | 300 – 3000 |
| Soft | 2000 – 4000 |
| Medium | 4500 – 9000 |
| Hard | 7000 – 20000 |
| Sandy | 30000 – 42500 |
| **Sandy** | |
| Silty | 5000 – 20000 |
| Not dense | 10000 – 25000 |
| Dense | 50000 – 100000 |
| **Sand and Gravel** | |
| Dense | 80000 – 200000 |
| Not dense | 50000 – 140000 |
| **Silt** | 2000 – 20000 |
| **Loess** | 15000 – 600000 |
| **Shale** | 140000 - 1400000 |

5. Poisson ratio (v)

   Poisson ratio is the ratio of lateral and longitudinal strain caused by lateral load. This parameter can be obtained by triaxial test on laboratory. The Table of poisson ratio can be seen in the Table 3.3 below.

**Table 3. 3 Poisson Ratio**

| Soil type | v |
|---|---|
| Saturated clay | 0,4 – 0,5 |
| Unsaturated clay | 0,1 – 0,3 |
| Sandy loam | 0,2 – 0,3 |
| Silt | 0,3 – 0,35 |
| Dense sand | 0,2 – 0,4 |
| Coarse sand (Pore number, e = 0.4-0.7) | 0,15 |
| Fine sand (Pore number, e = 0.4 - 0.7) | 0,25 |
| Stone (depending on type) | 0,1 – 0,4 |
| Loose | 0,1 – 0,3 |

6. Cohesion

   Cohesion on soil can be defined as the tensile strength among soil particles. Other than internal friction angle, cohesion is also one of the factors that determines the soil resistance towards deformation due to the soil movement on lateral direction. This parameter can be taken from Triaxial Test and Direct Shear Test. The table of cohesion can be seen in the Table 3.4 below.

**Table 3. 4 Cohesion**

| Soil Condition | Soil Type | c' (kN/m$^2$) |
|---|---|---|
| Poor | Soft and stiff clay with medium to high plasticity; silty clay; loose variable clay fill; loose sandy silt | 0 - 5 |
| Medium | Stiff sandy clay; gravelly clay; compacted clayey sand; sandy silt; compacted clay fill | 0 - 10 |
| Good | Gravelly sand; compacted sand; gravel and crushed sandstone fill; well-graded compacted sand | 0 - 5 |
| Very Good | Weakly weathered stone; controlled road base course fill; gravel and recycled concrete | 0 - 25 |

(Source: Bowles, 1996)

7. Internal friction angle

   As has been mentioned above, internal friction angle plays vital role in soil tensile strength. It is a critical factor that contributes to soil resistance towards soil lateral load. To put on a more detailed explanation, the relation between soil type and internal friction angle can be seen on the Table 3.5 below.

**Table 3. 5 Internal Friction Angle**

| Soil Condition | Soil Type | $\varphi'$ (°) |
|---|---|---|
| Poor | Soft and stiff clay with medium to high plasticity; silty clay; loose variable clay fill; loose sandy silt | 17 - 25 |
| Medium | Stiff sandy clay; gravelly clay; compacted clayey sand; sandy silt; compacted clay fill | 26 – 32 |
| Good | Gravelly sand; compacted sand; gravel and crushed sandstone fill; well-graded compacted sand | 32 – 37 |
| Very Good | Weakly weathered stone; controlled road base course fill; gravel and recycled concrete | 36 - 43 |

(Source: Bowles, 1996)

8. Permeability

   Physically, a soil consists of soil and void, this parameter will determine the speed of water penetrating through soil sample. This parameter will be applied as a coefficient. It plays essential role to help solving settlement issues on structures. The value of permeability coefficient can be obtained by conducting falling head, constant head test method, and also triaxial method on laboratory. The Table of permeability can be seen in the Table 3.6 below.

**Table 3. 6 Permeability**

| Soil Type | k |
|---|---|
| | cm/s |
| Fine Gravel | 1 - 100 |
| Coarse Sand | 1 - 0,01 |
| Fine Sand | 0,01 - 0,001 |
| Silt | 0,001 - 0,00001 |
| Clay | <0,000001 |

(Source: Bowles, 1996)

### 3.1.2 Soil Classification

Soil Classification System is a systematic classification system of soil types with similar properties into groups and sub-groups based on their use (Das, 1995). The systematic categorization of soils into distinct groups, based on shared physical and chemical properties, facilitates the comprehension, utilization, and differentiation of various soil types. This organization serves as a critical foundation for informed decision-making in engineering and construction projects.

The purpose of the soil classification system is to provide information on the characteristics and physical properties of soils that are useful for detailed studies of soil conditions as well as the needs of the engineer in determining technical properties such as compaction characteristics, soil strength, and specific gravity (Bowles, 1996). By finding out the soil classification, the soil behaviour will be known and the proper maintenance process of the upper structure will be discovered. There are several systems for classifying soils, but the most used systems are Unified Soil Classification System (USCS) and (American Association of State Highway and Transportation Officials) AASHTO.

1. USCS Classification Method

   In 1942, Arthur Casagrande developed the Unified Soil Classification method, which was subsequently adopted by the Army Corps of Engineers and the Bureau of Reclamation for regular usage. Casagrande first developed the method for airport building during the war, and in 1948 he published a report on it. It is currently modified and updated on a regular basis in ASTM (designation D 2487). Geotechnical engineers most frequently utilise this classification system. The soil classification based on USCS, the soil is divided into 2 categories:

   a. Coarse-grained soils

      In this category consists of gravel and sand which less than 50% of the soil passes the No. 200 sieve (F200 < 50).

   b. Fine-grained soils

      In this category with more than 50% passing through the No. 200 sieve (F200 ≥ 50).

      There are symbols used in USCS:

      G = gravel

      S = sand

      C = anorganic clay

      M = anorganic silt

      O = organic silt and organic clay

      Pt = peat

      W = well-graded

P = poorly-graded

H = high-plasticity

L = low-plasticity

Soil classification system of the USCS, can be seen in the Table 3.4 below.

**Table 3. 7 Unified Soil Classification System**

| Field identification procedures (excluding particles larger than 3 sq. inches and basing fractions on estimated weights) | | | | | Group symbols[a] | Typical names |
|---|---|---|---|---|---|---|
| Gravels (more than half of coarse fraction is larger than 4.75 mm) (For visual classifications, the 1/4" size may be used as equivalent to the No. 4 sieve size) | Clean gravels (little or no fines) | Wide range in grain size and substantial amounts of all intermediate particle sizes | | | GW | Well-graded gravels, gravel-sand mixtures, little or no fines |
| | | Predominantly one size or an range of sizes with some intermediate sizes missing | | | GP | Poorly graded gravels, gravel-sand mixtures, little or no fines |
| | Gravels with fines (appreciable amount of fines) | Non-plastic fines (for indentification procedures, see ML below) | | | GM | Silty gravels, poorly graded gravel-sand-silt mixtures |
| | | Plastic fines (for indentification procedures, see CL below) | | | GC | Clayey gravels, poorly graded gravel-sand-clay mixtures |
| Sands (more than half of coarse fraction is smaller than 4.75 mm) | Clean sands (little or no fines) | Wide range in grain sizes and substantial amounts of all intermediate particle sizes | | | SW | Well-graded sands, gravelly, little or no fines |
| | | Predominantly one size or a range of sizes with some intermediate sizes missing | | | SP | Poorly graded sands, gravelly sands, little or no fines |
| | Sands with fines (appreciable amount of fines) | Non-plastic fines (for indentification procedures, see ML below) | | | SM | Silty sands, poorly graded sand-silt mixtures |
| | | Plastic fines (for indentification procedures, see CL below) | | | SC | Clayey sands, poorly graded sand-clay mixtures |
| Identification procedures of fraction smaller than 0.425 mm | | | | | | |
| | | **Dry strength (crushing characteristics)** | **Dilatancy (reaction to shaking)** | **Toughness (consistency near plastic limit)** | | |
| Silts and clays (liquid limit less than 50) | | None to slight | Quick to slow | None | ML | Inorganic silts and very fine sands, rock flour, silty or clayey fine sands with slight plasticity |
| | | Medium to high | None to very slow | Medium | CL | Inorganic clays of low to medium plasticity, clays, sandy clays, siltyclays, lean clays |
| | | Slight to medium | Slow | Slight | OL | Organic silt sand, organic silt clays of low plasticity |
| Silts and clays (liquid limit greater than 50) | | Slight to medium | Slow to none | Slight to medium | MH | Inorganic silts, micaceous or diatomaceous fine sandy or silty soils, elastic silts |
| | | High to very high | None | High | CH | Inorganic clay of plasticity, fat clays |
| | | Medium to high | None to very slow | Slight to medium | OH | Organic clays of medium to high plasticity |
| High organic soils | | Readily identified by colour, odour, spongy feel, and frequently by fibrous texture | | | Pt | Peat and other highly organic soils |

(Source: Hardiyatmo, 2002)

2. AASHTO Classification Method

The AASHTO soil classification system is used to determine soil suitability for soil works, embankments, and roadbed materials which are subgrade, subbase, and base. The soils are categorized into eight groups, A-1 to A-7, with the

additional category A-8 for peat or muck. The soils with higher quality have smaller numbers, but the soil types in group A-3 have better material for road subgrades than the soils in group A-2. The AASHTO classification can be seen in the Table 3.5 below.

**Table 3. 8 AASHTO classification**

| AASHTO Soil Classification System (from AASHTO M 145 or ASTM D3282) | | | | | | | | | | | |
|---|---|---|---|---|---|---|---|---|---|---|---|
| **General Classification** | **Granular Materials (35% or less passing the 0.075 mm sieve)** | | | | | | | **Silt-Clay Materials (>35% passing the 0.075 mm sieve)** | | | |
| Group Classification | A-1 | | A-3 | A-2 | | | | A-4 | A-5 | A-6 | A-7 |
| | A-1-a | A-1-b | | A-2-4 | A-2-5 | A-2-6 | A-2-7 | | | | A-7-5 A-7-6 |
| Sieve Analysis, % passing | | | | | | | | | | | |
| 2.00 mm (No. 10) | 50 max | ... | ... | ... | ... | ... | ... | ... | ... | ... | ... |
| 0.425 (No. 40) | 30 max | 50 max | 51 min | ... | ... | ... | ... | ... | ... | ... | ... |
| 0.075 (No. 200) | 15 max | 25 max | 10 max | 35 max | 35 max | 35 max | 35 max | 36 min | 36 min | 36 min | 36 min |
| Characteristics of fraction passing 0.425 mm (No. 40) | | | | | | | | | | | |
| Liquid Limit | ... | | ... | 40 max | 41 min | 40 max | 41 min | 40 max | 41 min | 40 max | 41 min |
| Plasticity Index | 6 max | | N.P. | 10 max | 10 max | 11 min | 11 min | 10 max | 10 max | 11 min | 11 min[1] |
| Usual types of significant constituent materials | stone fragments, gravel and sand | | fine sand | silty or clayey gravel and sand | | | | silty soils | | clayey soils | |
| General rating as a subgrade | excellent to good | | | | | | | fair to poor | | | |

(Source: Hardiyatmo, 2002)

## 3.2 Soil Investigation

Soil investigation is an activity used to determine the condition of the soil surface and subsurface lithology as well as physical and mechanical parameters of the soil through laboratory tests. This series of activities is divided into three sequential stages, namely Geoelectric Measurement, Soil Investigation and Laboratory Testing. based on the results of soil investigation used as the basis for planning and construction of a building structure.

Geoelectric measurement is a geophysical measurement method that is often used in groundwater and subsurface lithology (rock) investigations. This method

has relatively good and representative results and depends on the resistivity value of the rock. The results of this method make it possible to model the subsurface showing high or low rock resistivity values.

Soil investigation is a comprehensive soil investigation activity, intended to provide information about soil conditions, soil and rock layers, soil types, groundwater Table, soil layer structure, and other information for foundation planning.

### 3.3 Soil Embankment Load

Based on the SNI (8460:2017) about the requirement of geotechnical design, there are live load, dead load, and earthquake load. Below, the loading will be specified as pavement load as dead load, traffic load as live load, while for earthquake load stays the same.

#### 3.3.1 Pavement Load

Pavement according to Sukirman (2010) is the layer of pavement that is located between the wheels of a vehicle and the subgrade. The road pavement serves to provide transport services and is expected not to experience significant damage during the period of use. Based on the binder material, pavement divide into 3 types, there are rigid pavement, flexible pavement, and composite pavement. The analysis procedure there are various pavement loads that are considered:

1. Thickness of rigid pavement,
2. Thickness of lean concrete,
3. Thickness of aggregate,
4. Pavement load.

### 3.3.2 Traffic load

Stability analysis is conducted by considering the traffic load. Traffic loads are uniform loads that must be taken into consideration on the entire width of the embankment surface. The traffic load can be seen in the Table 3.6 below.

**Table 3. 9 Traffic Load**

| Network System | Road Function | LHR | Traffic Load ($kN/m^2$) |
|---|---|---|---|
| Primer | Arteries | All | 15 |
| | Collector | >10.000 | 15 |
| | | <10.000 | 12 |
| Second | Arteries | >20.000 | 15 |
| | | <20.000 | 12 |
| | Collector | >6.000 | 12 |
| | | <6.000 | 10 |
| | Local | >500 | 10 |
| | | <500 | 10 |

(Source: Direktorat Bina Marga, 2017)

### 3.3.3 Earthquake load

Earthquake loads are loads caused by earthquakes that impact on a structure because of ground motions. The effect of earthquake load is considered in the planning of slope embankment that built in the area of settlement or involved in strategic importance criteria (SNI, 1726:2019). Planning is carried out to anticipate the collapse of transportation lane after the earthquake. The dynamic load of earthquake can increase the shear stress of slope, decrease the shear strength of soil, and decrease soil pore volume. Therefore, earthquake load can affect the slope stability because that load can affect the horizontal dynamic stress and vertical dynamic stress. Each region has its own earthquake value. So, earthquake zoning map will be used in designing the earthquake load based on the assigned area. The map can be seen in Figure 3.3.

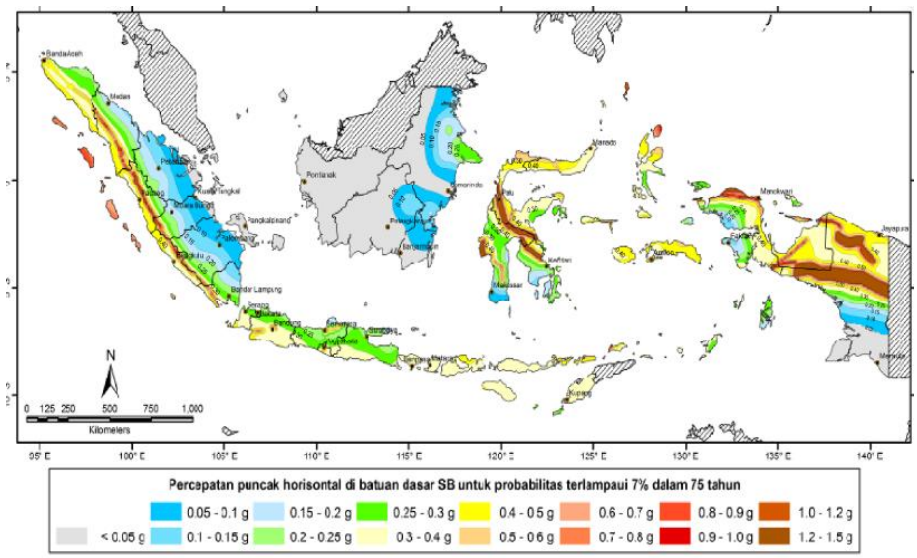


**Figure 3. 3 Earthquake Zoning Map**

(Source: SNI, 1726:2019)

### 3.4 Slope Stability

Slope is a soil surface that form particular tilt angle towards horizontal bodies. Slope can be formed by the natural geological process and also man-made. Slope that experience failure technically will automatically lose its stability due to the low safety factor (Soepandji, 1995). Therefore, slope stability is an important factor in cut and fill work, the rocks and excavation materials, which refers to the occupational health and safety of the labour and the succession of the works. Slope stability analysis is aimed to determine the safety factor.

As for the factors affecting the stability are soil condition, shear stress, water seepage flow, etc. Gravitational forces and seepage flow tend to create instability on natural slope, excavated slope, embankment slope, and also on soil dam. Based on its form, there are some types of slope failure. They are:

1. Flat failure (translation)

   Flat failure as known as translational failure is the simplest type of failure. This failure is caused by the movement of soil and rock masses on the sloping layer (Hardiyatmo, 1992). Flat failure can be seen in Figure 3.4 below.

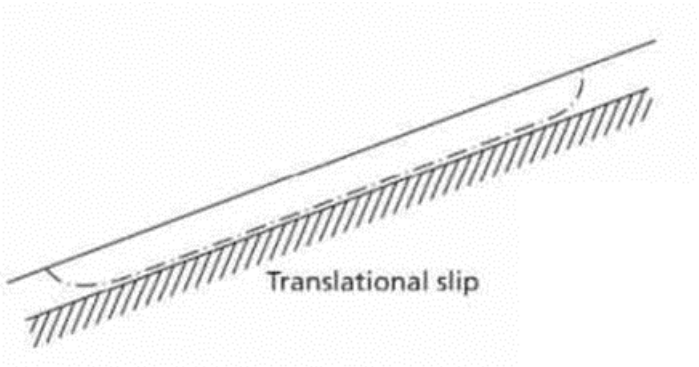


**Figure 3. 4 Flat Failure**

(Source: Hardiyatmo, 2002)

2. Rotation failure

Rotation failure is characterised by the curvilinear slope and rotation movement. The main causes of rotation failure are seepage forces of groundwater or increasing the slope in the residual soil. In this failure are globally that involving large masses of soil. Typically, it will be followed by smaller failure in the mass of moving soil (Hardiyatmo, 1992). The rotation failure can be seen in Figure 3.5 below.

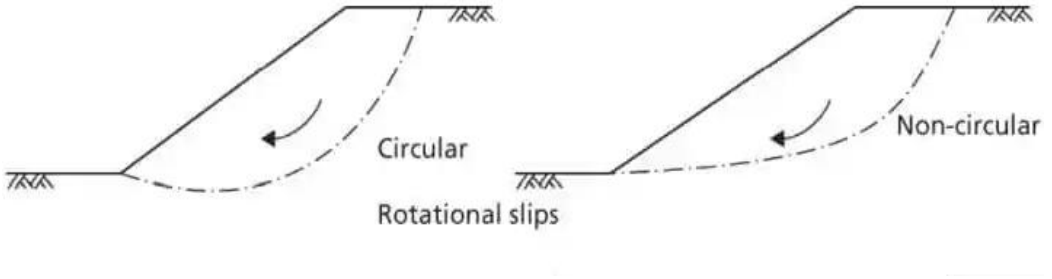


**Figure 3. 5 Rotation Failure**

(Source: Hardiyatmo, 2002)

3. Irregular failure

Irregular failure is a combination between flat failure and rotation failure. It can be categorized by other forms not of these two failures. This failure occurs in heterogeneous soil and have multiple different soil layers on the same slope. Irregular failure can be seen in Figure 3.6 below.

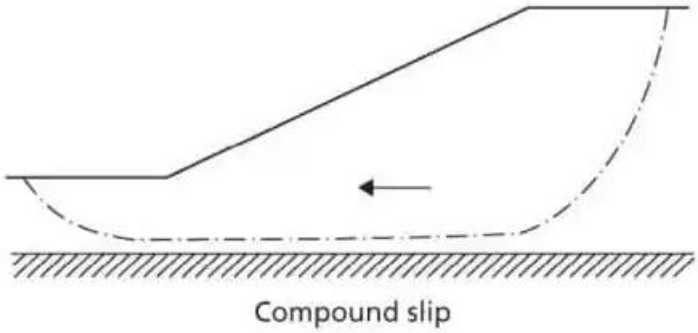


**Figure 3. 6 Irregular failure**

(Source: Hardiyatmo, 2002)

### 3.4.1 Safety Factor

The purpose of stability analysis of slope is to determine the safety factor of potential collapsed body. Based on Hardiyatmo (1992) there are some explanations made in terms of slope stability. They are:

1. Slope failure can occur across the particular collapse body surface and can be assumed as two-dimensional bodies problem.
2. The collapsed mass is assumed as a massive object,
3. Moving soil from the soil mass on every spot along the failure bodies is not depend on the orientation of potential collapsed body, and the average of soil shear force along the surface of the collapsed object,
4. Safety factor is defined by showing the average shear stress across the potential collapse body, and the average shear force of soil along the collapse surface.

Stability of the slope itself is represented by the Safety Factor (SF) value. The value of safety factor, that is required by the Departemen Pekerjaan Umum can be seen in the Table 3.10 and Table 3.11.

**Table 3. 10 Recommendation for safety factor of slope**

| Costs and consequences of slope failure | The level of uncertainty of the analysis conditions | |
|---|---|---|
| | Low[a] | High[b] |
| Repairing costs are worth the additional costs of designing more conservative slopes | 1,25 | 1,5 |
| Repairing costs outweigh the additional costs of designing more conservative slopes | 1,5 | 2,0 or more |
| a. The level of uncertainty in the analysis conditions is categorized as low, if the geological conditions can be understood, the soil conditions are uniform, the soil investigation is consistent, complete, and logical to the conditions in the field.<br>b. The level of uncertainty in the analysis conditions is categorized as high, if the geological conditions are very complex, soil conditions vary, and soil investigations are | | |

(Source: SNI, 8460:2017)

**Table 3. 11 Safety Factor of Slope**

| safety factor | slope status | failure intensity |
|---|---|---|
| SF<1,07 | unstable slope | unstable class |
| 1,074≤SF≥1,25 | critical slope | critical class |
| SF>1,25 | relatively stable slope | stable class |

(Source: Bowles, 1996)

### 3.4.2 Fellenius Method

Fellenius method is introduced by Fellenius (1927) used to analyse the stability of slope. Based on Hardiyatmo (1992), Fellenius method assume the forces on the right and left sides acting from any intersection of slope has to be zero resultant in the direction perpendicular to the landslide. By assuming this, vertical force equilibrium and other forces considering the pore water pressure. The modelling of fellenius method can be seen in Figure 3.7 below.

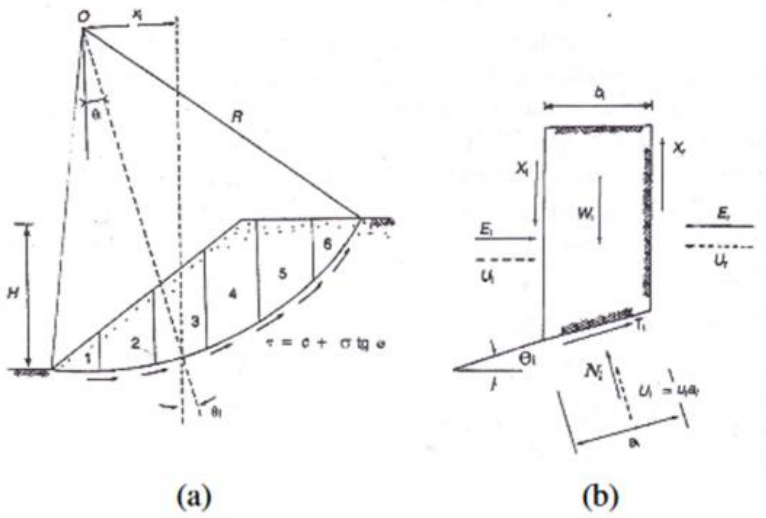


**Figure 3. 7 Modelling of Fellenius Method**

(Source: Hardiyatmo, 2002)

Based on the modelling and the concept of Fellenius method, some relations can be formulated in Equation 3.8 below.

$$Ni + Ui = Wi \cos\theta$$

Or

$$Ni = Wi \cos\theta - Ui$$

$$= Wi \cos\theta - Ui.\text{ai} \qquad (3.8)$$

Safety factor can be identified as,

$$FS = \frac{total\ moment\ of\ shear\ stress\ on\ failure\ body}{total\ moment\ of\ soil\ failure\ mass}$$

$$FS = \frac{\sum Mr}{\sum Md}$$

The moment arm of the soil mass of each intersection is R sin θ can be seen in Equation 3.9.

$$\sum Md = R \sum_{i=1}^{i=n} Wi\ sin\theta i \qquad (3.9)$$

With:

R = radius of failing body

n = total of intersection

$W_i$ = weight of intersection soil on-i (kN)

$\theta_i$ = define angle

Using the same step, the moment that hold the soil before failing, can be seen in Equation 3.10 below.

$$\sum Mr = R \sum_{i=1}^{i=n} (cai + Ni\ tg\varphi) \quad (3.10)$$

So, the safety factor formula can be seen in Equation 3.11 below,

$$FS = \frac{\sum_{i=1}^{i=n} (cai + Ni\ tg\varphi)}{\sum_{i=1}^{i=n} Wi\ sin\theta i} \quad (3.11)$$

With:

FS = safety factor

c = cohesion (kN/m$^2$)

$\varphi$ = friction angle (degree)

$a_i$ = length of curve circle on-i intersection ( m)

$W_i$ = weight of intersection soil on-i (kN)

$U_i$ = pore water pressure of intersection on-i

$\theta_i$ = define angle (degree)

If there are forces other than the weight of the soil, such as buildings on a slope, the moment due to this load is calculated as Md.

### 3.5 Slope Reinforcement Using Geotextile

Ideally, slopes must fulfil particular safety factor in order to ensure its stability in a short as well as long term. So, if the slopes have low stability level, then reinforcement have to be installed to protect the slopes from factors that can lead to failing, such as erosion and collapsing. One of the reinforcement methods for slopes is geotextile, which is used in this research.

Geotextile is commonly used for base soil reinforcement on pavement structures. It is also used for road embankment stabilisation located on the soft soil foundation. Installation of geotextile is functioned as separator between soil layers, also as reinforcement to increase the bearing capacity of base soil by the soil composite strength with geotextile (Rasdi, 2021). The materials used in creating geotextile are thread and polymer fibre, such as polyester (PET), polyamide (PM), polypropylene (PP), and polyethylene (PE).

### 3.5.1 Geotextile type

Generally, based on the method used, geotextile is divided into two types. They are woven geotextile and nonwoven geotextile. The explanation of those types can be seen below.

1. Woven geotextile

   This type of geotextile has bigger tensile strength compare to the nonwoven one. The structure of this geotextile is similar to rice sack made of woven synthetic fibers with protection from ultra violet and black in colour. This geotextile is functioned as stabilisation of base soil, especially for soil so the soil can be layered and not experiencing consolidation.

   Woven geotextile is not easily broken or teared during the installation on field. The double twist structure will ensure the compression stress up to 40 kN/m while used as separator or separating layer. Because, this function will be disturbed if the material is teared or broken. The woven geotextile can seen in Figure 3.8 below.

**Figure 3. 8 Woven Geotextile**

2. Nonwoven geotextile

   Nonwoven geotextile is made by sewing but the tissue or fibres is glued with one another by tying or using adhesive. The material used for this type of geotextile is made of polymer material polyester (PET) or polypropylene (PP). some function of nonwoven geotextile can be seen below.

a. Separator

   To prevent the contamination between one material to another this type of geotextile will be used. On the construction of soft soil type, nonwoven geotextile can prevent the rising of mud into the pavement system and also from the pumping effect that can destroy the road pavement. Therefore, geotextile can help compacting process of pavement system.

b. Filter

   By having permeable behaviour, nonwoven geotextile is aimed to prevent soil particles to be carried out by the water flow. The application of this geotextile is usually used as filter on underground drainage project.

c. Stabilator

   This function is also known as reinforcement function. Nonwoven geotextile can be seen on the Figure 3.9.

**Figure 3. 9 Non-Woven Geotextile**

### 3.5.2 Working Mechanism of Geotextile on field

The use of geotextile reinforcement on road construction project can help to prevent the local collapse on soft soil that have low bearing capacity. When the soil and geotextile are combined, the soil composite material that is reinforced will create high compressive and tensile strength, so the forced and deformation acting on there can be handled. Besides, geotextile is used to stabilize steep slope ($70^0$) and increase the safety factor. The working mechanism of geotextile on field. Can be seen in Figure 3.10 below.

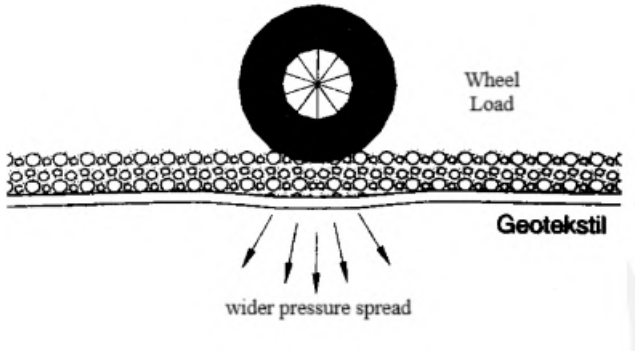


**Figure 3. 10 Working Mechanism of Geotextile on Field**

### 3.5.3 Slope Stability Analysis Using Geotextile

Slope stability analysis with reinforcement consist of two stability analysis, internal and external stability analysis. External stability consists of stability towards shears, rolls, eccentricity, and soil bearing capacity. While internal stability consists of stability towards internal forces that is calculated towards the length of geotextile (overlapping) and effective geotextile length. Each type of analysis will be explained below.

1. Internal stability

   Horizontal stress of soil is caused by the stress of the soil itself and the stress due to the load acting on the soil.

   The formula of coefficient of active soil can be seen in Equation 3.12.

$$\text{Ka} = \tan^2\left(45^o \frac{\varphi}{2}\right) \quad (3.12)$$

   Where:

   $Ka$ = coefficient of active soil

   $\varphi$ = shear angle ($^o$)

   Then, the Equation of horizontal stress of soil can be seen in Equation 3.13.

$$\sigma hc = \text{q. Ka} + \text{Ka . Hi.}\gamma \quad (3.13)$$

   Description:

   $\sigma hc$ = horizontal stress of soil (kN/m$^2$)

   $q$ = uniform load (kN/m)

   $Hi$ = height of observed land referring to soil surface (m)

   $\gamma$ = unit weight of soil (kN/m$^2$)

To find the vertical distance between geotextile (Sv) can be seen in the Equation 3.14.

$$Sv = \left(\frac{Tall}{\sigma hc.\ SF}\right) \quad (3.14)$$

Where:

$S_v$ = thickness of reinforcement layer (m)

$T_{all}$ = allowable tensile strength of reinforcement material (kN/m$^2$)

SF = safety factor

Analyzing the length of geotextile and failure body using angle of failure $\left(45° \frac{\varphi}{2}\right)$, can be seen in fgure 3.11.

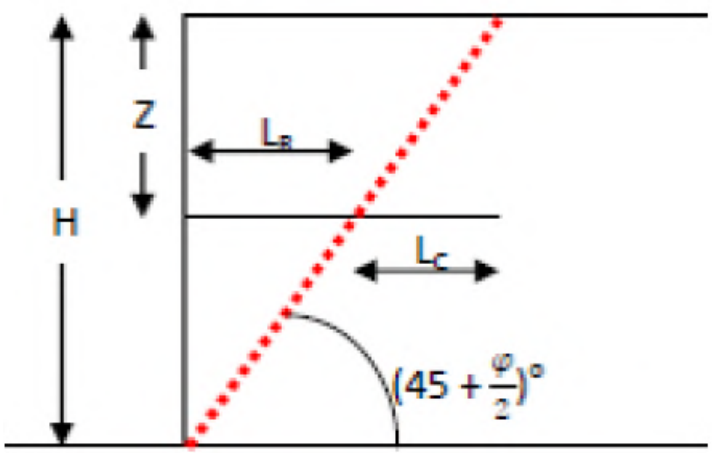


**Figure 3. 11 Failure Body and Length of Geotextile**
(Source: Suryolelono, 1993)

The largest length of geotextile in each zone is obtained from the calculation of the geotextile length (L) which corresponds to the results of the calculation of the geotextile vertical distance (Sv). The Equation of vertical soil stress can be seen in Equation 3.15.

$$\sigma v = \gamma . \text{Hi} \quad (3.15)$$

Where:

$\sigma_v$ = vertical soil stress

$\gamma$ = unit weight of soil (kN/m$^2$)

$H_i$ = height of observed land referring to soil surface (m)

For the length of geotextile in failure area, using the Equation 3.16.

$$L_R = \left( \frac{H - Zi}{\tan (45 + {}^{\varphi}/_{2})} \right) \quad (3.16)$$

Description:

$L_R$ = length of geotextile on active failure area (m)

H = height of soil embankment (m)

$Z_i$ = height of observed land referring to soil surface (m)

$\varphi$ = internal shear angle ($^o$)

For the calculation of the length of geotextile as an anchor, using the Equation 3.17.

$$L_c = \frac{1}{\beta} \frac{Tall}{(c + \sigma v . \tan \varphi)} \quad (3.17)$$

Description:

$L_c$ = length of geotextile as an anchor (m)

$T_{all}$ = allowable tensile strength of reinforcement material (kN/m$^2$)

$\beta$ = coefficient of soil interface to geotextile (used 0,67)

c = cohession (kN/m$^2$)

$\varphi$ = internal shear angle ($^o$)

The total length of geotextile can be calculate using Equation 3.18.

$$L_{tot} = L_R + L_c \quad (3.18)$$

Where:

$L_R$ = length of geotextile on active failure area (m)

$L_c$ = length of geotextile as an anchor (m)

For the length of geotextile overlapping (Lo) can be calculate using Equation 3.19.

$$L_o = \frac{1}{\beta} \frac{Tall}{4(c + \sigma v . \tan \varphi)} \geq 1 \text{ m} \quad (3.19)$$

Description:

$L_o$ = length of geotextile as an anchor (m)

$T_{all}$ = allowable tensile strength of reinforcement material (kN/m$^2$)

$\beta$ = coefficient of soil interface to geotextile (used 0,67)

c = cohession (kN/m$^2$)

$\varphi$ = internal shear angle ($^o$)

2. External stability

The calculation of external stability is used to examine three types of stability. they are.

a. Stability toward rolling

The equation of stability towards rolling can ben seen in Equation 3.20.

$$SF = \frac{L^2 . (\frac{1}{2} . q . \frac{1}{2} . \gamma . H)}{\frac{1}{2} . q . ka . H^2 . \gamma - c\sqrt{ka . H^2}} \quad (3.20)$$

Where:

SF = active soil coefficient

L = geotextile length (m)

H = soil layer height (m)

c = cohession (kN/m$^2$)

γ = unit weight of soil (kN/m$^3$)

q = load above soil (kN/m)

b. Stability toward shear

1) Resisting force

The Equation of resisting force can be seen in Equation 3.21.

$$F = \left[Cg + \frac{Wtotal}{lg} . tan\delta\right] lg \quad (3.21)$$

Where:

F = resisting force (kN)

$C_g$ = viscosity between geotextile and foundation subgrade = $\frac{2}{3}$c

$W_{total}$ = total of passive force (kN)

$\delta$ = $\frac{2}{3}\varphi$ (friction angle of foundation subgrade)

$L_g$ = length of lowest geotextile (m)

2) Driving force

The Equation of driving force can be seen in Equation 3.22.

$$F = Ea + Eq \quad (3.22)$$

Where:

E = driving force (kN)

$E_a$ = active force due to soil (kN)

$E_q$ = active force due to load (kN)

The Equation of stability toward shear can be seen in Equation 3.23.

$$SF = \frac{FI}{E} > 1{,}5 \quad (3.23)$$

Where:

FI = resisting force (kN)

E = driving force (kN)

c. Stability toward soil bearing capacity

Calculation of stability toward bearing capacity is based on the load acting above.

1) Allowable soil bearing capacity

The Equation of allowable soil bearing capacity can be seen in Equation 3.24.

$$\sigma_{ult} = c.Nc + q.Nq + 0{,}5.\gamma.L.N\gamma \quad (3.24)$$

Description:

$\sigma_{ult}$ = allowable soil bearing capacity ($kN/m^2$)

c = soil cohession ($kN/m^2$)

$N_c$, $N_q$, $N\gamma$ = Terzaghi bearing capacity factor

$\gamma$ = unit weight of soil ($kN/m^3$)

L = length of geotextile (m)

2) Bearing capacity of soil occurs

The Equation of soil bearing capacity occurs can be seen in Equation 3.25.

$$\sigma_{occurs} = H.\gamma. + q \quad (3.25)$$

Where:

$\sigma_{occurs}$ = bearing capacity ($kN/m^2$)

H = height of embankment (m)

$\gamma$ = unit weight of soil ($kN/m^3$)

q = load above soil (kN/m)

So, the calculation of stability toward soil bearing capacity can use the Equation 3.26.

$$SF = \frac{\sigma ult}{\sigma occurs} > 1{,}5 \quad (3.26)$$

Where:

SF = safety factor

$\sigma_{ult}$ = allowable soil bearing capacity ($kN/m^2$)

$\sigma_{occurs}$ = bearing capacity ($kN/m^2$)

### 3.6 Settlement

Additional loading on the certain soil layer will result in the addition of stress on soil particle, therefore, soil will experience settlement. Soil particles deformation and the discharge of pore water through soil pores become one of the factors of the settlement occurrence. The cause of massive settlement is consolidation settlement during loading of the soil.

#### 3.6.1 Consolidation Settlement

Additional loading on top of a saturated soil layer will cause increasing pore water pressure and resulting in the water to forcefully finding way out from the soil pores, therefore the volume will decrease. The amount of consolidation settlement will depend on the soil geologic. Soils on certain depth will experience pre-consolidation effective stress, which is the biggest effective stress of soil. This stress can be smaller or equal in amount with current effective overburden. While normally consolidates is the state where effective overburden stress on the maximum level (Das, 1995). The formula for normally consolidated state can be seen on Equation 3.27.

$$S_c = H \frac{C_c}{1 + e_o} \log \frac{P_o + \Delta p}{P_o} \quad (3.27)$$

With,

$S_c$ = primary settlement (m)

$\Delta_p$ = change of vertical stress ($kN/m^2$)

$c_c$ = soil compression index

$e_o$ = pore number

H = soil layer thickness (m)

$P_o$ = effective overburden stress ($kN/m^2$)

### 3.6.2 Settlement Calculation Parameter

Some additional parameter is needed to calculate how big the settlement occurs on certain soil layer. Those parameters are effective overburden stress ($P_o$), soil compression ($C_c$), and soil stress distribution ( $\Delta p$ ). The explanation of the parameters can be seen below.

1. Effective Overburden Stress ($P_o$)

   This parameter is effective vertical stress of existing soil added with load or soil layer above the reviewed soil (Satindra, 2018). The formula for effective overburden can be seen on Equation 3.28.

   $$P_o = \gamma' x\, H \qquad (3.28)$$

   With,

   $P_o$ = effective overburden stress

   $\gamma'$ = soil layer thickness

   H = effective soil volume weight

2. Soil Compression Index ($C_c$)

   Based on Terzaghi and Peck (1967), to obtain soil compression index on undisturbed clay soil, method used is empirical equation (Barimbing, 2017). The calculation of this index can be done by using formula in Equation 3.29.

   $$C_c = 0.009(LL - 10) \qquad (3.29)$$

   LL symbol above means liquid limit. Equation 3.35 above is applied for inorganic clay soil calculation that has low to medium sensitivity with 30% of error rate. If the sensitivity exceeds 4 on the equation above, it is suggested not to be used. For clay soil, remolded is suggested as mentioned on Equation 3.30 and figure of relationship of soil compression index graph ($C_c$) that can be seen on Figure 3.12.

   $$C_c = 0.007(LL - 100) \qquad (3.30)$$

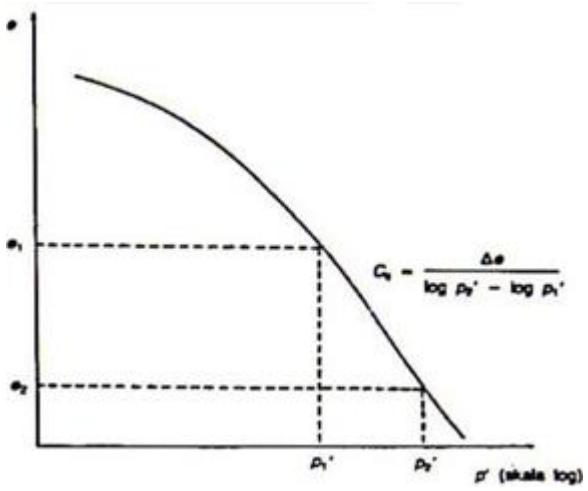

**Figure 3. 12 Soil Compression Index ($C_c$)**

(Source: Hardiyatmo, 2002)

This $C_c$ value is taken based on the soil behaviors on certain location determined in Azzous (1976) that can be seen on Equation 3.31 to 3.34.

$C_c = 0.0115$ wn (for organic soil, peat) (3.31)

$C_c = 0.0046(LL - 9)$ (for Brasilia clay) (3.32)

$C_c = 0.01$ wn (for Chicago clay) (3.33)

$C_c = 0.208\ e_o + 0.0083$ (for Chicago clay) (3.34)

The wn notation means original water content and pore number of the existing soil (%)

3. Soil Stress Distribution ($\Delta p$)

   This parameter occurs because of loading on top of the soil viewed by the centre point of every soil layer. The equation for soil stress distribution can be seen on Equation 3.35.

   $\Delta p = q\ x\ I\ x\ H$ (3.35)

   The equation to find "q" value can be seen on Equation 3.36.

   $q = \gamma_{embankment}\ x\ H$ (3.36)

With,

$\Delta_P$ = vertical stress change

$\gamma_{embankment}$ = embankment soil volume weight

H = soil layer thickness

$q$ = embankment weight

$I$ = influential factor

To determine the influential factor can be done to see the Figure 3.13.

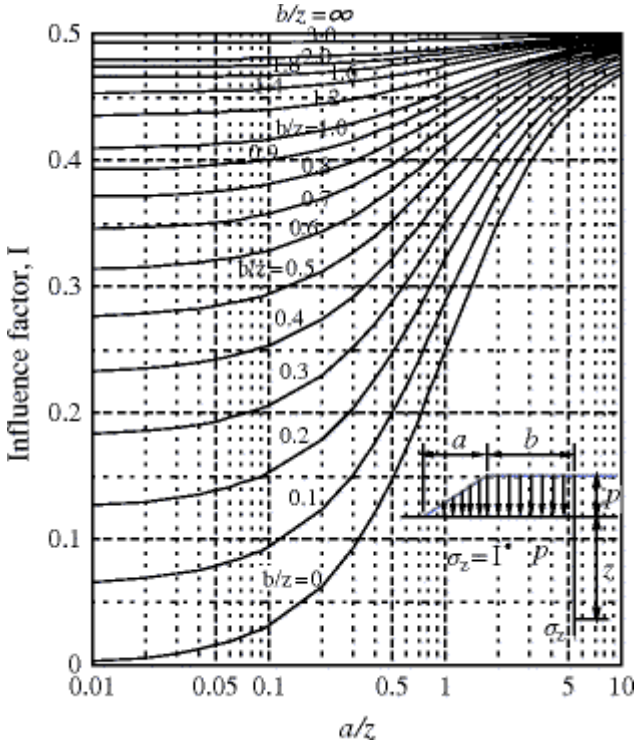


**Figure 3. 13 Influential Factor (Osterberg,1957)**
(Source: Hardiyatmo, 2002)

## 3.7 PLAXIS

PLAXIS is a computer program for analysis in the geotechnical field. in the analysis process of stability and deformation in the PLAXIS program using the finite element method. PLAXIS program also can be used for displacement analysis, stresses that occur in the soil, slope safety factor, and consolidation. Using the PLAXIS program, the site conditions can be modelled in plane strain as well as asymmetrically. The various site conditions simulated in the PLAXIS program are

specifically aimed at applying and implementing the site implementation steps through the working stages of the program.

The steps in the analysis using the PLAXIS programs:

1. PLAXIS input

   The modelling using the PLAXIS program is adjusted to the conditions in the field. The PLAXIS input is creating and adjusting the geometry, soil paramater, and load model. The PLAXIS input be seen in the Figure 3.14 below.

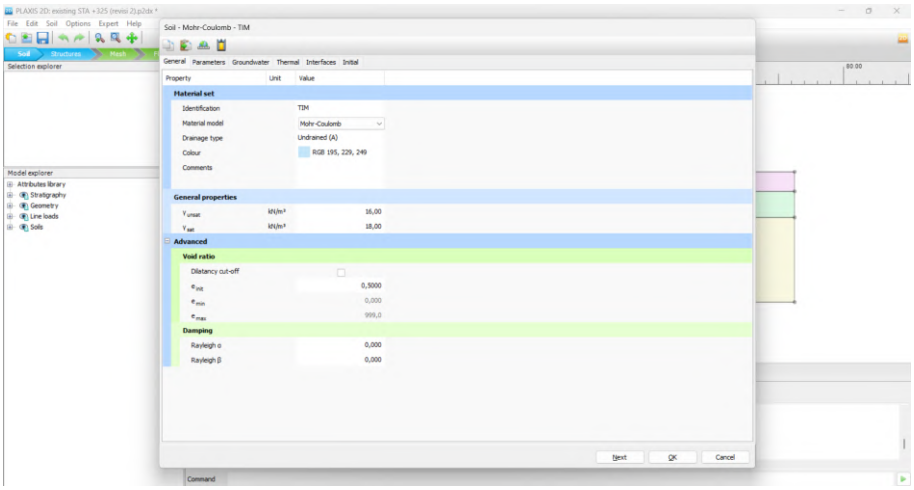


**Figure 3. 14 PLAXIS Input**

2. PLAXIS calculation

   PLAXIS Calculation is performed after the input process is completed. The calculation step can be performed by selecting the calculate toolbar at the end of input or by selecting calculation program in the start menu. The PLAXIS calculation can be seen in the Figure 3.15 below.

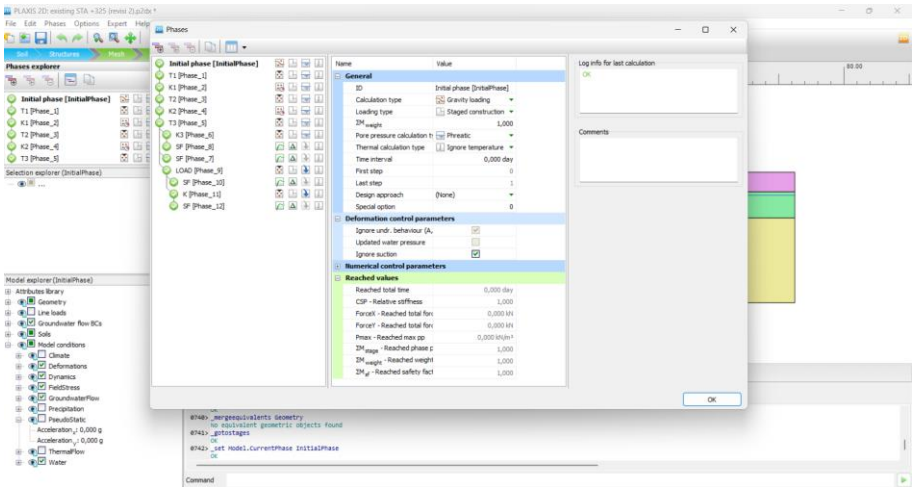

**Figure 3. 15 PLAXIS Calculation**

3. PLAXIS output

   PLAXIS output can be done by selecting the PLAXIS output toolbar, or from the start menu. The output phase results can be displayed in the form of numbers, images, and curves. The PLAXIS output can be seen in Figure 3.16 below.

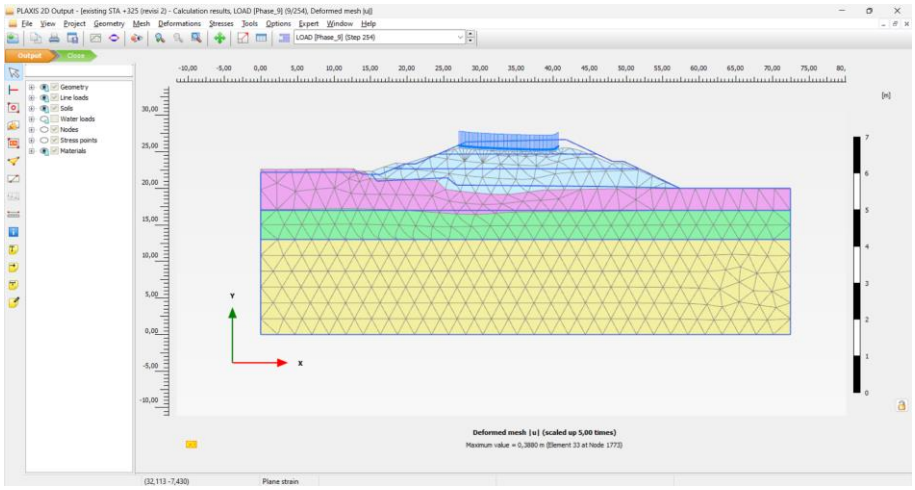

**Figure 3. 16 PLAXIS Calculation**

4. PLAXIS curve

   The PLAXIS Curves Program can be used to illustrate the load relationship curves, stress-strain diagrams of locations. The PLAXIS curve can be seen in the Figure 3.17 below.

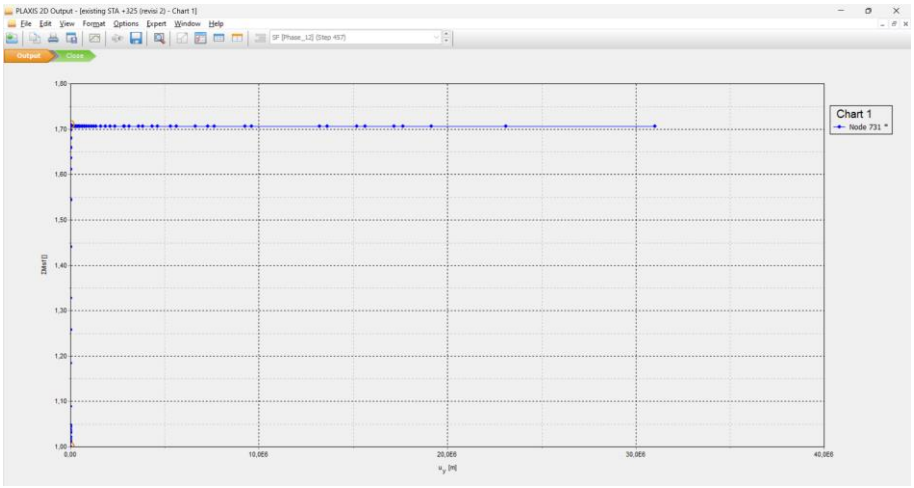


**Figure 3. 17 PLAXIS Curve**

# CHAPTER IV
# METHODOLOGY

## 4.1 Research Method

The research object to be carried out is an embankment soil located in the Tawang-Ngalang segment IV road and bridge construction project in the area Nglegi, Kapanewon Patuk, Gunungkidul. The research that will be carried out is an analysis of the slope stability of the geotextile reinforcement on that project. This research is using quantitative and modelling methods for the analysis process. The research will investigate the occurrence of certain conditions through quantitative data collection and data analysis using a technical approach.

## 4.2 Research Location

The location of the research object is in the Tawang-Ngalang road and brigde construction project which is in Nglegi, Kapanewon Patuk, Gunungkidul. The location of the research can be seen in Figure 4.1.

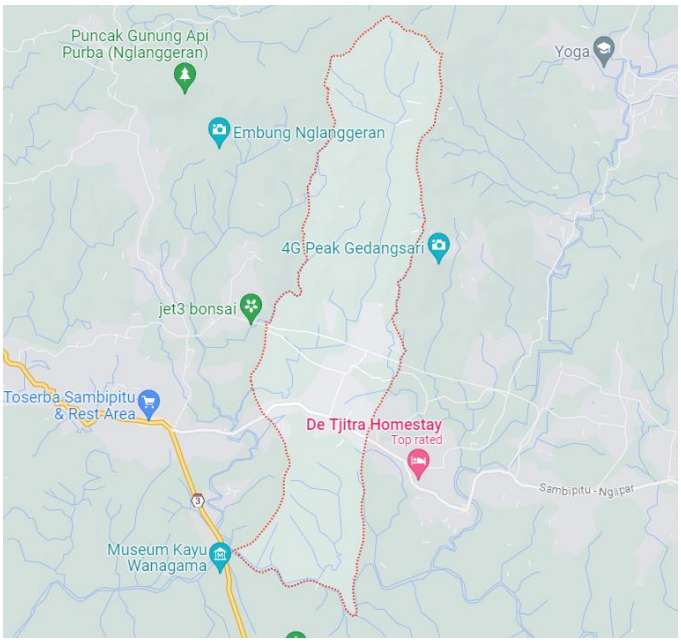


**Figure 4. 1 Research Location**

(Source: Google Earth, 2023)

## 4.3 Data Collection

The data used in this research is secondary data. The data is obtained from PT Geomine Bara Studio that have collected data. The collection data used can be seen below:

1. Soil Investigation Data

   This data includes standard penetration test method (SPT) data with ground water elevation of 3.5 m, soil profile, and laboratory data of STA 5+325 of Tawang-Ngalang Segment IV Road and Bridge Project. The data can be seen in Table 4.1.

**Table 4. 1 N-SPT Result**

| Depth (m) | N-SPT | Lithology |
|---|---|---|
| 0 | 0 | Clayey sands, Reddish brown |
| 1 | 6 | |
| 2 | 12 | |
| 3 | 12 | |
| 4 | 12 | Sandy clay, medium to high plasticity, medium consistency |
| 5 | 36 | |
| 6 | 60 | |
| 7 | 60 | |
| 8 | 60 | Andesitic breccia and massive strong rock |
| 9 | 60 | |
| 10 | 60 | |
| 11 | 60 | |
| 12 | 60 | |
| 13 | 60 | |
| 14 | 60 | |
| 15 | 60 | |
| 16 | 60 | |
| 17 | 60 | |
| 18 | 60 | |
| 19 | 60 | |
| 20 | 60 | |

(Source: PT Geomine Bara Studio)

2. Detailed Engineering Drawing

   In this research used the drawing to find the existing elevation, and the contour of the area. The existing elevation can be seen in Figure 4.1 below.

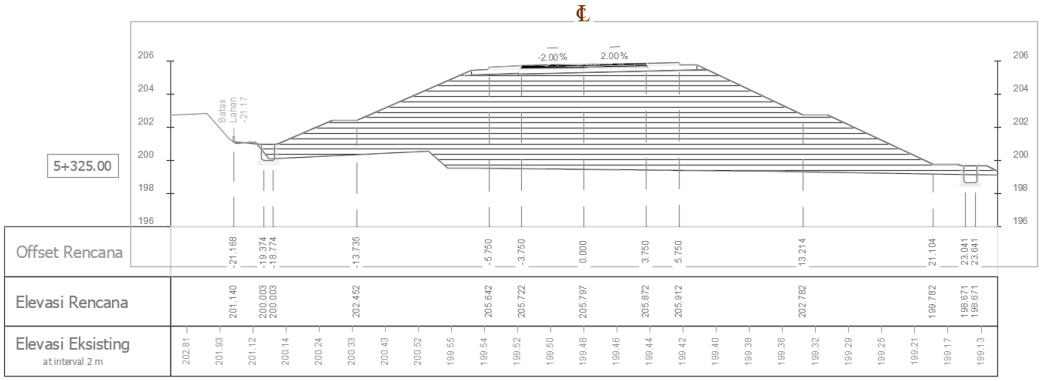


**Figure 4. 2 Existing Elevation**
(Source: PT Geomine Bara Studio)

## 4.4 Research Procedure

The stages that must be completed for the research can be seen below.

1. Identifying the problem used in the final project and creating the problem formulation.
2. Reviewing the literature that related to the problem to gather information regarding the research from some sources, including books, academic journals, and other research.
3. Collecting the data includes soil investigation data (field data and laboratory data), and Detailed Engineering Drawing (DED) are used to analysis, calculation, and design.
4. Modelling the original slope and designing slope reinforcement.
5. Calculating the safety factor (SF) using the PLAXIS Program and using the Fellenius method.
6. Analysing the result from the calculation and the modelling.
7. Concluding the result of research and suggesting that can be improved for the other research.

## 4.5 Variation of Models

The model variations of the embankment is made on the PLAXIS v20.

1. Existing Embankment

   Embankment slopes in the original condition have a various variety of materials. This is because the embankment material used selected material to fill the topographic conditions that are not suitable for the construction site.

2. Non-reinforced Embankment with alternative internal angle

   In this research the author will use the alternative internal angle as the basic parameter for the embankment stability. The alternative that will be used of 20°. Later, this height variations will be used for the bottom line to discover the safest and most effective embankment model for the current research location.

3. Reinforced Embankment

   After obtaining the analysis result for the existing condition, designing geotextile reinforcement will be conducted to reach each safe state according to the safety factor required on Table 3.7 and Table 3.8.

4. Reinforced Embankment with alternative internal angle

   As for this stage, the analysis process will be conducted in the same way as the analysis stability of embankment in existing condition, but the internal angle will differ as has been mentioned on point 2.

As for the variation of loading used for the stability analysis of embankment can be seen below.

1. Internal Load

   The variation of the loading is used in vertical and horizontal direction. The internal load that acts on the embankment are the soil embankment load, pore water pressure, and the structural load. So, that reinforcement is needed to prevent the occurrence of collapse.

2. Traffic Load

   Based on “Departemen Pekerjaan Umum tahun 2009 tentang Persyaratan Teknis Jalan dan Kriteria Perencanaan Teknis Jalan”, the traffic load is added

to the entire width of the road surface and is determined based on the road class. So, it can be determined the traffic load is 15 kN/$m^2$.

Other than those two, dynamic loading will also be applied to the models of embankment on PLAXIS V20. they are:

1. Without Earthquake

   Without earthquake load soil stability analysis refers to the assessment of soil stability under normal conditions, without taking into consideration the effects of earthquake activity. This analysis is important in geotechnical engineering to evaluate the stability and safety of structures and infrastructure in non-seismic scenarios. Factors such as soil composition, groundwater level, and external loads are usually considered in this analysis to ensure soil stability and prevent slope failure or soil movement.

2. With earthquake

   The analysis of slope stability, it is very important to consider the effect of earthquake loads on the factor of safety. The effect of earthquake loads on soil stability is very significant. Analysis of soil stability under earthquake loading has a particularly important effect in geotechnical engineering. Based on the SNI 8460:2017, earthquake plan for excavation and embankment slopes is determined with a probability of exceeding the magnitude during the 50-year plan life of 2% or equivalent to a return period of 500 years with reference to earthquake maps The earthquake load used is the seismic load due to earthquake, which is in accordance with the location of the Gunungkidul is 0.3-0.4 g according to the earthquake zoning map.

### 4.6 Research Flowchart

The research flowchart shows the steps of the research methodology to be carried out visually. The research flowchart helps the researcher visualize and plan the research process systematically so that it can be followed clearly and structurally. The research stages are illustrated sequentially with arrows and symbols. The flowchart of research can be seen below.

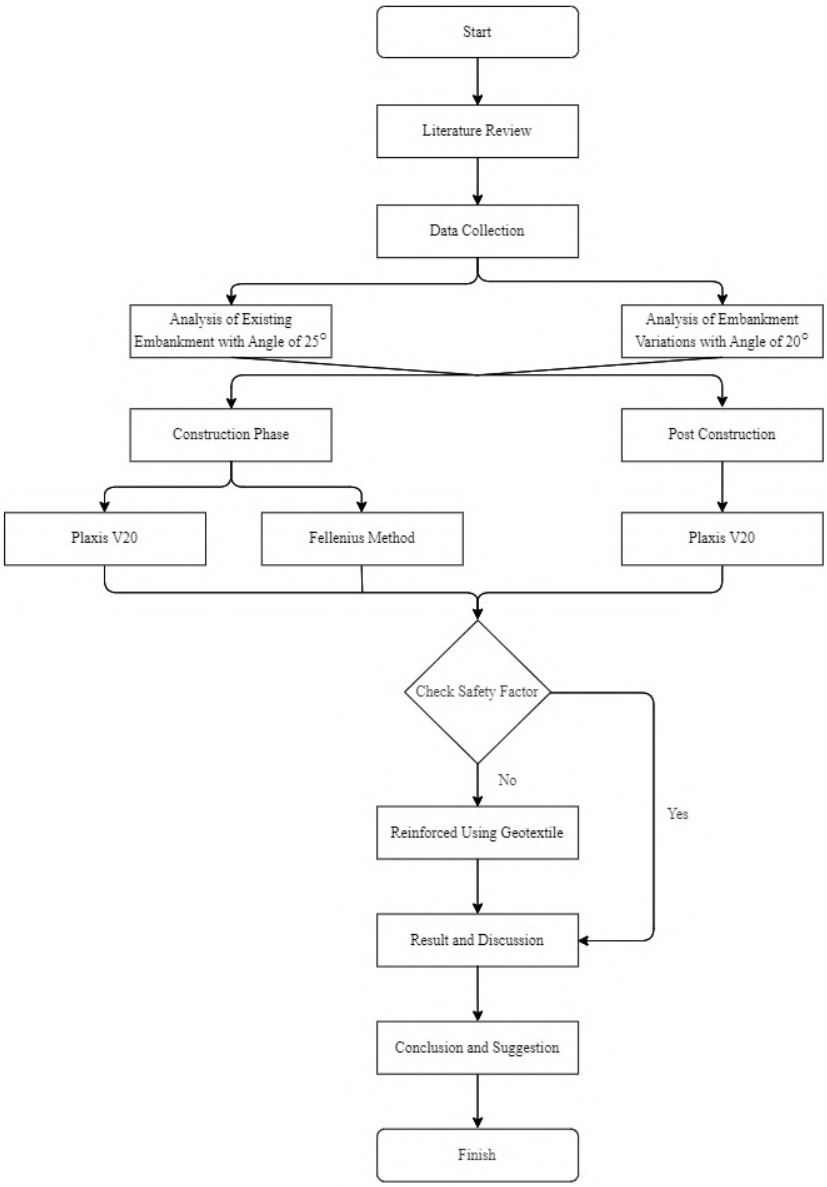


**Figure 4. 3 The Flowchart of Research**

# CHAPTER V
# ANALYSIS AND RESULT

## 5.1 Embankment Stability

The stability of slope is determined by the factor of safety. This value will be obtained by both static and finite element method of PLAXIS 2D V20. The analysis will use existing condition of embankment slope without reinforcement. The analysis will be conducted using data on STA 5 + 325 on Tawang-Ngalang Segment IV Road and Bridge Construction. The existing embankment slope is 6,75 m with internal angle of 25°. Then geotextile will be used as the reinforcement option for the slope to achieve the 1.5 factor of safety. The longitudinal cut of the analysis location can be seen on Figure 4.1.

The data used in this research is secondary data obtained from boring result, laboratory data, and detailed engineering drawings from PT. Geomine Bara Studio and PT. Aneka Dharma Persada.

## 5.2 Parameter data

The analysis of embankment stability in this research requires the parameter data such as soil investigation data, various load types, and geotextile parameter.

### 5.2.1 Soil parameter

Soil parameter data from the field is needed to analysis of road embankment stability. Soil parameter in this research used the field and laboratory data from PT. Geomine Bara Studio. The soil parameter data can be seen on Table 5.1.

**Table 5. 1 Soil Parameter Data**

| Parameter | Unit | Embankment | Layer 1 | Layer 2 | Layer 3 |
|---|---|---|---|---|---|
| Model | - | Mohr Coulomb | | | Hoek-brown |
| Type | - | Undrained | Drained | Drained | Drained |
| H | m | 6.75 | 3 | 4 | 13 |
| $\gamma_{sat}$ | kN/m³ | 16.52 | 16.20 | 18.15 | 22.89 |
| $\gamma_{unsat}$ | kN/m³ | 12.49 | 15.51 | 13.31 | 22.26 |
| $\gamma_{w}$ | kN/m³ | 9.81 | 9.81 | 9.81 | 9.81 |

**Continuation Table 5.1 Soil Parameter Data**

| | | | | | |
|---|---|---|---|---|---|
| c | kN/m² | 10.79 | 14.72 | 19.62 | |
| φ | ° | 14.50 | 15.41 | 5.51 | |
| v | | 0.26 | 0.27 | 0.28 | 0.30 |
| $K_x$ | m/day | 0.00005 | 0.00031 | 0.00002 | |
| $K_y$ | m/day | 0.00005 | 0.00031 | 0.00002 | |
| $E_{ref}$ | kN/m² | 3605 | 3723 | 37784 | 236180 |

(Source: PT. Geomine Bara Studio)

### 5.2.2 Load parameter

The working loads on embankment slope are pavement load, traffic load and earthquake load.

1. Pavement and traffic load

   Based on the secondary data, the pavement load is 10 kN/m$^2$. While, the traffic load used is obtained from Departemen Pekerjaan Umum (2009), can be seen on Table 3.9.

2. Earthquake data

   Earthquake parameters can vary into different kind of data. But for the earthquake data used on PLAXIS as the Finite Element Method is represented by the value of Peak Ground Acceleration (PGA). The area of Gunungkidul district has Peak Ground Acceleration (PGA) between 0.3 – 0.4 g, under the type of dynamic earthquake load.

   The earthquake analysis will be conducted using data from Earthquake zoning map. The earthquake data that is in accordance with Gunungkidul earthquake data is earthquake data of Victoria, Mexico, in 1978 taken from www.strongmotioncenter.org. They both has the same PGA of 0.367, with time interval of 2.6 seconds under the assumption that at that exact time, the peak ground acceleration has passed.

   Based on SNI 8460:2017 for analysis using PLAXIS V20 based on Finite Element Method, the earthquake value is represented using horizontal seismic coefficient or Kh. This value is taken from half of PGA value of the area which

is 0.1835 g. The graph of relationship between acceleration and earthquake time can be seen on Figure 5.1.

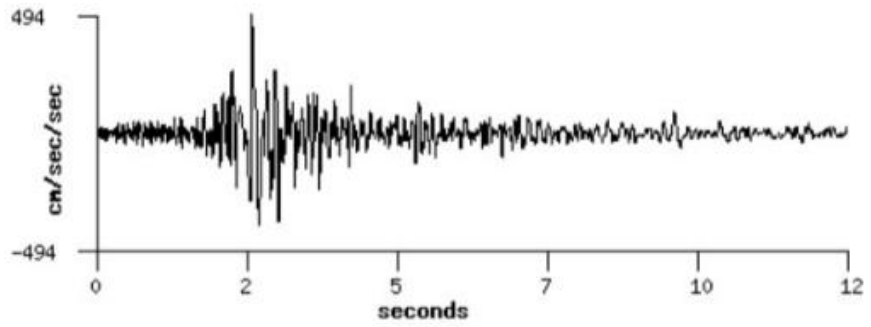


**Figure 5. 1 Graph of Relationship between Acceleration and Earthquake Time**
(Source: Earthquake data of Victoria, Mexico in 1978)

### 5.2.3 Geotextile data

Geotextile UW-250 is a geotextile reinforcement that will be used in this research. It is produced by PT. Tekindo Geosistem with allowable tensile strength and strain of 52 kN/m$^2$ and 20% obtained from the production brochure. Those values then will be input into PLAXIS V20 that can be seen on Table 5.2.

**Table 5. 2 Geotextile Data**

| Parameter | Notation | Value | Unit |
|---|---|---|---|
| Tensile Strength | T | 52 | kN/m |
| Strain | Ɛ | 20 | % |
| Normal Stiffness | EA | 260 | kN/m |

(Source: PT. Teknindo Geosistem Unggul)

For the calculation of geotextile reinforcement, woven geotextile will be used as additional reinforcement for soil embankment, using the data on Table 5.2. Then those value will be calculated first into a normal stiffness (*EA*) value that will be calculated below.

$$EA = \frac{Fg}{\Delta l / l}$$

$$= \frac{52}{0.2}$$

$$= 260\ kN/m$$

## 5.3 Analysis of Existing Embankment Stability Without Reinforcement

The analysis of Embankment slope using PLAXIS V20. The modelling for the embankment construction phase using the soil embankment based on the field. The embankment that will be used is STA 5+325 of Tawang-Ngalang Segment IV Road. The width of the existing embankment is 42.3 meters, the height is 6.75 meters, and the angle of the slope is 25º. For the embankment variation with an angle of 20º, the width of embankment is 47.88 meters, and the height is 6.75 meters. The cross section existing of STA 5+325 of Tawang-Ngalang Segment IV Road and the embankment variation with angle of 20º can be seen in Figure 5.2 and Figure 5.3.

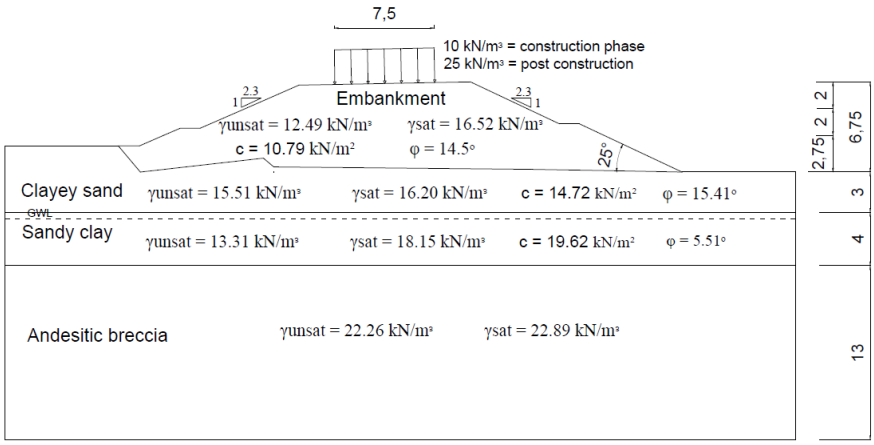


**Figure 5. 2 Cross Section of STA 5+325 Of Tawang-Ngalang Segment IV Road with Angle Of 25 º**

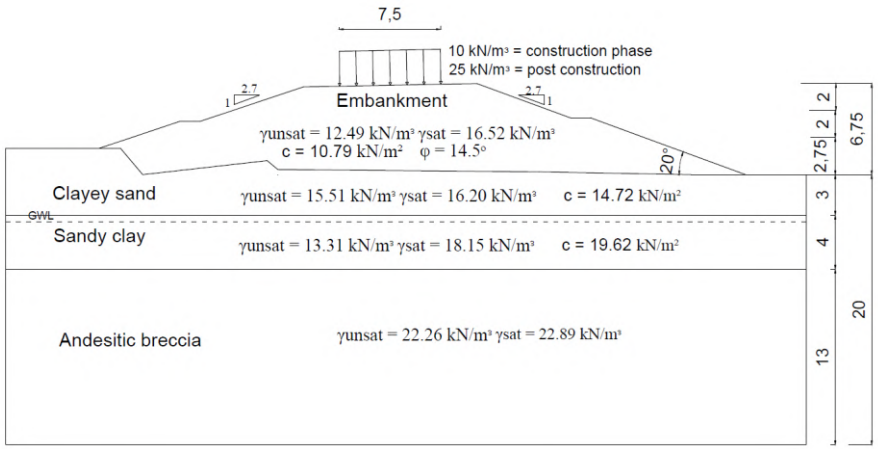


**Figure 5. 3 Cross Section of Embankment Variation with Angle Of 20º**

### 5.3.1 Analysis of Construction Phase Existing Embankment

The stability analysis of the existing embankment with internal slope angle of 25º is conducted in three phases. The first phase assumes that the embankment is completed to a height 2.75 meters, followed by an analysis of the embankment condition. The analysis is continued at height of 4.75 meters, and 6.75 meters, by adding pavement load of 10 kN/m. The stability of embankments with internal slope angle of 20º using the same analytical method applied to the existing embankment condition. Detailed calculations and results are presented in the appendix. The construction phase can be seen in the Figure 5.4.

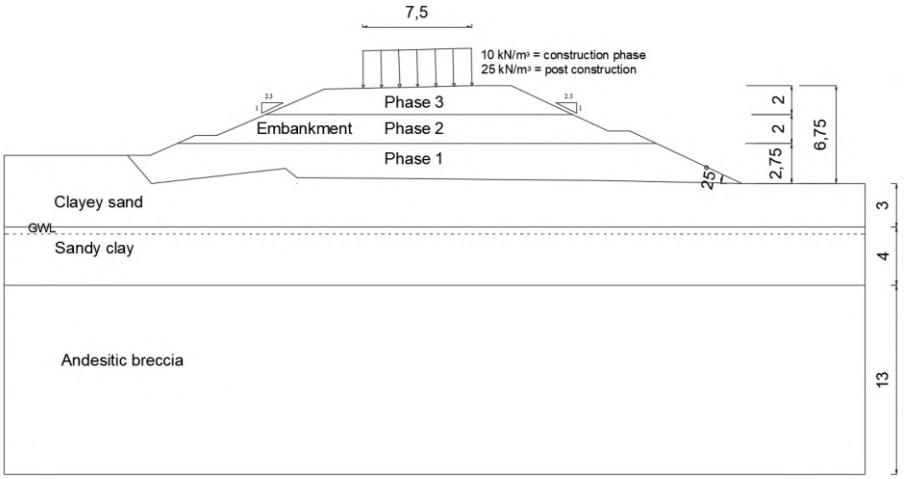


**Figure 5. 4 Construction Phase**

1. Embankment Phase 1

   The phase 1 of existing embankment with angle of 25º is done to the height of 2.75 m. In order to know the deformation occurring on the location due to the loads mentioned before, deformed mesh is necessary. Deformed Mesh of existing embankment phase 1 without reinforcement based on PLAXIS V20 analysis can be seen in Figure 5.5.

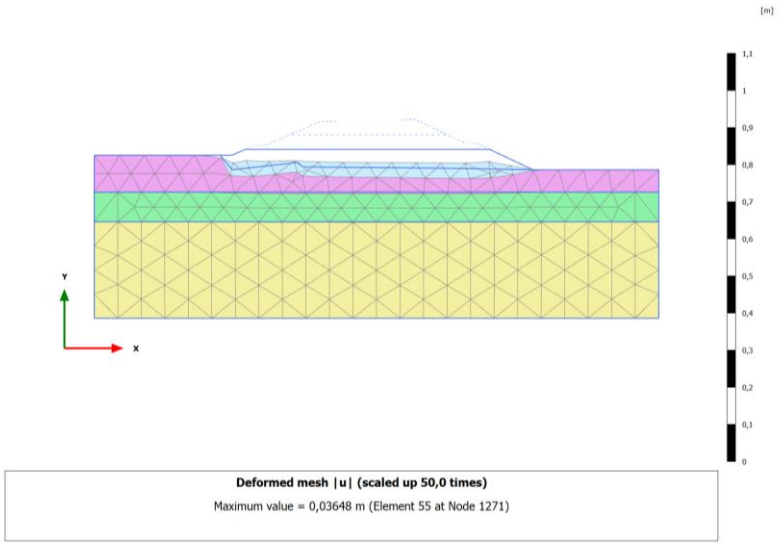


**Figure 5. 5 Deformed Mesh of Existing Embankment Phase 1 Without Reinforcement**

Displacement occurs on phase 1 of existing embankment with angle of 25º without reinforcement due to embankment load. Based on the indicator on PLAXIS V20, the bigger displacement shows redder colour. While smaller displacement indicated by the shade of blue. The displacement value of existing embankment phase 1 without reinforcement due to embankment load is 0.03648 m can be seen in Figure 5.6.

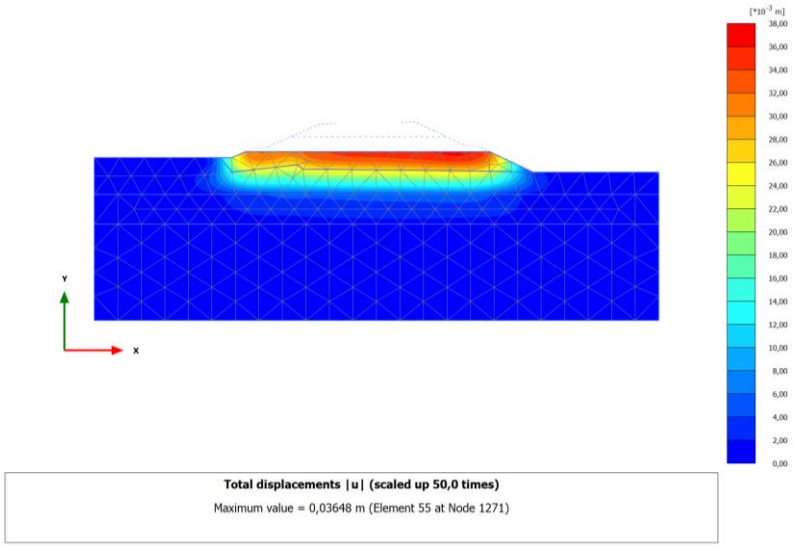


**Figure 5. 6 Displacement of Existing Embankment Phase 1 Without Reinforcement Due to Embankment Load**

The effective stress is used to calculate the factor of safety for embankment slope. Also, to identify the potentially failed slope area. The maximum amount effective stress of existing embankment phase 1 without reinforcement due to embankment load is 5.329 x $10^{-15}$ kN/$m^2$, can be seen in Figure 5.7.

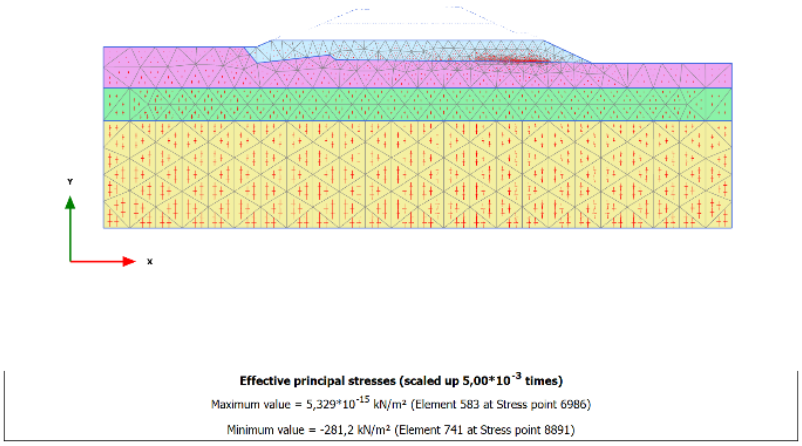


**Figure 5. 7 Effective Stress of Existing Embankment Phase 1 Without Reinforcement Due to Embankment Load**

Based on the PLAXIS V20 analysis, the type of the slope failure is rotation failure. The analysis result on PLAXIS V20 shows the factor of safety is 3.479. The stability analysis result show that the slope is in safe condition, with a factor of safety already meet the minimum requirement. Potential failure area on existing embankment phase 1 with angle of 25º without reinforcement due to embankment load can be seen in Figure 5.8.

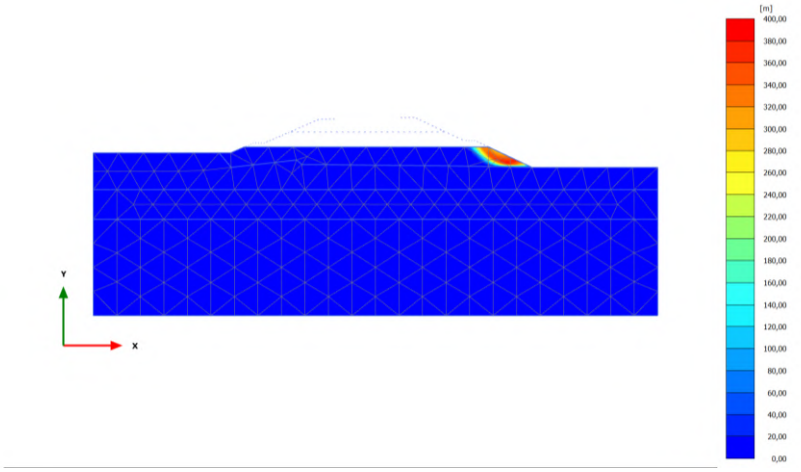


**Figure 5. 8 Potential Failure Area on Existing Embankment Phase 1 With Angle Of 25º Without Reinforcement Due To Embankment Load**

2. Embankment Phase 2

   The phase 2 of existing embankment with angle of 25º is done to the height of 4.75 m. In order to know the deformation occurring on the location due to the loads mentioned before, deformed mesh is necessary. Deformed Mesh existing embankment phase 2 without reinforcement based on PLAXIS V20 analysis can be seen in Figure 5.9.

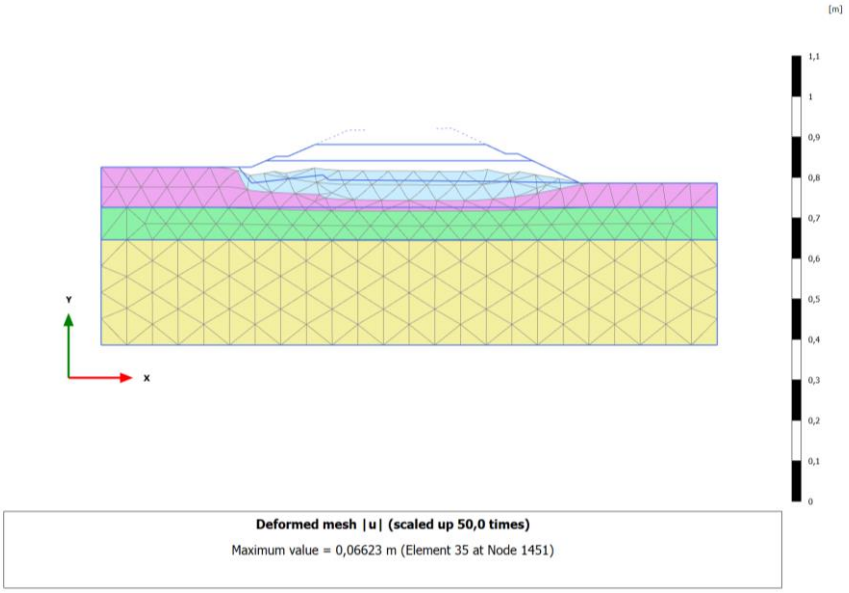


**Figure 5. 9 Deformed Mesh Existing Embankment Phase 2 Without Reinforcement Due to Embankment Load**

Displacement occurs on phase 2 of existing embankment with angle of 25º without reinforcement due to embankment load. Based on the indicator on PLAXIS V20, the bigger displacement shows redder colour. While smaller displacement indicated by the shade of blue. The displacement value of existing embankment phase 2 without reinforcement due to embankment load is 0.06623 m can be seen in Figure 5.10.

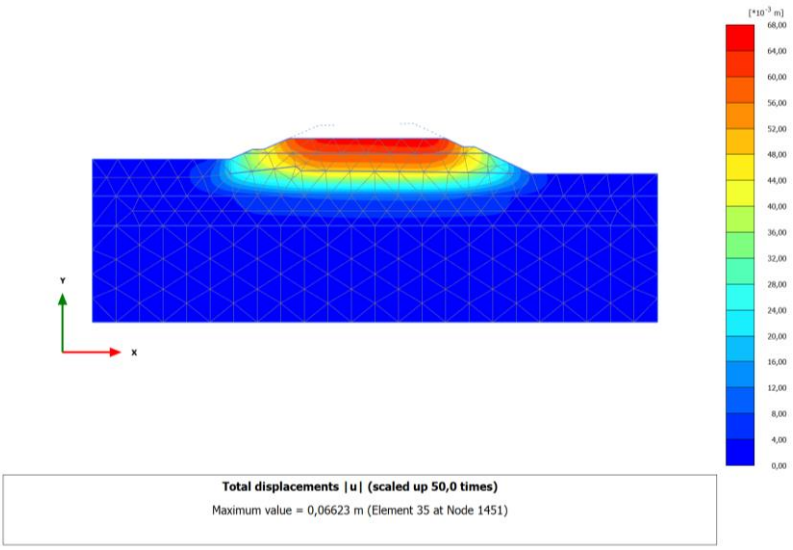


**Figure 5. 10 Displacement Value of Existing Embankment Phase 2 Without Reinforcement Due to Embankment Load**

The effective stress is used to calculate the factor of safety for embankment slope. Also, to identify the potentially failed slope area. The maximum amount effective stress of existing embankment phase 2 without reinforcement due to embankment load is 8.882 x $10^{-15}$ kN/$m^2$, can be seen in Figure 5.11.

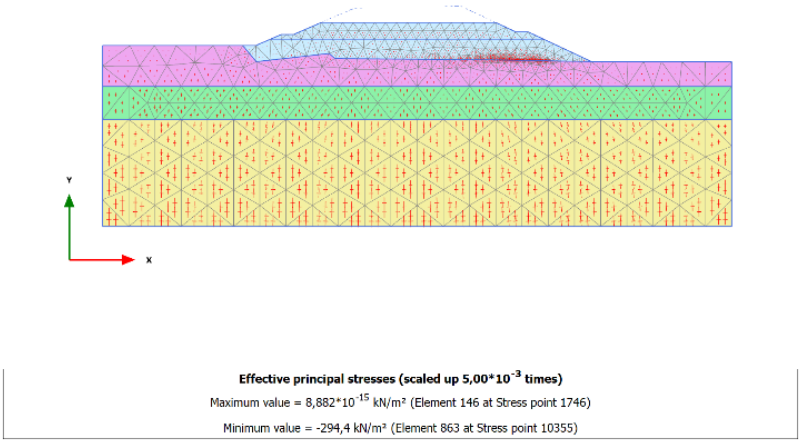


**Figure 5. 11 Effective Stress of Existing Embankment Phase 2 Without Reinforcement Due to Embankment Load**

Based on the PLAXIS V20 analysis, the type of the slope failure is rotation failure. The analysis result on PLAXIS V20 shows the factor of safety is 2.234. The stability analysis result show that the slope is in safe condition, with a factor of safety already meet the minimum requirement. Potential failure area on existing embankment phase 2 with angle of 25º without reinforcement due to embankment load can be seen in Figure 5.12.

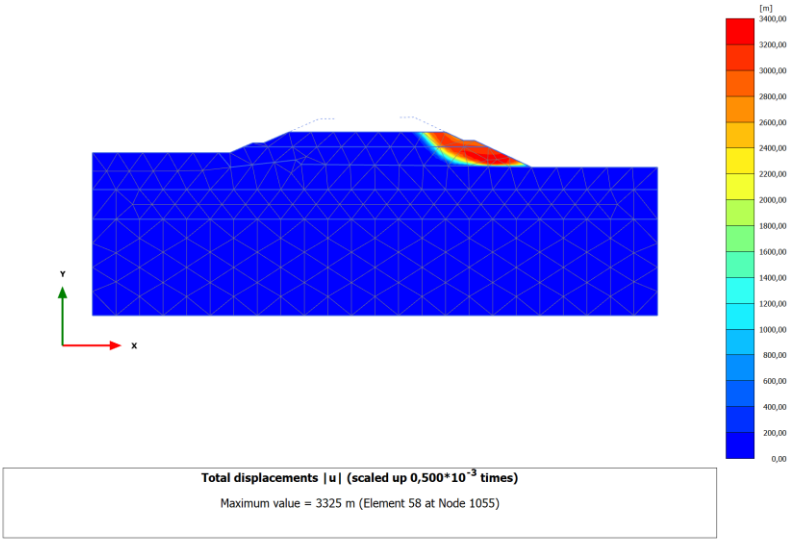


**Figure 5. 12 Potential Failure Area on Existing Embankment Phase 2 With Angle Of 25º Without Reinforcement Due to Embankment Load**

3. Embankment Phase 3

   The phase 3 of existing embankment with angle of 25º is done to the height of 6.75 m. The pavement load of 10 kN/m$^2$ and earthquake load is added to embankment phase 3 analysis. In order to know the deformation occurring on the location due to the loads mentioned before, deformed mesh is necessary. Therefore, the analysis result can't be shown on PLAXIS V20. Deformed Mesh for the existing embankment phase 3 with angle of 25º by adding pavement load, and existing embankment phase 3 with angle of 25º by adding pavement and earthquake loads without reinforcement based on PLAXIS V20 analysis can be seen on Figure 5.13 and Figure 5.14.

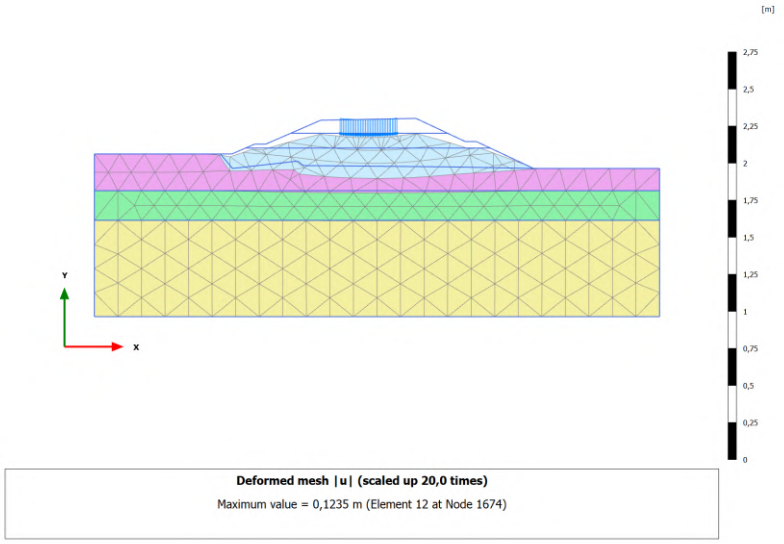


**Figure 5. 13 Deformed Mesh for Existing Embankment with Angle Of 25º By Adding Pavement Load Without Reinforcement**

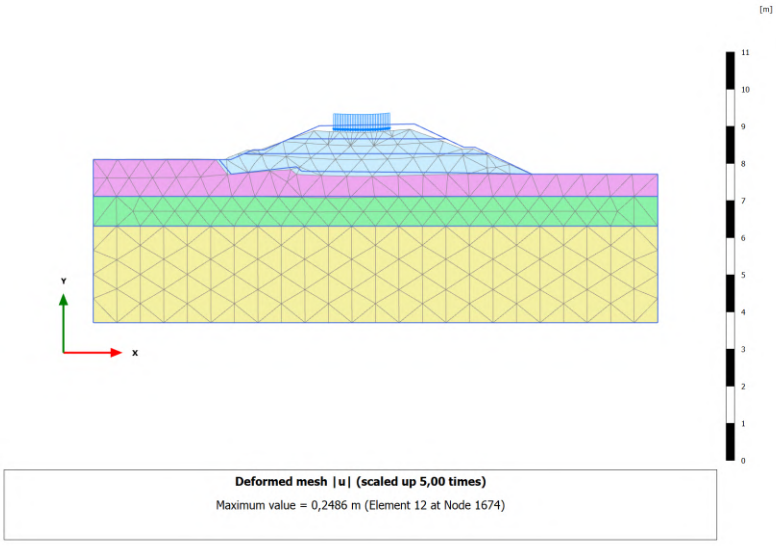


**Figure 5. 14 Deformed Mesh for Existing Embankment with Angle Of 25º By Adding Pavement and Earthquake Loads Without Reinforcement**

Displacement occurs on phase 3 of existing embankment with angle of 25º without reinforcement. Based on the indicator on PLAXIS V20, the bigger displacement shows redder colour. While smaller displacement indicated by the shade of blue. The displacement value of the existing embankment with angle of 25º by adding pavement load without reinforcement is 0.1235 m, while analysis result for existing embankment with angle of 25º by adding pavement

and earthquake loads on PLAXIS V20 is 0.2486 m. The displacement value of the existing embankment with angle of 25º by adding pavement load, and the existing embankment phase 3 with angle of 25º by adding pavement and earthquake loads without reinforcement can be seen on Figure 5.15 and Figure 5.16.

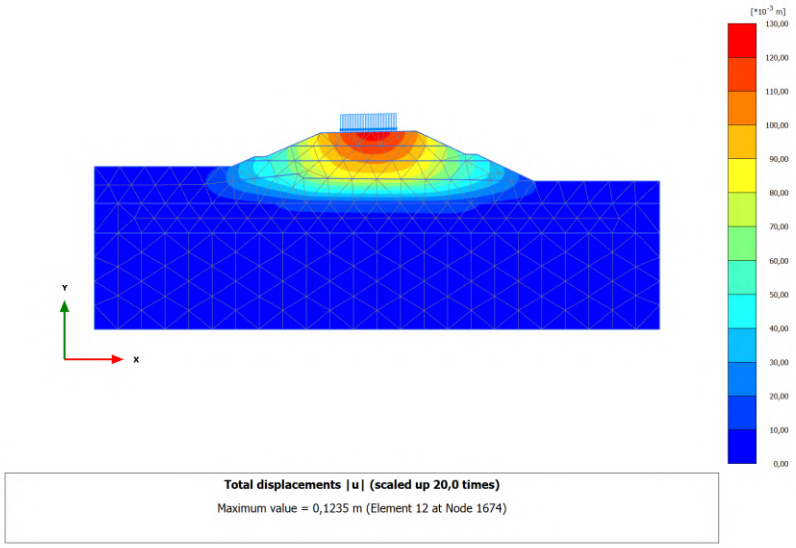


**Figure 5. 15 Displacement Value of Existing Embankment Phase 3 With Angle Of 25º By Adding Pavement Load Without Reinforcement**

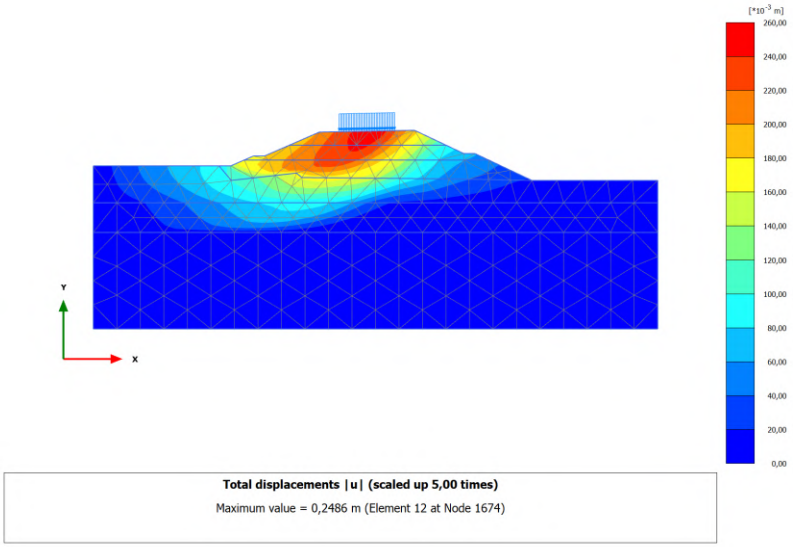


**Figure 5. 16 Displacement Value of Existing Embankment Phase 3 With Angle Of 25º By Adding Pavement and Earthquake Loads Without Reinforcement**

The effective stress is used to calculate the factor of safety for embankment slope. Also, to identify the potentially failed slope area. The maximum amount effective stress of existing embankment phase 3 with angle of 25º by adding pavement load without reinforcement is 0.1421 x $10^{-15}$ kN/$m^2$, while the analysis result for existing embankment phase 3 with angle of 25º by adding pavement and earthquake loads is 49.37 kN/$m^2$. The effective stress of existing embankment phase 3 with angle of 25º by adding pavement load, and the existing embankment phase 3 with angle of 25º by adding pavement and earthquake loads without reinforcement without reinforcement can be seen in Figure 5.17 and Figure 5.18.

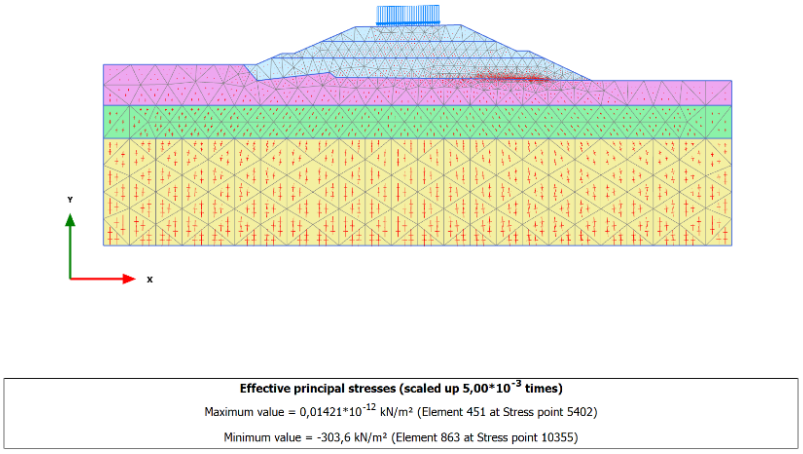


**Figure 5. 17 Effective Stress of Existing Embankment Phase 3 With Angle Of 25º By Adding Pavement Load Without Reinforcement**

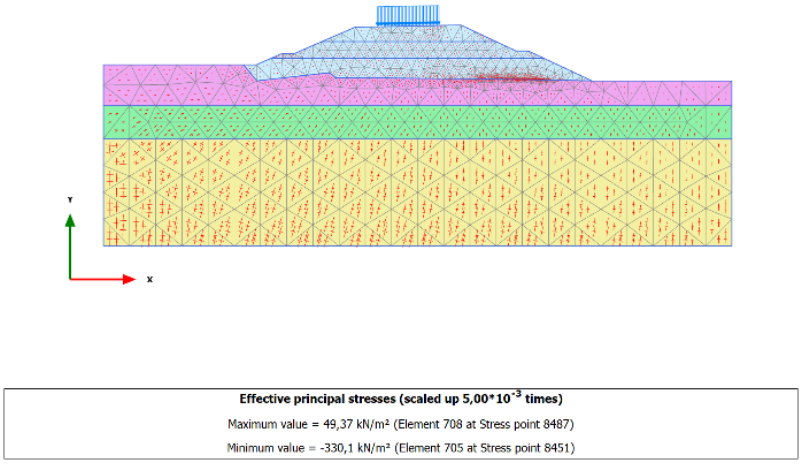


**Figure 5. 18 Effective Stress of Existing Embankment Phase 3 With Angle Of 25º By Adding Pavement And Earthquake Loads Without Reinforcement**

Based on the PLAXIS V20 analysis, the type of the slope failure is rotation failure. The analysis result for existing embankment phase 3 with angle of 25º by adding pavement load on PLAXIS V20 shows the factor of safety is 1.444. While the analysis result for existing embankment phase 3 with angle of 25º by adding pavement and earthquake loads on PLAXIS V20 is 1.1048. Potential failure area on the existing embankment phase 3 with angle of 25º by adding pavement load, and existing embankment phase 3 with angle of 25º by adding pavement and earthquake loads without reinforcement can be seen on Figure 5.19 and Figure 5.20.

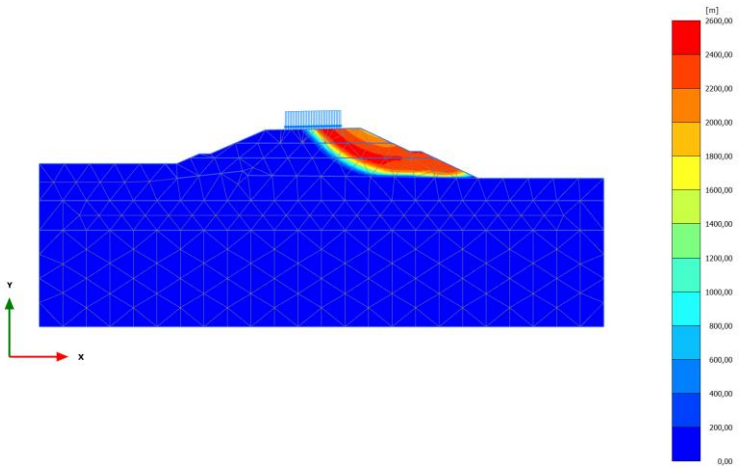


**Figure 5. 19 Potential Failure Area on Existing Embankment Phase 3 With Angle of 25º By Adding Pavement Load Without Reinforcement**

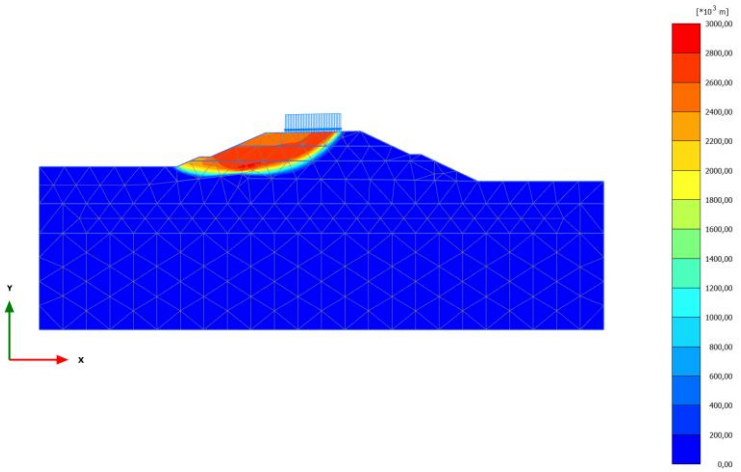


**Figure 5. 20 Potential Failure Area on Existing Embankment Phase 3 With Angle of 25º By Adding Pavement and Earthquake Loads Without Reinforcement**

The analysis using PLAXIS indicated a total consolidation settlement of 0.1405 meter for the existing embankment phase 3 with angle of 25º after a 365-day consolidation period. Consolidation settlement of existing embankment phase 3 with angle of 25º can be seen on Figure 5.21.

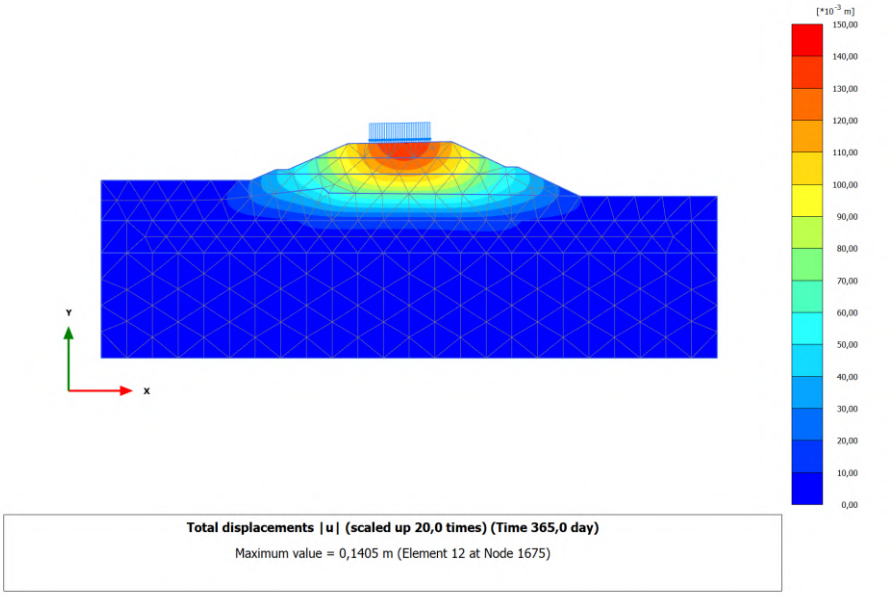


**Figure 5. 21 Consolidation Settlement of Existing Embankment Phase 3 With Angle Of 25º**

### 5.3.2 Analysis of Post-Construction Existing Embankment

Post construction embankment means that road constructing can be started. The road structure load and traffic loads of 25 kN/$^2$, and earthquake load is added to the post-construction analysis. In order to know the deformation occurring on the location due to the loads mentioned before, deformed mesh is necessary. The analysis result for existing embankment with angle of 25º by adding pavement, traffic and earthquake loads on PLAXIS V20 is collapse. Therefore, the analysis result can't be shown on PLAXIS V20. Deformed Mesh for the existing

embankment with angle of 25º by adding the road structure and traffic load without reinforcement based on PLAXIS V20 analysis can be seen on Figure 5.22.

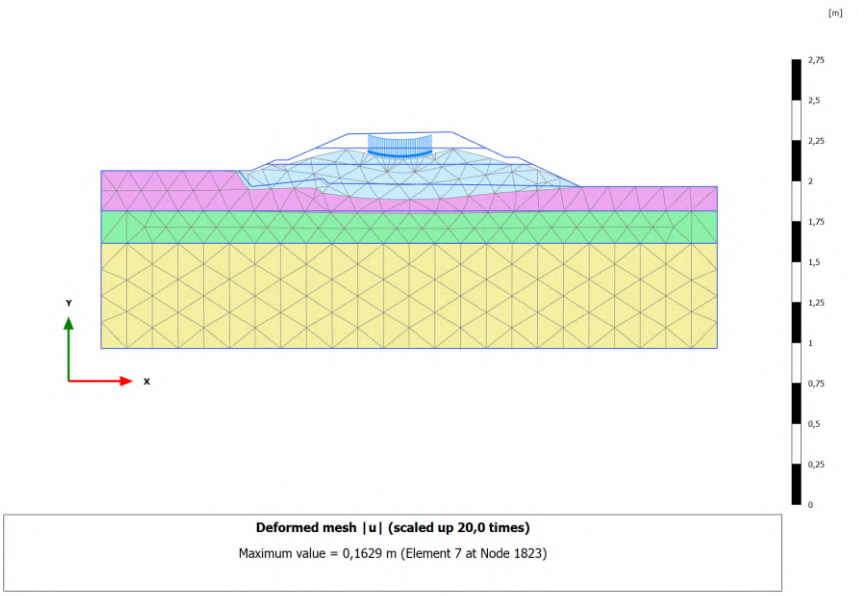


**Figure 5. 22 Deformed Mesh for Existing Embankment with Angle of 25º By Adding Road Structure and Traffic Loads Without Reinforcement**

Displacement occurs on post construction embankment with angle of 25º without reinforcement. Based on the indicator on PLAXIS V20, the bigger displacement shows redder colour. While smaller displacement indicated by the shade of blue. The displacement value of the existing embankment with angle of 25º by adding the road structure load without reinforcement is 0.1629 m, while the analysis result for existing embankment with angle of 25º by adding pavement, traffic, and earthquake loads on PLAXIS V20 shows that slope is collapse. Therefore, the analysis result can't be shown on PLAXIS V20. The displacement of the existing embankment with angle of 25º by adding the road structure and traffic loads without reinforcement can be seen on Figure 5.23.

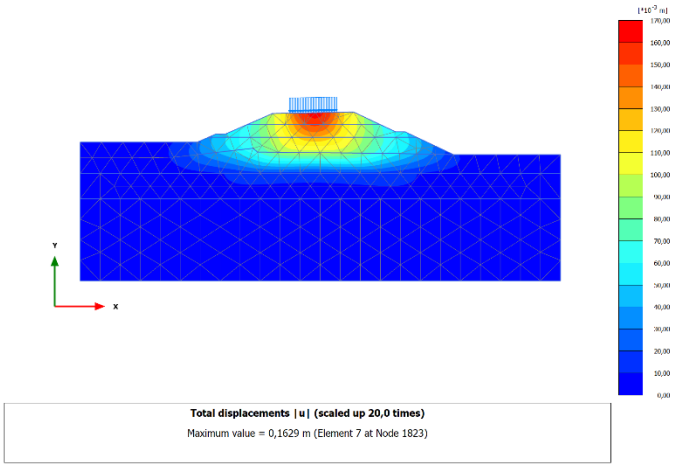


**Figure 5. 23 Displacement Value of Existing Embankment with Angle of 25º By Adding Road Structure and Traffic Loads Without Reinforcement**

The effective stress is used to calculate the factor of safety for embankment slope. Also, to identify the potentially failed slope area. The maximum amount effective stress of existing embankment with angle of 25º by adding pavement load without reinforcement is 0.01776 x $10^{-15}$ kN/$m^2$, while the analysis result for existing embankment with angle of 25º by adding pavement and earthquake loads on PLAXIS V20 shows that slope is collapse. Therefore, the analysis result can't be shown on PLAXIS V20. The effective stress of existing embankment with angle of 25º by adding road structure and traffic load without reinforcement can be seen in Figure 5.24.

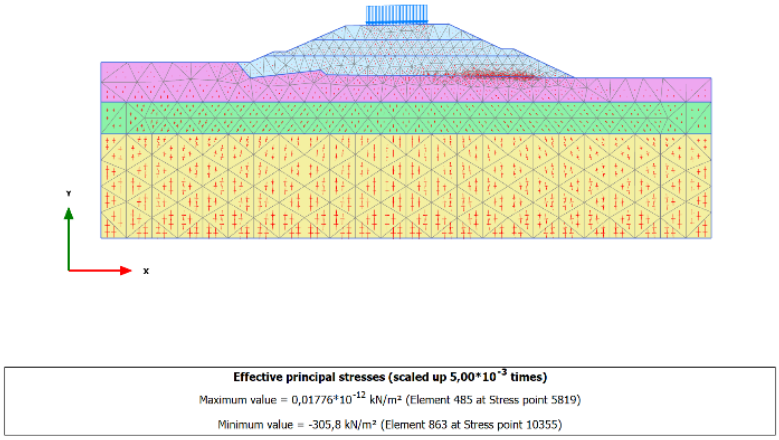


**Figure 5. 24 Effective Stress of Existing Embankment with Angle Of 25º By Adding Road Structure Load Without Reinforcement**

Based on the PLAXIS V20 analysis, the type of the slope failure is rotation failure. The analysis result for existing embankment with angle of 25º by adding the road structure load on PLAXIS V20 shows the factor of safety is 1.211. While the analysis result for existing embankment with angle of 25º by adding the road structure, traffic and earthquake loads on PLAXIS V20 shows that slope is collapse. Therefore, the analysis result can't be shown on PLAXIS V20. Potential failure area on the existing embankment with angle of 25º by the road structure and traffic loads without reinforcement can be seen on Figure 5.25.

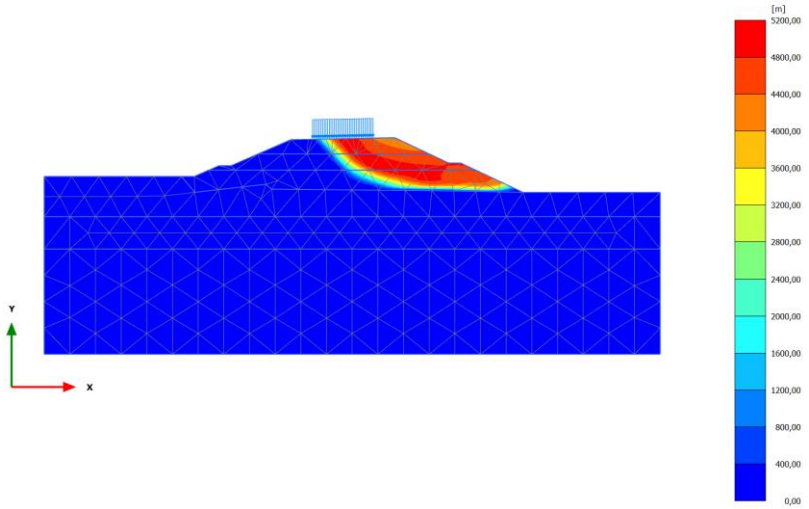


**Figure 5. 25 Potential Failure Area on Existing Embankment with Angle of 25º By Adding Road Structure Load Without Reinforcement**

The analysis using PLAXIS indicated a total consolidation settlement of 0.1905 meter for the existing embankment phase 3 with angle of 25º after a 365-day consolidation period. Consolidation settlement of existing embankment post-construction with angle of 25º can be seen on Figure 5.26.

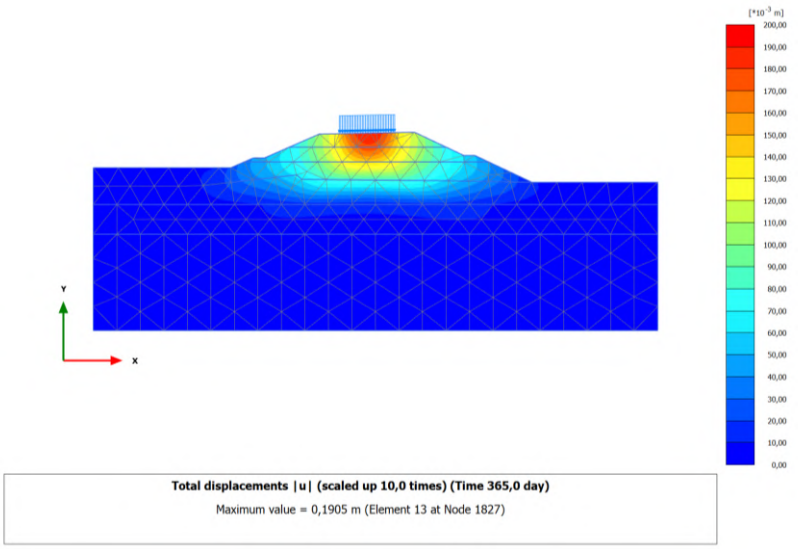


**Figure 5. 26 Consolidation Settlement of Existing Embankment Post-Construction with Angle of 25º**

### 5.3.3 Fellenius method

The analysis of embankment stability using PLAXIS V20 program based on the finite element method on will be compared with the Fellenius method analysis. The calculation of Fellenius method is used to compare and confirm the factor of safety on existing embankment on the post construction PLAXIS V20 program. As has been mentioned in sub-chapter 3.4.2, method of slices is used as the base of calculation of Fellenius method. Therefore, the method of slice applied on the slope failure can be seen in Figure 5.27.

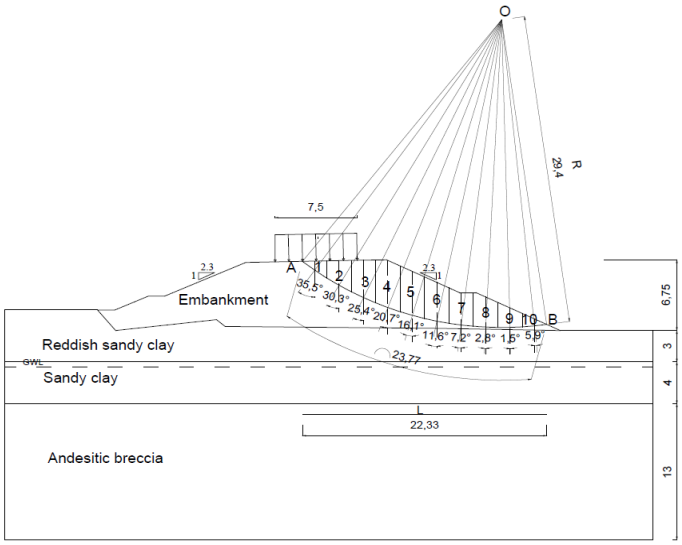


**Figure 5. 27 The Method of Slice**

Based on the Figure 5.19 the horizontal length of slope failure is 22.326 m, and the slope failure section will be divided into 10 slices in this calculation of Fellenius method. The radius of the slope failure on the existing embankment with slope angle 25° is 29.4 m. The calculation steps of slope stability using Fellenius method.

1. Calculation of each slice length

   $L = \frac{22.326}{10} = 2.2326\ m$

2. Calculation of each slice weight

   $W = \gamma \text{ x } A$

   For the slices with upper load, the weight can be determined by the equation below.

   $W = (\gamma \text{ x } A) + (q \text{ x } L)$

   The load (q) for this calculation used pavement and traffic load of 25 kN/m$^2$. Meanwhile, the length (L) used the slices with upper load.

   The calculation example of each slice weight can be seen below.

   $\gamma_1$ = 12.49 kN/m$^3$

   $L_1$ = 2.2326 m

   $A_1$ = 1.891 m$^2$

   $A_4$ = 9.795 m$^2$

   $W_1 = \gamma_1 \text{ x } A_1 + (q \text{ x } L_1)$

   $= (12.49 \text{ x } 1.891) + (25 \text{ x } 2.2326)$

   $= 79.437\ kN$

   $W_4 = \gamma_4 \text{ x } A_4$

   $= 12.49\ x\ 9.795$

   $= 122.859\ kN$

   The recapitulation of each slice weight can be seen in Table 5.3.

3. Calculation of Wi sin α of each slice

   The calculation example of Wi sin α of each slice can be seen below.

   $\alpha_1$ = 35.5°

   $\alpha_6$ = 20.7°

   Slice 1 = $W_1 \text{ x } \sin \alpha$

$= 79.437 \text{ x } \sin 35.5^{o}$

$= 46.129\ kN/m$

Slice 4 $= W_4 \text{ x } \sin \alpha$

$= 122.859 \text{ x } \sin 20.7^{o}$

$= 43.243\ kN/m$

4. Calculation of Wi cos α of each slice

Slice 1 $= W_1 \text{ x } \cos \alpha$

$= 79.437 \text{ x } \cos 35.5^{o}$

$= 64.671\ kN/m$

Slice 4 $= W_4 \text{ x } \cos \alpha$

$= 122.859 \text{ x } \cos 20.7^{o}$

$= 114.438 kN/m$

The recapitulation of calculation steps using Fellenius method for entire slices can be seen in Table 5.3.

**Table 5. 3 Recapitulation of Calculation Steps Using Fellenius Method**

| Slice | Soil layer | A | Wi | α | Wi cos α | Wi sin α |
|---|---|---|---|---|---|---|
| | | (m²) | kN | (°) | | |
| 1 | 1 | 1.891 | 79.437 | 35.5 | 64.671 | 46.129 |
| 2 | 1 | 5.225 | 121.077 | 30.3 | 104.538 | 61.087 |
| 3 | 1 | 7.962 | 112.859 | 25.4 | 101.950 | 48.409 |
| 4 | 1 | 9.795 | 122.336 | 20.7 | 114.438 | 43.243 |
| 5 | 1 | 9.352 | 116.804 | 16.1 | 112.223 | 32.391 |
| 6 | 1 | 8.243 | 102.956 | 11.6 | 100.853 | 20.702 |
| 7 | 1 | 7.112 | 88.823 | 7.2 | 88.122 | 11.132 |
| 8 | 1 | 6.390 | 79.807 | 2.8 | 79.712 | 3.899 |
| 9 | 1 | 4.120 | 51.458 | 1.5 | 51.440 | 1.347 |
| 10 | 1 | 1.458 | 18.215 | 5.9 | 18.119 | 1.872 |
| Total | | | | | 836.066 | 270.212 |

5. Failure capacity given by cohesion component

Based on Figure 5.26, the length of curve line on layer 1 (A-B) is 23.77 m. Therefore, the calculation is:

a $= 23.77$ m

$c_1$ = 10.79 kN/m²

$c_1a_1$ = (10.79 x 23.77)

= 256.478 kN/m

6. Calculation of the factor of safety

$$SF = \frac{(\Sigma ci\alpha i)+(\text{Tan } \varphi \times \Sigma W \times \cos \alpha))}{(\Sigma W \sin\alpha)+(q \times L))}$$

$$= \frac{(256.478)+(\text{Tan } 14.5 \times 836.066))}{(216.221+(25 \times 7.5))}$$

=1.196

Based on the calculation results of the factor of safety on the existing embankment with a slope angle of 25º using the Fellenius method is 1.196. The result obtained using the Fellenius method is used as a comparison and to verify the results of the PLAXIS V20 analysis. The analysis and calculations performed for the post-construction stage without seismic loads. The results of the manual calculation are not much different from the PLAXIS analysis result, which is 1.211.

**5.4 Primary Consolidation Calculation**

The calculation of consolidation settlement is using the Terzaghi method. The compression index and void ratio data used in this analysis were obtained empirically from secondary data. The objective of this analysis is used to compare and verify the consolidation settlement of the embankment, as previously determined using PLAXIS V20. This analysis is conducted using normally consolidated principles. Where the consolidation settlement calculation for layer 1 can be done by using formula from Equation 3.27.

Layer 1:

$Cc_1$ = 0.1077

$eo_1$ = 0.678

The next step is to discover the value of effective overburden stress (Po). The calculation can be done using Equation 3.28.

$Po_1$ = $\gamma_1$ x $H_1$

= 16.2 x 3

= 48.6 kN/$m^2$

After that, soil stress distribution value must be discovered (ΔP). But before discovering the value, there are some values that have to be calculated first before obtaining the (ΔP) value. They are q, a/z, and b/z to obtain coefficient in soil stress distribution value (ΔP).

$qo$ = ($\gamma_{embankment}$ x $H_{embankment}$) + pavement load

= (16.52 x 6.75) + 10

= 121.51 kN/$m^3$

$a/z_1$ = 7.935 / 1.5

= 5.29

$b/z_1$ = 12.87 / 1.5

= 8.58

The value of the empirical parameter I, obtained from Figure 3.13 (Osterberg's chart), is 0.5.

$\Delta P_1$ = qo x $I_1$

= 121.51 x 0.5

= 60.755 kN/$m^2$

Then, the value of primary consolidation can be trully determined using Equation 3.28.

$Sc_1$ = $\frac{Cc\ x\ H}{1+eo} log \frac{Po+ \Delta P}{Po}$

= $\frac{0.1077\ x\ 3}{1+0.678} log \frac{48.6 + 60.755}{48.6}$

= 0.0678 m

The calculation for the preceeding layer is similar in the process. Therefore, the recapitulation of each value of each layer can be seen on the Table 5.4 below.

**Table 5. 4 Recapitulation of Consolidation Settlement**

| Name | H (m) | I | Δp (kN/m$^2$) | Po (kN/m$^3$) | Cc | eo | Sc (m) |
|---|---|---|---|---|---|---|---|
| Soil Layer 1 | 3 | 0.5 | 60.755 | 48.6 | 0.1077 | 0.678 | 0.0678 |
| Soil Layer 2 | 4 | 0.47 | 57.1097 | 86.865 | 0.1585 | 0.896 | 0.0734 |
| Soil Layer 3 | 13 | 0.44 | 106.9288 | 256.905 | 0 | 0.224 | 0.0000 |
| Total | | | | | | | 0.1412 |

Based on the calculation results of the consolidation settlement on the existing embankment with a slope angle of 25º using the Terzaghi method is 0.1412 m. The result obtained using the Terzaghi method is used as a comparison and to verify the results of the PLAXIS V20 analysis. The analysis and calculations performed for the construction stage without seismic loads. The results of the manual calculation are not much different from the PLAXIS analysis result, which is 1.1405 m.

## 5.5 Geotextile calculation

The geotextile calculation is used to calculate the geotextile requirements in the analysed embankment. Geotextile reinforcement calculation, per-zone method is used to determine tensile strength distribution in slopes. While the division of the zone can be seen on Figure 5.28.

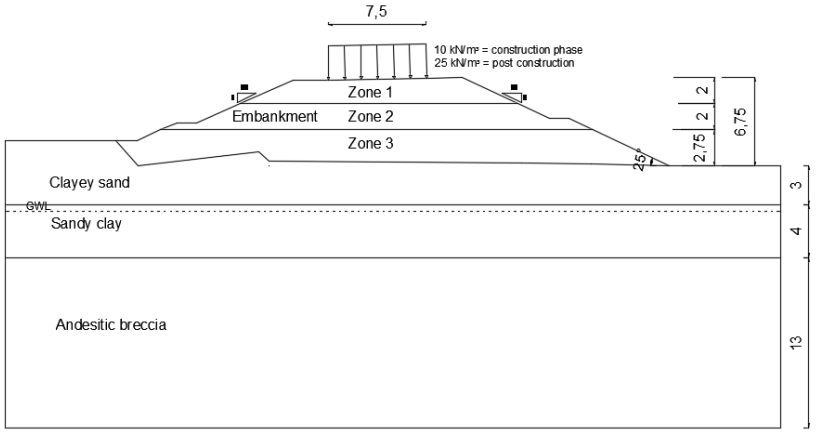


**Figure 5. 28 Division of The Zone**

### 5.5.1 Parameter Data

Parameter required for geotextile calculation is basic parameter of geotextile type, embankment soil parameter, loads working on the embankment, and coefficient of soil bearing capacity.

The data for the analysis of internal and external stability.

1. Geotextile
   a. Type = Woven geotextile
   b. Ultimate tensile strength = 52 kN/m
   c. Allowable tensile strength = 26 kN/m
   d. Normal stiffness = 260 kN/m
2. Embankment soil
   a. Bulk unit weight ($\gamma b$) = 12.49 kN/m$^3$
   b. Cohesion ($c$) = 10.79 kN/m$^2$
   c. Internal friction angle ($\varphi$) = 14.5$^o$
3. Load
   a. Pavement load = 10 kN/m$^2$
   b. Traffic load = 15 kN/m$^2$

   So, the total load that distributed to the embankment is 25 kN/m$^2$
4. Soil bearing capacity coefficient

   The data of soil bearing capacity coefficient refer to the Departemen Pekerjaan Umum (2009) that can be seen on Table 5.5.

**Table 5. 5 Soil Bearing Capacity Coefficient**

| φ | Nc | Nq | Nγ |
|---|---|---|---|
| 10 | 8.35 | 2.47 | 1.22 |
| 11 | 8.8 | 2.71 | 1.44 |
| 12 | 9.28 | 2.97 | 1.69 |
| 13 | 9.81 | 3.26 | 1.97 |
| 14 | 10.37 | 3.59 | 2.29 |
| 14.5 | 10.40 | 3.64 | 2.36 |
| 15 | 10.98 | 3.94 | 2.65 |
| 16 | 11.63 | 4.34 | 3.06 |
| 17 | 12.34 | 4.77 | 3.53 |

**Continuation Table 5.5 Soil Bearing Capacity Coefficient**

| | | | |
|---|---|---|---|
| 18 | 13.1 | 5.26 | 4.07 |
| 19 | 13.93 | 5.8 | 4.68 |
| 20 | 14.83 | 6.4 | 5.39 |

Source: Departemen Pekerjaan Umum (2009)

### 5.5.2 External stability calculation

External stability calculation is used to determine the vertical distance between geotextile layers (Sv) and minimum required geotextile length (L). The calculation can be seen below.

1. vertical distance between geotextile layers (Sv),

$\text{Ka} = tan^2((45^0 - \left(\frac{\varphi}{2}\right)))$

$= tan^2((45^0 - \left(\frac{14.5}{2}\right)))$

= 0.578

a. Zone 1

$\sigma_{hc1}$ $= \text{q x Ka} - 2 \text{ x } c \text{ x } \sqrt{Ka} + \text{Ka x H}_1 \text{x } \gamma_b$

$= (25 \text{ x } 0.6) - (2 \text{ x } 10.79 \text{ x } \sqrt{0.6}) + (0.6 \text{ x } 2 \text{ x } 12.49)$

= 13.255 kN/m$^2$

SF = 1.5 (used)

$S_{Vi} = \frac{\text{Ta}}{\sigma_{hc1} \text{ x SF}}$

$= \frac{26}{13.225 \text{ x } 1.5}$

= 1.308 m

$S_{Vi}$ used = 1 m (used for zone 1)

The amount of geotextile layers $= \frac{2}{1} = 2$

= 2 layers (used for zone 1)

Based on the calculation of vertical distance between geotextile layers is 1 meter, and the amount of geotextile layers is 2 for zone 1.

b. Zone 2

$\sigma_{hc2}$ $= \text{Ka x } H_2 \text{ x } \gamma_b - 2 \text{ x } c \text{ x } \sqrt{Ka}$

$= (0.6 \text{ x } 4 \text{ x } 12.49) - (2 \text{ x } 10.79 \text{ x } \sqrt{0.6\ })$

$= 13.243 \text{ kN/m}^2$

SF $= 1.5$ (used)

$S_{Vi}$ $= \frac{\text{Ta}}{\sigma_{hc1} \text{ x SF}}$

$= \frac{26}{13.243 \text{ x } 1.5}$

$= 1.309$ m

$S_{Vi}$ used $= 1$ m (used for zone 2)

The amount of geotextile layers $= \frac{2}{1} = 2$

$= 2$ layers (used for zone 2)

Based on the calculation of vertical distance between geotextile layers is 1 meter, and the amount of geotextile layers is 2 for zone 2.

c. Zone 3

$\sigma_{hc2}$ $= \text{Ka x } H_2 \text{ x } \gamma_b - 2 \text{ x } c \text{ x } \sqrt{Ka}$

$= (0.6 \text{ x } 6.75 \text{ x } 12.49) - (2 \text{ x } 10.79 \text{ x } \sqrt{0.6\ })$

$= 33.834 \text{ kN/m2}$

SF $= 1.5$ (used)

$S_{V3}$ $= \frac{\text{Ta}}{\sigma_{hc1} \text{ x SF}}$

$= \frac{26}{33.834 \text{ x } 1.5}$

$= 0.512$ m

$S_{V3}$ used $= 0.5$ m (used for zone 3)

The amount of geotextile layers $= \frac{2.75}{0.5} = 5.5$

$= 6$ layers (used for zone 3)

Based on the calculation of vertical distance between geotextile layers is 0.5 meter, and the amount of geotextile layers is 6 for zone 1.

2. Determining geotextile length based on the working forces

   Zone 1

   a. Stability toward eccentricity

$$\frac{1}{6}xL \geq e$$

$$e = \frac{\sum \text{MD}}{Rv}$$

$$\sum \text{MD} = \left(q\ x\ ka\ x\ \frac{1}{2}x\ H^2\right) + \left(\frac{1}{2}x\ Ka\ x\ \gamma b\ x\ H^2\ x\ \frac{1}{3}x\ H\right) - (2\ x\ c\ x\sqrt{Ka}\ x\ \frac{1}{2}x\ H^2)$$

$$Rv = (H\ x\ \gamma b\ x\ L) + (q\ x\ L)$$

$$\frac{1}{6}L \geq \frac{\left(\text{q x ka x }\frac{1}{2}\text{x H}^2\right)+\left(\frac{1}{2}\text{x Ka x }\gamma\text{b x H}^2\text{ x }\frac{1}{3}\text{x H}\right)-(2\text{ x c x }\sqrt{\text{Ka}}\text{ x }\frac{1}{2}\text{x H}^2)}{(\text{Hx }\gamma\text{b x L})+(\text{q x L})}$$

$$\frac{\text{L}}{6} \geq \frac{\left(25\ x\ 0.6\ x\ \frac{1}{2}\ x\ 2^2\right)+\left(\frac{1}{2}x\ 0.6\ x\ 12.49\ x\ 2^2\ x\ \frac{1}{3}x\ 2\right)-\left(2\ x\ 10.79\ x\ \sqrt{0.6}\ x\ \frac{1}{2}x\ 2^2\right)}{(2\ x\ 12.49\ x\ L)+(25\ x\ L)}$$

$$\frac{\text{L}}{6} \geq \frac{6.542}{49.98L}$$

$$49.98L^2 = 39.25$$

$$L^2 = \frac{39.25}{49.98}$$

$$L = \sqrt{0.786}$$

$$L = 0.886m$$

   The calculated geotextile length of zone 1 to resist eccentricity on soil embankment is 1 m.

   b. Stability toward rolling

$$\text{SF} = \frac{\sum \text{MR}}{\sum MD} = \frac{resistance\ moment}{rolling\ moment} \geq 1.5$$

$$\sum MR = \left(\frac{1}{2}x\ q\ x\ L^2\right) + \left(\frac{1}{2}x\ \gamma b\ x\ H\ x\ L^2\right)$$

$$\sum MD = \left(q\ x\ ka\ x\ \frac{1}{2}x\ H^2\right) + \left(\frac{1}{2}x\ Ka\ x\ \gamma b\ x\ H^2\ x\ \frac{1}{3}x\ H\right) - (2\ x\ c\ x\sqrt{Ka}\ x\ \frac{1}{2}x\ H^2)$$

$$\text{SF} = \frac{\left(\frac{1}{2}x\ q\ x\ L^2\right)+\left(\frac{1}{2}x\ \gamma b\ x\ H\ x\ L^2\right)}{\left(q\ x\ ka\ x\ \frac{1}{2}x\ H^2\right)+\left(\frac{1}{2}x\ Ka\ x\ \gamma b\ x\ H^2\ x\ \frac{1}{3}x\ H\right)-(2\ x\ c\ x\sqrt{Ka}\ x\ \frac{1}{2}x\ H^2)}$$

$$\text{SF} = \frac{\left(\frac{1}{2}x\ 25\ x\ L^2\right)+\left(\frac{1}{2}x\ 12.49\ x\ 2\ x\ L^2\right)}{\left(25\ x\ 0.6\ x\ \frac{1}{2}\ x\ 2^2\right)+\left(\frac{1}{2}x\ 0.6\ x\ 12.49\ x\ 2^2\ x\ \frac{1}{3}x\ 2\right)-(2\ x\ 10.79\ x\sqrt{0.6}\ x\ \frac{1}{2}x\ 2^2)}$$

$$1.5 = \frac{24.99L^2}{6.542}$$

$$24.99L^2 = 9.812$$

$L^2 = \frac{9.812}{24.99}$

$L = \sqrt{0.393}$

$L = 0.627\ m$

The calculated geotextile length of zone 1 to resist rolling on soil embankment is 1 m.

c. Stability toward shear

$SF = \frac{(q\ x\ tan\delta\ x\ L)+(H\ x\ \gamma_b\ x\ tan\delta\ x\ L)}{(q\ x\ ka\ x\ H)+\left(\frac{1}{2}\ x\ Ka\ x\ \gamma_b\ x\ H^2\right)-(2\ x\ c\ x\sqrt{Ka}\ x\ H)}$

Shear resistance on reinforcement base ($\delta = \frac{2}{3} x\ 14.5 = 9.667$)

$SF = \frac{(25\ x\ tan(9.667)\ x\ L)+(2\ x\ 12.49\ x\ tan(9.667)\ x\ L)}{(25\ x\ 0.6\ x\ 2)+\left(\frac{1}{2}\ x\ 0.6\ x\ 12.49\ x\ 2^2\right)-\left(2\ x\ 10.79\ x\ \sqrt{0.6}\ x\ 2\right)}$

$1.5 = \frac{8.513L}{11.534}$

$8.513L = 17.3$

$L = \frac{17.3}{8.513}$

$L = 2.032\ m$

The calculated geotextile length of zone 1 to resist shear on soil embankment is 2.5 m.

d. Stability toward bearing capacity of soil

$L \leq \frac{\sigma ult}{(H\ x\ \gamma_b)+q}$

$qult = (c\ x\ Nc) + (0.5\ x\ L\ x\ \gamma_b\ x\ N\gamma)$

$= (10.79\ x\ 10.4) + (0.5\ x\ L\ x\ 12.49\ x 2.36)$

$= (168.301) + (14.756)$

$\sigma ult = qult\ x\ SF$

$= (168.301) + (14.756) x\ 1.5$

$= 178.342 + 22.134L$

$L \leq \frac{178.342+22.134L}{(2\ x\ 12.49)+25}$

$49.98L \leq 178.342 + 22.134L$

$$L = \frac{178.342}{(49.98-22.134)}$$

$$L = \frac{178.342}{27.846}$$

$$L = 6.044\ m$$

The calculated geotextile length of zone 1 to resist bearing capacity on soil embankment is 6.5 m.

Zone 2

a. Stability toward eccentricity

$$\frac{1}{6}xL \geq e$$

$$e = \frac{\sum \text{MD}}{Rv}$$

$$\sum \text{MD} = \left(q\ x\ ka\ x\ \frac{1}{2}x\ H^2\right) + \left(\frac{1}{2}x\ Ka\ x\ \gamma b\ x\ H^2 x\ \frac{1}{3}x\ H\right) - (2\ x\ c\ x\sqrt{Ka}\ x\ \frac{1}{2}x\ H^2)$$

$$Rv = (H\ x\ \gamma b\ x\ L) + (q\ x\ L)$$

$$\frac{1}{6}L \geq \frac{\left(\text{q x ka x }\frac{1}{2}\text{x H}^2\right)+\left(\frac{1}{2}\text{x Ka x }\gamma\text{b x H}^2\text{ x }\frac{1}{3}\text{x H}\right)-(2\text{ x c x }\sqrt{\text{Ka}}\text{ x }\frac{1}{2}\text{x H}^2)}{(\text{H x }\gamma\text{b x L})+(\text{q x L})}$$

$$\frac{\text{L}}{6} \geq \frac{\left(25\ x\ 0.6\ x\ \frac{1}{2}\ x\ 4^2\right)+\left(\frac{1}{2}\ x\ 0.6\ x\ 12.49\ x\ 4^2\ x\ \frac{1}{3}\ x\ 4\right)-\left(2\ x\ 10.79\ x\ \sqrt{0.6}\ x\ \frac{1}{2}\ x\ 4^2\right)}{(4\ x\ 12.49\ x\ L)+(25\ x\ L)}$$

$$\frac{\text{L}}{6} \geq \frac{66.102}{74.96L}$$

$$74.96L^2 = 396.612$$

$$L^2 = \frac{396.612}{74.96}$$

$$L = \sqrt{5.921}$$

$$L = 2.3\ m$$

The calculated geotextile length of zone 2 to resist eccentricity on soil embankment is 2.5 m.

b. Stability toward rolling

$$\text{SF} = \frac{\sum \text{MR}}{\sum MD} = \frac{resistance\ moment}{rolling\ moment} \geq 1.5$$

$$\sum MR = \left(\frac{1}{2}x\ q\ x\ L^2\right) + \left(\frac{1}{2}x\ \gamma b\ x\ H\ x\ L^2\right)$$

$$\sum MD = \left(q\ x\ ka\ x\ \frac{1}{2}x\ H^2\right) + \left(\frac{1}{2}x\ Ka\ x\ \gamma b\ x\ H^2 x\ \frac{1}{3}x\ H\right) - (2\ x\ c\ x\sqrt{Ka}\ x\ \frac{1}{2}xH^2)$$

$$SF = \frac{\left(\frac{1}{2} x\ q\ x\ L^2\right)+\left(\frac{1}{2} x\ \gamma b\ x\ H\ x\ L^2\right)}{\left(q\ x\ ka\ x \frac{1}{2} x\ H^2\right)+\left(\frac{1}{2} x\ Ka\ x\ \gamma b\ x\ H^2\ x \frac{1}{3} x\ H\right)-(2\ x\ c\ x\sqrt{Ka}\ x \frac{1}{2} x\ H^2)}$$

$$SF = \frac{\left(\frac{1}{2} x\ 25\ x\ L^2\right)+\left(\frac{1}{2} x\ 12.49\ x\ 4\ x\ L^2\right)}{\left(25\ x\ 0.6\ x \frac{1}{2} x\ 4^2\right)+\left(\frac{1}{2} x\ 0.6\ x\ 14.49\ x\ 4^2 x \frac{1}{3} x\ 4\right)-(2\ x\ 10.79\ x\sqrt{0.6}\ x \frac{1}{2} x\ 4^2)}$$

$$1.5 = \frac{37.48L^2}{66.102}$$

$$37.48L^2 = 99.153$$

$$L^2 = \frac{99.153}{37.48}$$

$$L = \sqrt{2.646}$$

$$L = 1.626\ m$$

The calculated geotextile length of zone 2 to resist rolling on soil embankment is 2 m.

c. Stability toward shear

$$SF = \frac{(q\ x\ tan\delta\ x\ L)+(H\ x\ \gamma_b\ x\ tan\delta\ x\ L)}{(q\ x\ ka\ x\ H)+\left(\frac{1}{2} x\ Ka\ x\ \gamma_b\ x\ H^2\right)-(2\ x\ c\ x\sqrt{Ka}\ x\ H)}$$

Shear resistance on reinforcement base ($\delta = \frac{2}{3} x 14.5 = 9.667$)

$$SF = \frac{(25\ x\ tan(9.667)\ x\ L)+(4\ x\ 16\ x\ tan(9.667)\ x\ L)}{(25\ x\ 0.6\ x\ 4)+\left(\frac{1}{2} x\ 0.6\ x\ 12.49\ x\ 4^2\right)-\left(2\ x\ 10.79\ x\sqrt{0.6}\ x\ 4\right)}$$

$$1.5 = \frac{12.768L}{53.019}$$

$$13.668L = 79.528$$

$$L = \frac{79.528}{13.668}$$

$$L = 6.229\ m$$

The calculated geotextile length of zone 2 to resist shear on soil embankment is 6.5 m.

d. Stability toward bearing capacity of soil

$$L \leq \frac{\sigma ult}{(H\ x\ \gamma_b)+q}$$

$$qult = (c\ x\ Nc) + (0.5\ x\ L\ x\ \gamma_b\ x\ N\gamma)$$

$$= (10.79x10.4) + (0.5\ x\ L\ x\ 12.49\ x2.36)$$

$$= (168.301) + (14.756)$$

$\sigma ult \quad = qult \text{ x SF}$

$= (168.301) + (14.756) \text{x } 1.5$

$= 178.342 + 22.134L$

$L \quad \leq \frac{178.342 + 22.134L}{(4 \text{ x } 12.49)+25}$

$74.96L \leq 178.342 + 22.134L$

$L \quad = \frac{178.342}{(74.96-22.134)}$

$L \quad = \frac{178.342}{52.826}$

$L \quad = 3.186\ m$

The calculated geotextile length of zone 2 to resist bearing capacity on soil embankment is 3.5 m.

Zone 3

a. Stability toward eccentricity

$\frac{1}{6}xL \quad \geq e$

$e \quad = \frac{\sum \text{MD}}{Rv}$

$\sum \text{MD} \quad = \left(q\ x\ ka\ x \frac{1}{2} x\ H^2\right) + \left(\frac{1}{2} x\ Ka\ x\ \gamma b\ x\ H^2 x \frac{1}{3} x\ H\right) - (2\ x\ c\ x \sqrt{Ka}\ x \frac{1}{2} x\ H^2)$

$Rv \quad = (H\ x\ \gamma b\ x\ L) + (q\ x\ L)$

$\frac{1}{6}L \quad \geq \frac{\left(\text{q x ka x } \frac{1}{2} \text{x H}^2\right)+\left(\frac{1}{2} \text{x Ka x } \gamma\text{b x H}^2 \text{ x} \frac{1}{3} \text{x H}\right)-(2 \text{ x c x } \sqrt{\text{Ka}} \text{ x} \frac{1}{2} \text{x H}^2)}{(\text{H x } \gamma\text{b x L})+(\text{q x L})}$

$\frac{\text{L}}{6} \quad \geq \frac{\left(25\ x\ 0.6\ x \frac{1}{2} x\ 6.75^2\right)+\left(\frac{1}{2} x\ 0.6\ x\ 12.49\ x\ 6.75^2 x \frac{1}{3} x\ 6.75\right)-\left(2\ x\ 10.79\ x \sqrt{0.6}\ x \frac{1}{2} x\ 6.75^2\right)}{(6.75\ x\ 12.49\ x\ L)+(25\ x\ L)}$

$\frac{\text{L}}{6} \quad \geq \frac{344.604}{109.308L}$

$109.308L^2 = 2067.625$

$L^2 \quad = \frac{2067.625}{109.308}$

$L \quad = \sqrt{18.916}$

$L \quad = 4.349\ m$

The calculated geotextile length of zone 3 to resist eccentricity on soil embankment is 4.5 m.

b. Stability toward rolling

$$\text{SF} = \frac{\sum \text{MR}}{\sum MD} = \frac{resistance\ moment}{rolling\ moment} \geq 1.5$$

$$\sum MR = \left(\frac{1}{2}\ x\ q\ x\ L^2\right) + \left(\frac{1}{2} x\ \gamma b\ x\ H\ x\ L^2\right)$$

$$\sum MD = \left(q\ x\ ka\ x \frac{1}{2} x\ H^2\right) + \left(\frac{1}{2} x\ Ka\ x\ \gamma b\ x\ H^2 x \frac{1}{3} x\ H\right) - (2\ x\ c\ x\sqrt{Ka}\ x \frac{1}{2} x\ H^2)$$

$$\text{SF} = \frac{\left(\frac{1}{2} x\ q\ x\ L^2\right)+\left(\frac{1}{2} x\ \gamma b\ x\ H\ x\ L^2\right)}{\left(q\ x\ ka\ x \frac{1}{2} x\ H^2\right)+\left(\frac{1}{2} x\ Ka\ x\ \gamma b\ x\ H^2\ x \frac{1}{3} x\ H\right)-(2\ x\ c\ x\sqrt{Ka}\ x \frac{1}{2} x\ H^2)}$$

$$\text{SF} = \frac{\left(\frac{1}{2} x\ 25\ x\ L^2\right)+\left(\frac{1}{2} x\ 12.49\ x\ 6.75\ x\ L^2\right)}{\left(25\ x\ 0.6\ x \frac{1}{2} x\ 6.75^2\right)+\left(\frac{1}{2} x\ 0.6\ x\ 14.49\ x\ 6.75^2 x \frac{1}{3} x\ 6.75\right)-(2\ x\ 10.79\ x\sqrt{0.6}\ x \frac{1}{2} x\ 6.75^2)}$$

$$1.5 = \frac{54.654L^2}{344.604}$$

$$54.654L^2 = 516.906$$

$$L^2 = \frac{516.906}{54.654}$$

$$L = \sqrt{9.458}$$

$$L = 3.075\ m$$

The calculated geotextile length of zone 3 to resist rolling on soil embankment is 3.5 m.

c. Stability toward shear

$$\text{SF} = \frac{(q\ x\ tan\delta\ x\ L)+(H\ x\ \gamma_b\ x\ tan\delta\ x\ L)}{(q\ x\ ka\ x\ H)+\left(\frac{1}{2} x\ Ka\ x\ \gamma_b\ x\ H^2\right)-(2\ x\ c\ x\sqrt{Ka}\ x\ H)}$$

Shear resistance on reinforcement base ($\delta = \frac{2}{3} x 14.5 = 9.667$)

$$\text{SF} = \frac{(25\ x\ tan(9.667)\ x\ L)+(6.75\ x\ 16\ x\ tan(9.667)\ x\ L)}{(25\ x\ 0.6\ x\ 6.75)+\left(\frac{1}{2} x\ 0.6\ x\ 12.49\ x\ 6.75^2\right)-\left(2\ x\ 10.79\ x\sqrt{0.6}\ x\ 6.75\right)}$$

$$1.5 = \frac{18.619L}{158.966}$$

$$19.93L = 238.45$$

$$\text{L} = \frac{238.45}{19.93}$$

$$L = 12.807\ m$$

The calculated geotextile length of zone 3 to resist shear on soil embankment is 13 m.

d. Stability toward bearing capacity of soil

$L \quad \leq \frac{\sigma ult}{(H \times \gamma_b)+q}$

$qult \quad = (c \times Nc) + (0.5 \times L \times \gamma_b \times N\gamma)$

$= (10.79x10.4) + (0.5\ x\ L\ x\ 12.49\ x2.36)$

$= (168.301) + (14.756)$

$\sigma ult \quad = qult \times SF$

$= (168.301) + (14.756) \times 1.5$

$= 178.342 + 22.134L$

$L \quad \leq \frac{178.342+22.134L}{(6.75 \times 12.49)+25}$

$109.308L \leq 178.342 + 22.134L$

$L \quad = \frac{178.342}{(109.308-22.134)}$

$L \quad = \frac{178.342}{87.173}$

$L \quad = 1.931m$

The calculated geotextile length of zone 3 to resist bearing capacity on soil embankment is 2 m.

### 5.5.3 Internal stability calculation

Internal stability calculation is used to determine the geotextile overlapping length (Lo), geotextile effective length (Le), geotextile length on active zone (Lz), and geotextile total length (L) The calculation can be seen below.

1. Geotextile overlapping length (Lo)

$Lo \quad = \frac{\sigma hc \times Svi \times SF}{2 \times \gamma_b \times Zi \times \tan \varphi}$

For the calculation of geotextile overlapping length number 1 on zone 1

$\sigma hc \quad = 12.475 kN/m^2$

$SF \quad = 1.5$

$Sv1 \quad = 1\ m$

$Zi \quad = 1\ m$

$Lo \quad = \frac{\sigma hc \times Svi \times SF}{2 \times \gamma_b \times Zi \times \tan \varphi}$

$$= \frac{13.255 \text{ x } 1 \text{ x } 1.5}{2 \text{ x } 12.49 \text{ x } 1 \text{ x } \tan 14.5}$$

$= 3.078$ m

Based on the calculation overlapping length, the length used is 3.5 m. The recapitulation of the geotextile overlapping length will be shown in Table 5.6.

**Table 5. 6 Recapitulation of Geotextile Overlapping Length**

| Zone | Geotextile | Svi | Zi (m) | Lo (m) | Lo used (m) |
|---|---|---|---|---|---|
| 1 | Geotextile - 1 | 1 | 1 | 3.078 | 3.5 |
| | Geotextile - 2 | 1 | 2 | 1.539 | 2 |
| 2 | Geotextile - 3 | 1 | 3 | 1.025 | 1.5 |
| | Geotextile - 4 | 1 | 4 | 0.769 | 1 |
| 3 | Geotextile - 5 | 0.5 | 4.5 | 0.873 | 1 |
| | Geotextile - 6 | 0.5 | 5 | 0.786 | 1 |
| | Geotextile - 7 | 0.5 | 5.5 | 0.714 | 1 |
| | Geotextile - 8 | 0.5 | 6 | 0.655 | 1 |
| | Geotextile - 9 | 0.5 | 6.5 | 0.604 | 1 |
| | Geotextile - 10 | 0.5 | 6.75 | 0.582 | 1 |

2. Geotextile effective length (Le)

$$\text{Le} = \frac{\text{SF x Svi x Ka x } \gamma_{b} \text{ x Zi}}{2 \text{ x } \gamma_{b} \text{ x Zi x tan } \varphi}$$

For the calculation of geotextile effective length number 1 on zone 1

$$\text{Le} = \frac{1.5 \text{ x } 1 \text{ x } 0.6 \text{ x } 12.49 \text{ x } 1}{2 \text{ x } 12.49 \text{ x } 1 \text{ x } \tan 14.5}$$

$$= 1.739\ m$$

Based on the calculation effective length, the length used is 2 m. The recapitulation of the geotextile effective length will be shown in Table 5.7.

**Table 5. 7 Recapitulation of Geotextile Effective Length**

| Zone | Geotextile | Svi | Zi (m) | Le (m) | Le pakai (m) |
|---|---|---|---|---|---|
| 1 | Geotextile - 1 | 1 | 1 | 1.739 | 2 |
| | Geotextile - 2 | 1 | 2 | 1.739 | 2 |
| 2 | Geotextile - 3 | 1 | 3 | 1.739 | 2 |
| | Geotextile - 4 | 1 | 4 | 1.739 | 2 |
| 3 | Geotextile - 5 | 0.5 | 4.5 | 0.869 | 1 |
| | Geotextile - 5 | 0.5 | 4.5 | 0.869 | 1 |

**Continuation Table 5. 7 Recapitulation of Geotextile Effective Length**

| | | | | | |
|---|---|---|---|---|---|
| 3 | Geotextile - 6 | 0.5 | 5 | 0.869 | 1 |
| | Geotextile - 7 | 0.5 | 5.5 | 0.869 | 1 |
| | Geotextile - 8 | 0.5 | 6 | 0.869 | 1 |
| | Geotextile - 9 | 0.5 | 6.5 | 0.869 | 1 |
| | Geotextile - 10 | 0.5 | 6.75 | 0.869 | 1 |

3. Geotextile length on active zone (Lz)

   Lz =(H-Zi). $\tan(45° - \frac{\varphi}{2})$

   For the calculation of geotextile length on active zone number 1 on zone 1

   Lz =(2-1). $\tan(45° - \frac{14.5}{2})$

   $= 0.774\ m$

Based on the calculation of geotextile length on active zone, the length used is 1 m. The recapitulation of the geotextile length on active zone will be shown in Table 5.8.

**Table 5. 8 Recapitulation of Geotextile Length on Active Zone**

| Zone | Geotextile | Svi | Zi (m) | Lz (m) | Lz used (m) |
|---|---|---|---|---|---|
| 1 | Geotextile - 1 | 1 | 1 | 0.774 | 1 |
| | Geotextile - 2 | 1 | 2 | 0.000 | 1 |
| 2 | Geotextile - 3 | 1 | 3 | 0.774 | 1 |
| | Geotextile - 4 | 1 | 4 | 0.000 | 1 |
| 3 | Geotextile - 5 | 0.5 | 4.5 | 1.742 | 2 |
| | Geotextile - 6 | 0.5 | 5 | 1.355 | 1.5 |
| | Geotextile - 7 | 0.5 | 5.5 | 0.968 | 1 |
| | Geotextile - 8 | 0.5 | 6 | 0.581 | 1 |
| | Geotextile - 9 | 0.5 | 6.5 | 0.194 | 1 |
| | Geotextile - 10 | 0.5 | 6.75 | 0.000 | 1 |

4. Geotextile total length

   Ltotal = Lo + Sv + Le + Lz

   For the calculation of geotextile total length number 1 on zone 1

   Ltotal =3.5 + 1 + 2 + 1

   = 7.5 $m$

Based on the calculation of geotextile total length, the length used is 7.5 m. The recapitulation of the geotextile total length will be shown in Table 5.9.

**Table 5. 9 Recapitulation of Geotextile Total Length**

| Zone | Geotextile | Svi | Zi (m) | Lo (m) | Le (m) | Lz (m) | Ltotal (m) |
|---|---|---|---|---|---|---|---|
| 1 | Geotextile - 1 | 1 | 1 | 3.5 | 2 | 1 | 7.5 |
| | Geotextile - 2 | 1 | 2 | 2 | 2 | 1 | 6 |
| 2 | Geotextile - 3 | 1 | 3 | 1.5 | 2 | 1 | 5.5 |
| | Geotextile - 4 | 1 | 4 | 1 | 2 | 1 | 5 |
| 3 | Geotextile - 5 | 0.5 | 4.5 | 1 | 1 | 2 | 4.5 |
| | Geotextile - 6 | 0.5 | 5 | 1 | 1 | 1.5 | 4 |
| | Geotextile - 7 | 0.5 | 5.5 | 1 | 1 | 1 | 3.5 |
| | Geotextile - 8 | 0.5 | 6 | 1 | 1 | 1 | 3.5 |
| | Geotextile - 9 | 0.5 | 6.5 | 1 | 1 | 1 | 3.5 |
| | Geotextile - 10 | 0.5 | 6.75 | 1 | 1 | 1 | 3.5 |

### 5.5.4 Control of Tensile Strength between Soil and Geotextile

The control of tensile strength between soil and geotextile is to know the vertical load that transferred by the soil embankment. The geotextile will be tensioned and redistribute the stress to the passive soil resistance. Therefore, control of tensile strength is required to ensure the geotextiles are able to withstand the working tensile strength by calculating the occurring shear stress. The working tensile strength on geotextile can be determined by equation below.

1. Zone 1

$$\tau = c + \sigma\, x \tan\varphi$$
$$= 10.79 + (\tfrac{1}{2}\, x\, 1\, x\, 12.49\, x \tan 14.5)$$
$$= 10.919\ kN/m$$

2. Zone 2

$$\tau = c + \sigma\, x \tan\varphi$$
$$= 10.79 + (\tfrac{1}{2}\, x\, 1\, x\, 12.49\, x \tan 14.5)$$
$$= 10.919\ kN/m$$

3. Zone 2

$$\tau = c + \sigma\, x \tan\varphi$$

$= 10.79 + (\frac{1}{2}\ x\ 0.5\ x\ 12.49\ x \tan 14.5)$

$= 10.855\ kN/m$

Working tensile strength on geotextile.

$T = (\tau_1 + \tau_2 + \tau_3)$

$= 10.919\ + 10.919\ + 10.855$

$= 32.693\ kN/m\ <$ 52 kN/m

Based on the calculation of working tensile strength on geotextile obtained 32.693 kN/m, while the allowable tensile strength on geotextile used is 52 kN/m. It can be concluded that the allowable tensile strength is exceeding the working tensile strength. Therefore, the geotextiles are able to withstand the working tensile strength.

## 5.6 Embankment of Existing Condition Using Geotextile Reinforcement

The analysis of Embankment slope using geotextile reinforcement on PLAXIS V20. The modelling for the embankment construction phase using the soil embankment based on the field. The embankment that will be used is STA 5+325 of Tawang-Ngalang Segment IV Road. The width of the existing embankment is 42.3 meters, the height is 6.75 meters, and the angle of the slope is 25º.

### 5.6.1 Analysis of Construction Phase Existing Embankment Using Geotextile Reinforcement

The stability analysis of the existing embankment using geotextile with internal slope angle of 25º is conducted in three phases. The first phase assumes that the embankment is completed to a height 2.75 meters, followed by an analysis of the embankment condition. The analysis is continued at height of 4.75 meters, and 6.75 meters, by adding pavement load of 10 kN/m. The construction phase can be seen in Figure 5.4.

1. Embankment Phase 1

   The phase 1 of existing embankment with angle of 25º is done to the height of 2.75 m. In order to know the deformation occurring on the location due to the loads mentioned before, deformed mesh is necessary. Deformed Mesh existing embankment phase 1 using geotextile based on PLAXIS V20 analysis can be seen in Figure 5.29.

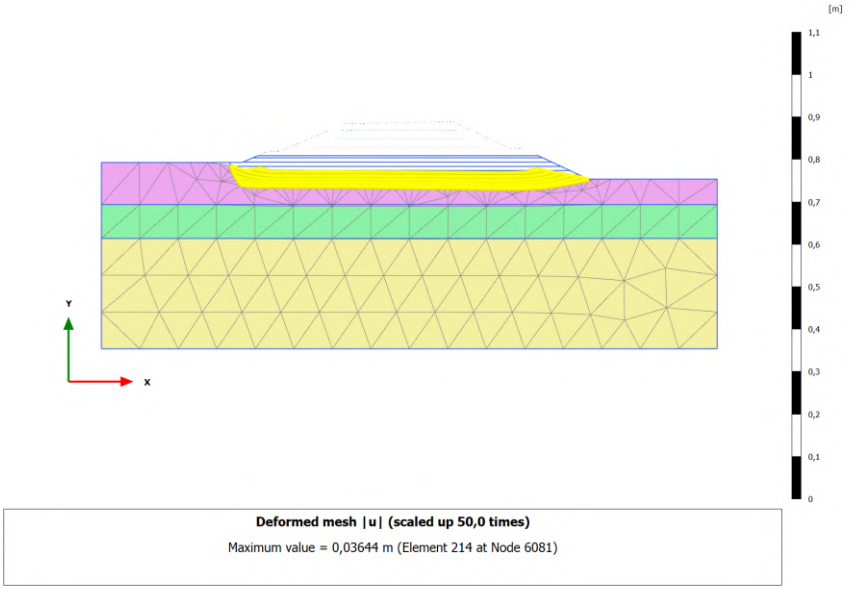


**Figure 5. 29 Deformed Mesh Existing Embankment Phase 1 Using Geotextile Due to Embankment Load**

Displacement occurs on phase 1 of existing embankment with angle of 25º without reinforcement due to embankment load. Based on the indicator on PLAXIS V20, the bigger displacement shows redder colour. While smaller displacement indicated by the shade of blue. The displacement value of existing embankment phase 1 using geotextile due to embankment load is 0.03644 m can be seen in Figure 5.30.

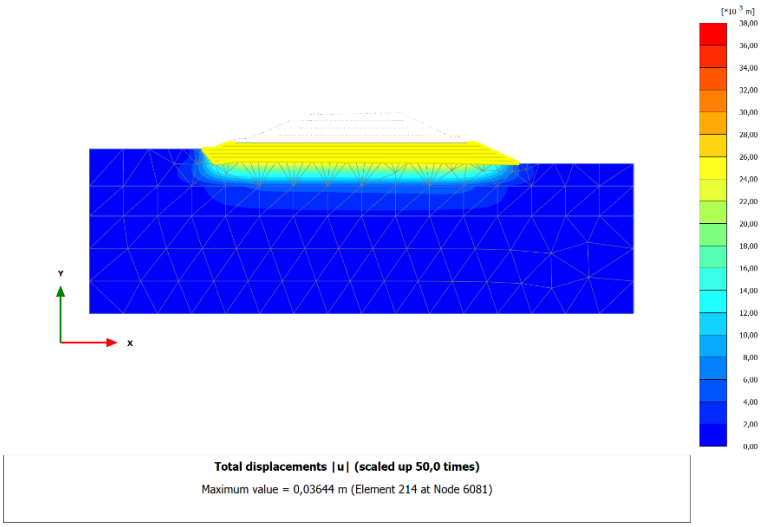


**Figure 5. 30 Displacement Value of Existing Embankment Phase 1 Using Geotextile Due to Embankment Load**

The effective stress is used to calculate the factor of safety for embankment slope. Also, to identify the potentially failed slope area. The maximum amount effective stress of existing embankment phase 1 using geotextile due to embankment load is 5.329 x $10^{-15}$ kN/$m^2$, can be seen in Figure 5.31.

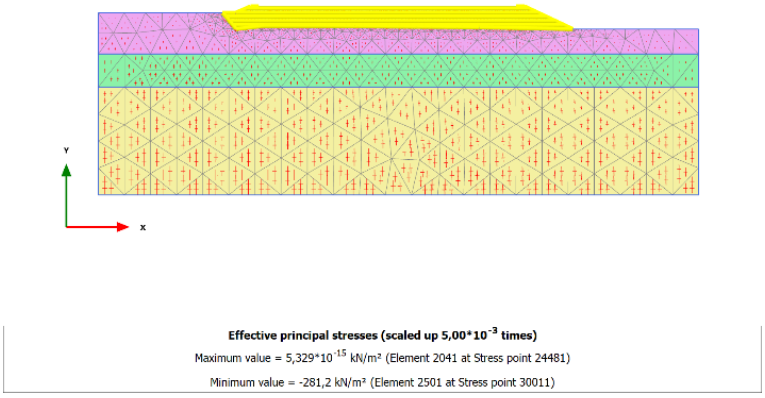


**Figure 5. 31 Effective Stress of Existing Embankment Phase 1 Using Geotextile Due to Embankment**

Based on the PLAXIS V20 analysis, the type of the slope failure is rotation failure. The analysis result on PLAXIS V20 shows the factor of safety is 3.861. The stability analysis result show that the slope is in safe condition, with a factor of safety already meet the minimum requirement. Potential failure area on existing embankment phase 1 with angle of 25º using geotextile due to embankment load can be seen in Figure 5.32.

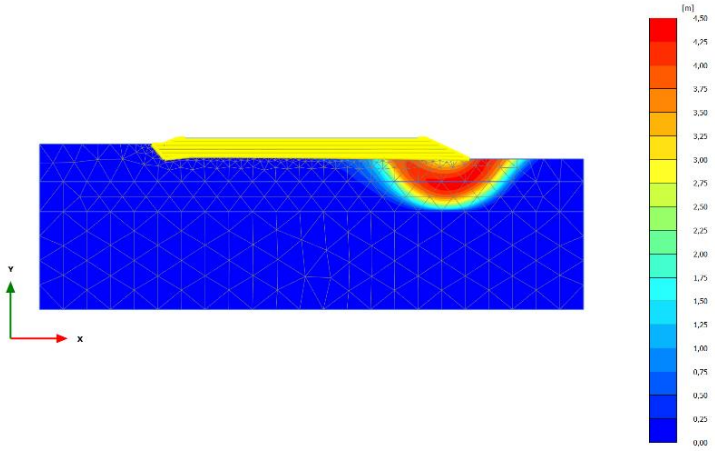

**Figure 5. 32 Potential Failure Area on Existing Embankment Phase 1 With Angle Of 25º Using Geotextile Due to Embankment Load**

2. Embankment Phase 2

   The phase 2 of existing embankment with angle of 25º is done to the height of 4.75 m. In order to know the deformation occurring on the location due to the loads mentioned before, deformed mesh is necessary. Deformed Mesh existing embankment phase 2 using geotextile reinforcement based on PLAXIS V20 analysis can be seen in Figure 5.33.

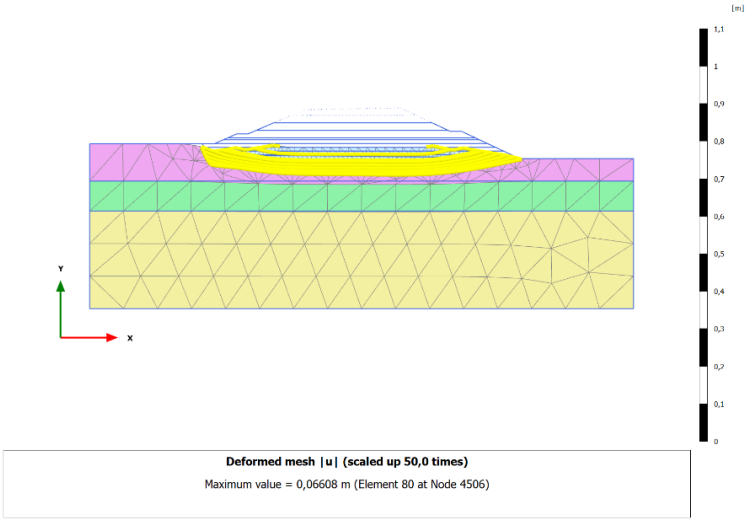


**Figure 5. 33 Deformed Mesh of Existing Embankment Phase 2 Using Geotextile Reinforcement Due to Embankment Load**

Displacement occurs on phase 1 of existing embankment with angle of 25º without reinforcement due to embankment load. Based on the indicator on PLAXIS V20, the bigger displacement shows redder colour. While smaller displacement indicated by the shade of blue. The displacement value of existing embankment phase 2 using geotextile due to embankment load is 0.06608 m can be seen in Figure 5.34.

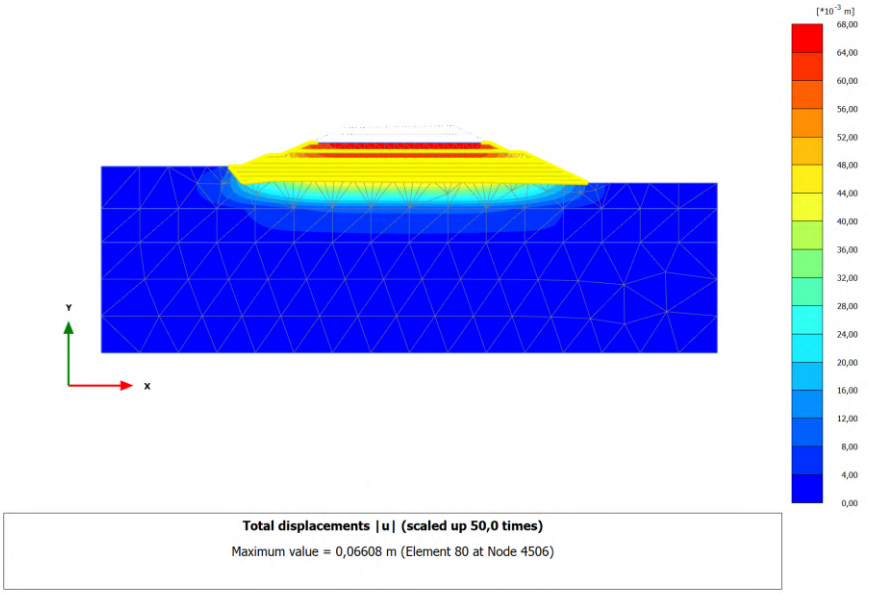


**Figure 5. 34 Displacement Value of Existing Embankment Phase 2 Using Geotextile Due to Embankment Load**

The effective stress is used to calculate the factor of safety for embankment slope. Also, to identify the potentially failed slope area. The maximum amount effective stress of existing embankment phase 2 using geotextile due to embankment load is 8.882 x $10^{-15}$ kN/$m^2$, can be seen in Figure 5.35.

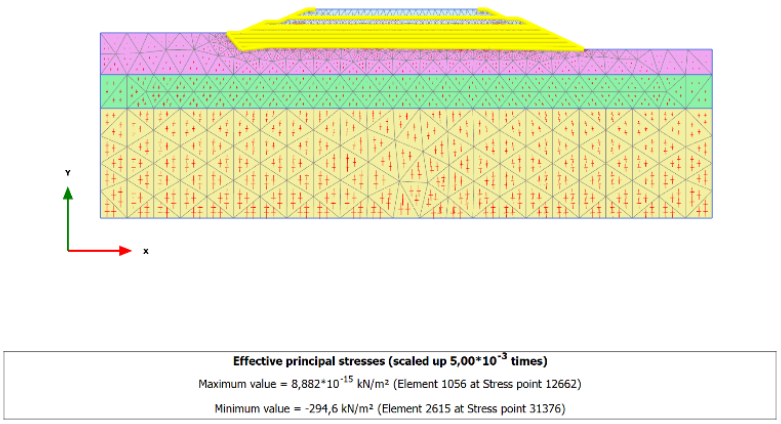


**Figure 5. 35 Effective Stress of Existing Embankment Phase 2 Using Geotextile Due to Embankment Load**

Based on the PLAXIS V20 analysis, the type of the slope failure is rotation failure. The analysis result on PLAXIS V20 shows the factor of safety is 2.393. The stability analysis result show that the slope is in safe condition, with a factor of safety already meet the minimum requirement. Potential failure area on existing embankment phase 2 with angle of 25º using geotextile due to embankment load can be seen in Figure 5.36.

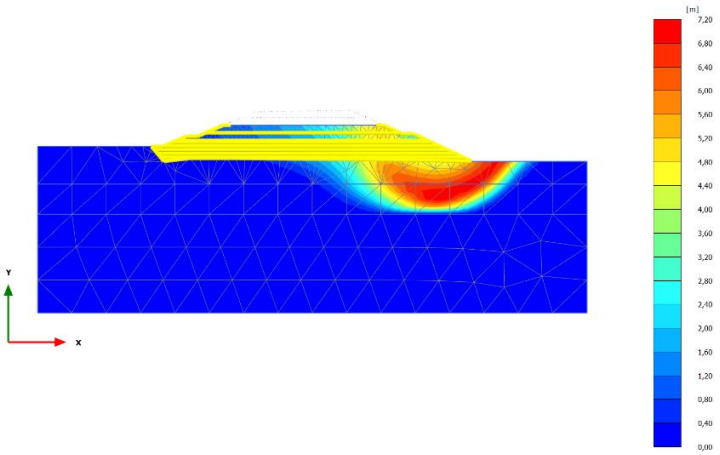

**Figure 5. 36 Potential Failure Area on Existing Embankment Phase 2 with Angle of 25º Using Geotextile Due to Embankment Load**

3. Embankment Phase 3

The phase 3 of existing embankment with angle of 25º is done to the height of 6.75 m. The pavement load of 10 kN/m$^2$ and earthquake load is added to

embankment phase 3 analysis. In order to know the deformation occurring on the location due to the loads mentioned before, deformed mesh is necessary. Deformed Mesh for the existing embankment with angle of 25º by adding pavement and earthquake loads using geotextile based on PLAXIS V20 analysis can be seen on Figure 5.37 and 5.38.

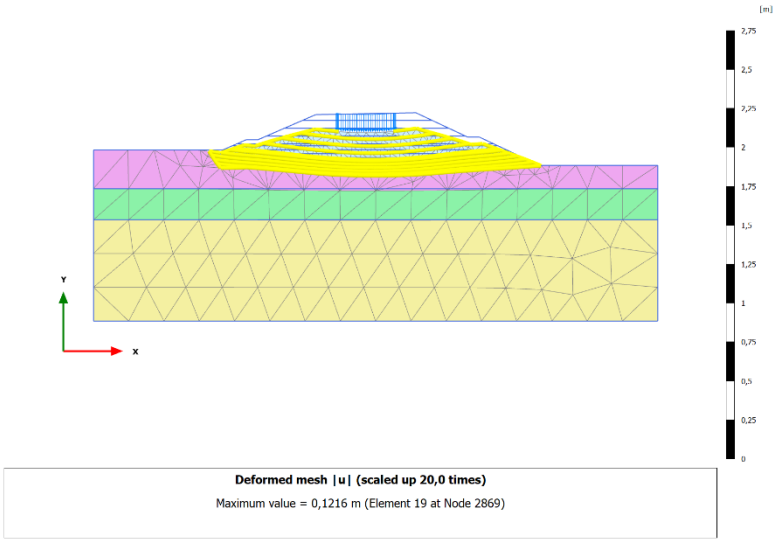


**Figure 5. 37 Deformed Mesh for Existing Embankment with Angle of 25º By Adding Pavement Load Using Geotextile**

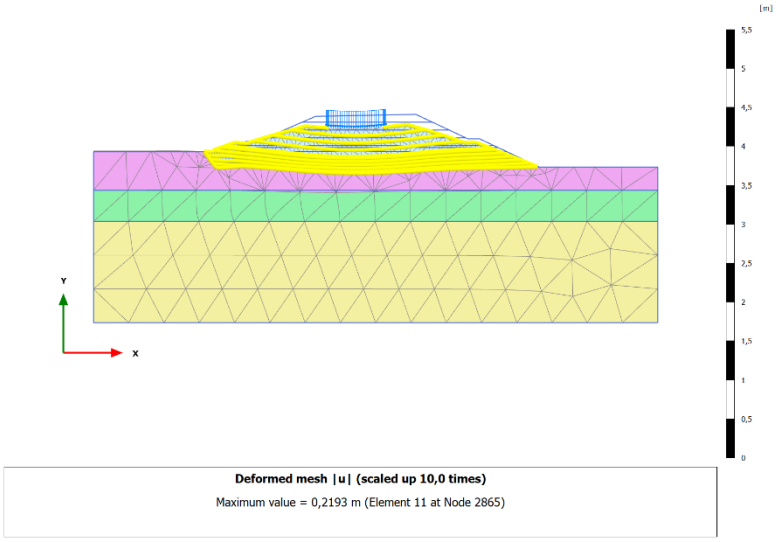


**Figure 5. 38 Deformed Mesh for Existing Embankment Angle of 25º By Adding Pavement and Earthquake Loads Using Geotextile**

Vertical displacement occurs on phase 3 of existing embankment with angle of 25º using geotextile. Based on the indicator on PLAXIS V20, the bigger

displacement shows redder colour. While smaller displacement indicated by the shade of blue. The displacement value of the existing embankment with angle of 25º by adding pavement load using geotextile is 0.1216 m, while the displacement value of the existing embankment with angle of 25º by adding pavement and earthquake loads using geotextile 0.2193 m can be seen on Figure 5.39 and Figure 5.40.

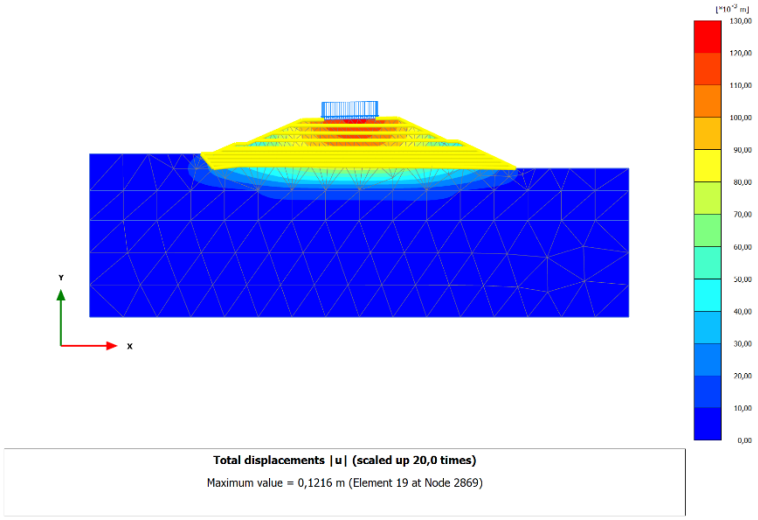


**Figure 5. 39 Displacement Value of Existing Embankment with Angle of 25º By Adding Pavement Load Using Geotextile**

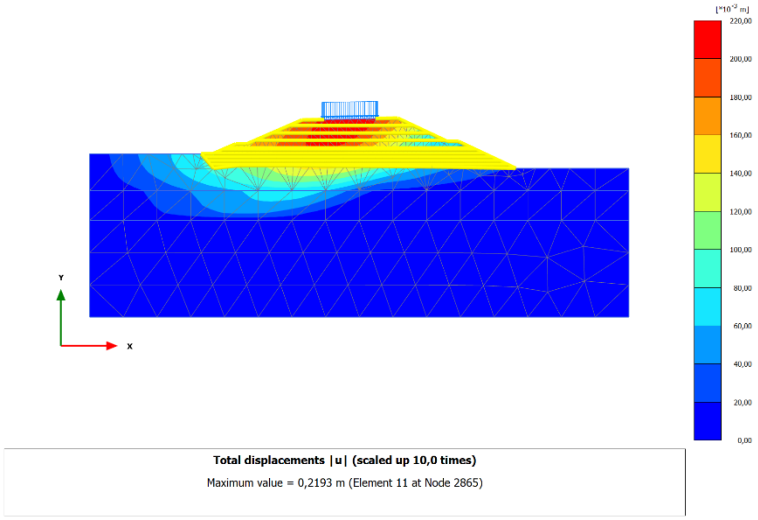


**Figure 5. 40 Displacement Value of Existing Embankment with Angle of 25º By Adding Pavement and Earthquake Loads Using Geotextile**

The effective stress is used to calculate the factor of safety for embankment slope. Also, to identify the potentially failed slope area. The maximum amount effective stress of existing embankment phase 3 using geotextile due to road structure load is 0.01776 x $10^{-12}$ kN/$m^2$, while the maximum amount effective stress of existing embankment phase 3 using geotextile due to road structure and earthquake load is 58.59 kN/$m^2$.  can be seen in Figure 5.41 and Figure 5.42.

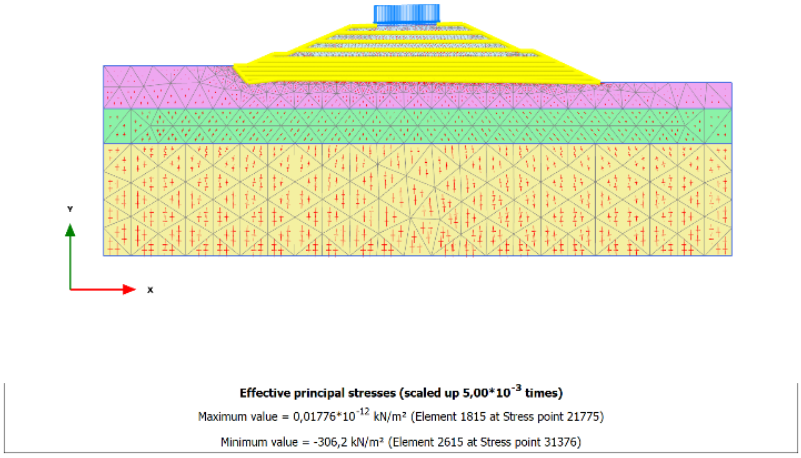


**Figure 5. 41 Effective Stress of Existing Embankment Phase 3 Using Geotextile By Adding Road Structure Load**

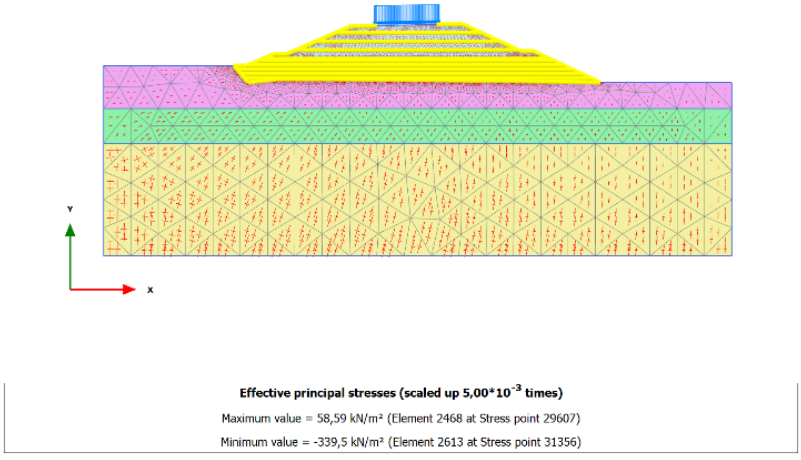


**Figure 5. 42 Effective Stress of Existing Embankment Phase 3 Using Geotextile By Adding Road Structure and Earthquake Load**

Based on the PLAXIS V20 analysis, the type of the slope failure is rotation failure. The analysis result for existing embankment with angle of 25º by adding pavement load on PLAXIS V20 shows the factor of safety is 2.984. While the analysis result for existing embankment with angle of 25º by adding pavement and earthquake loads on PLAXIS V20 shows the factor of safety is 1.048. Potential failure area on the existing embankment with angle of 25º by adding pavement and earthquake loads using geotextile can be seen on Figure 5.43 and Figure 5.44.

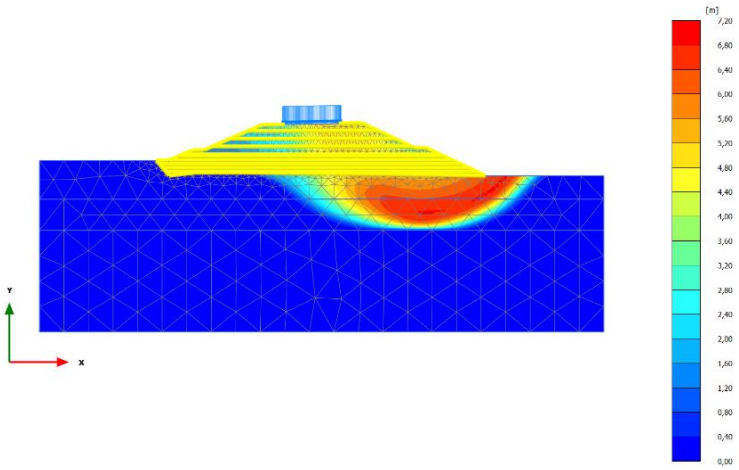


**Figure 5. 43 Potential Failure Area on Existing Embankment with Angle of 25º By Adding Pavement Load Using Geotextile**

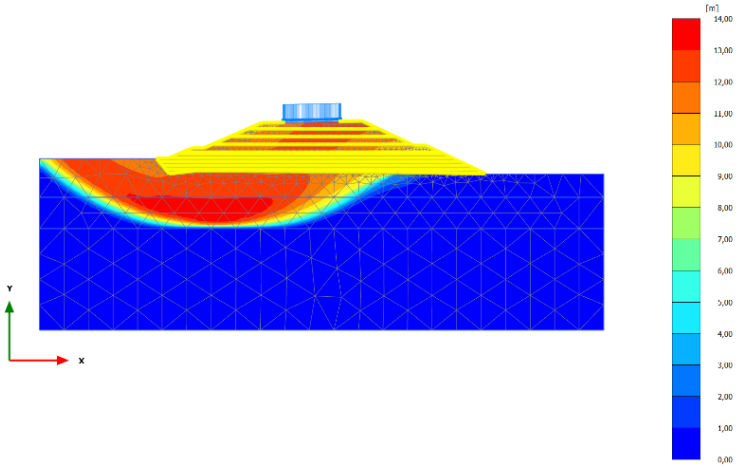


**Figure 5. 44 Potential Failure Area on Existing Embankment with Angle of 25º By Adding Pavement and Earthquake Loads Using Geotextile**

The analysis using PLAXIS indicated a total consolidation settlement of 0.1378 meter for the existing embankment phase 3 using geotextile with angle of 25º after a 365-day consolidation period. Consolidation settlement of existing embankment phase 3 with angle of 25º can be seen on Figure 5.45.

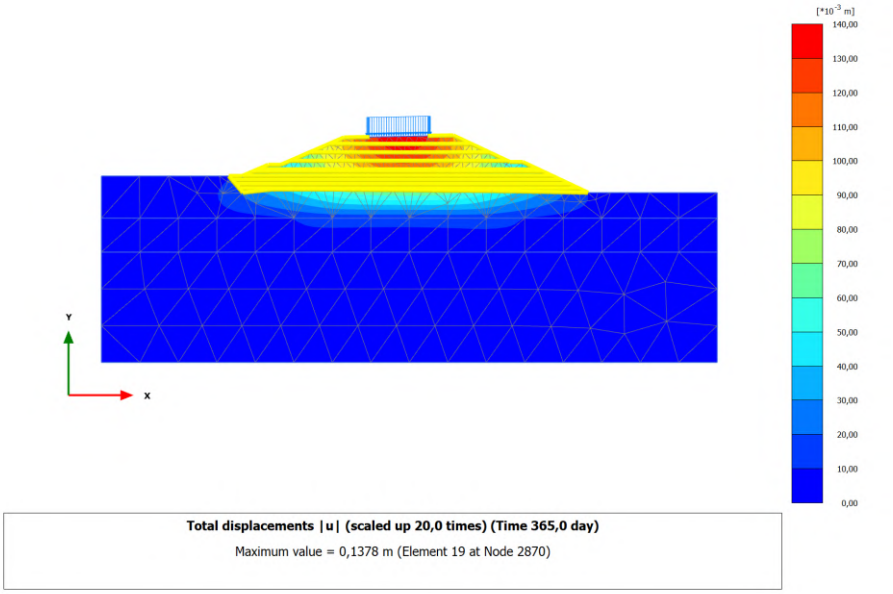


**Figure 5. 45 Consolidation Settlement of Existing Embankment Phase 3 Using Geotextile with Angle of 25º**

### 5.6.2 Analysis of Post-Construction Existing Embankment Using Geotextile Reinforcement

Post construction embankment means that road constructing can be started. The road structure and traffic loads of 25 kN/$^2$ and earthquake load is added to the post-construction analysis. In order to know the deformation occurring on the location due to the loads mentioned before, deformed mesh is necessary. Deformed Mesh for the existing embankment with angle of 25º by adding the road structure load and earthquake load using geotextile based on PLAXIS V20 analysis can be seen on Figure 5.46 and Figure 3.47.

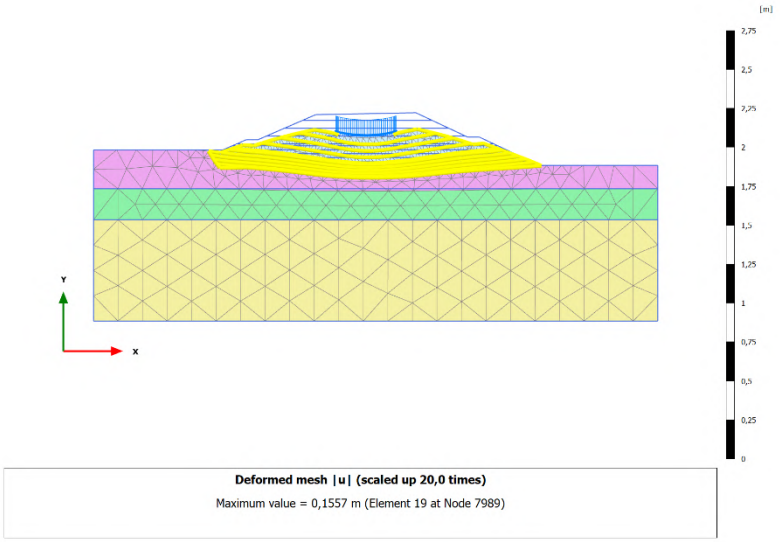


**Figure 5. 46 Deformed Mesh for Existing Embankment with Angle Of 25º By Adding Road Structure Load Using Reinforcement**

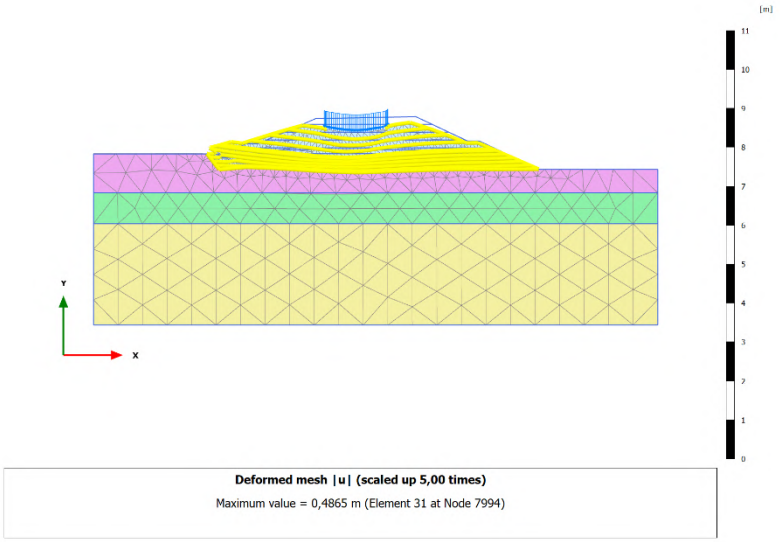


**Figure 5. 47 Deformed Mesh for Existing Embankment with Angle Of 25º By Adding Road Structure and Earthquake Loads Using Reinforcement**

Vertical displacement occurs on post construction embankment with angle of 25º without reinforcement. Based on the indicator on PLAXIS V20, the bigger displacement shows redder colour. While smaller displacement indicated by the shade of blue. The displacement value of the existing embankment with angle of 25º by adding the road structure load using geotextile is 0.1557 m, while displacement value of the existing embankment with angle of 25º by adding the

road structure load and earthquake load using geotextile is 0.4865 m can be seen on Figure 5.48 and Figure 5.49.

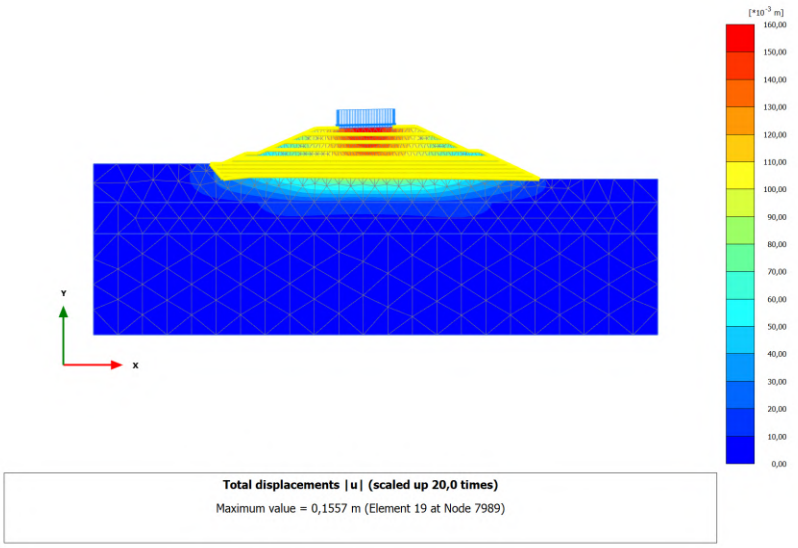


**Figure 5. 48 Displacement Value of Existing Embankment with Angle Of 25º By Adding Road Structure Load Using Geotextile**

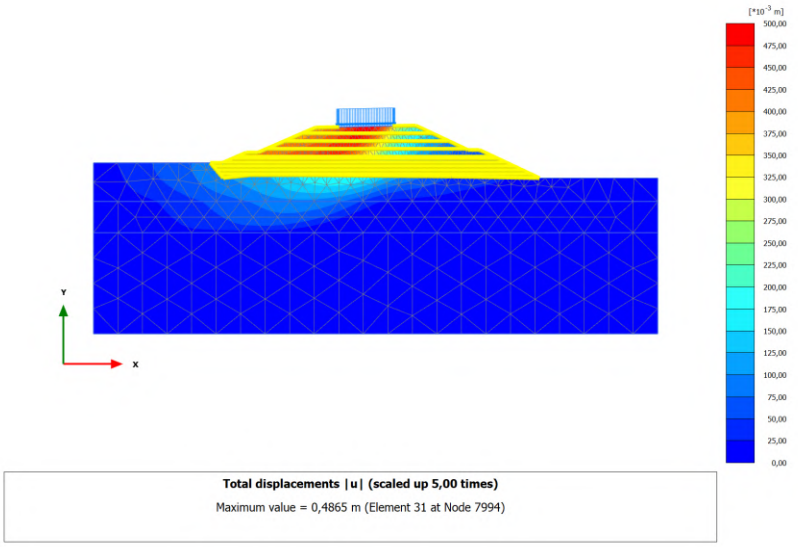


**Figure 5. 49 Displacement Value of Existing Embankment with Angle Of 25º By Adding Road Structure and Earthquake Load Using Geotextile**

The effective stress is used to calculate the factor of safety for embankment slope. Also, to identify the potentially failed slope area. The maximum amount effective stress of existing embankment with angle of 25º by adding pavement load using geotextile is 0.01776 x $10^{-12}$ kN/$m^{-12}$ kN/$m^2$, while the maximum amount effective

stress of existing embankment phase 3 using geotextile due to road structure and earthquake load is 58.59 kN/m$^2$. The effective stress of existing embankment with angle of 25º by adding road structure and earthquake load using geotextile can be seen in Figure 5.50 and Figure 5.51.

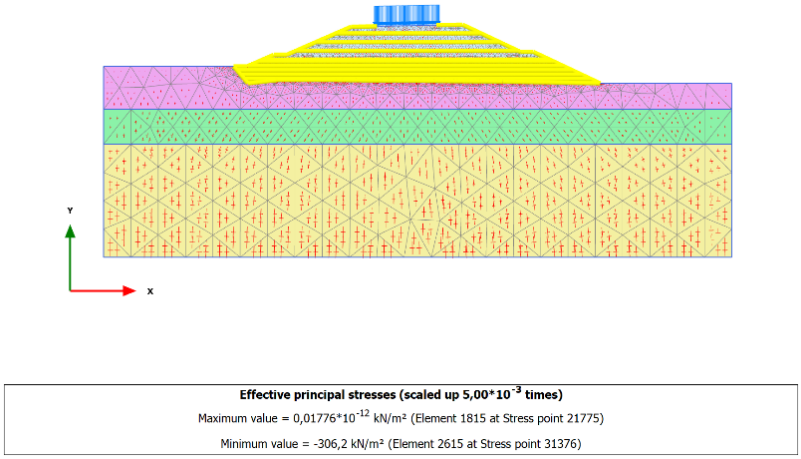


**Figure 5. 50 Effective Stress of Existing Embankment with Angle Of 25º By Adding Road Structure Using Geotextile**

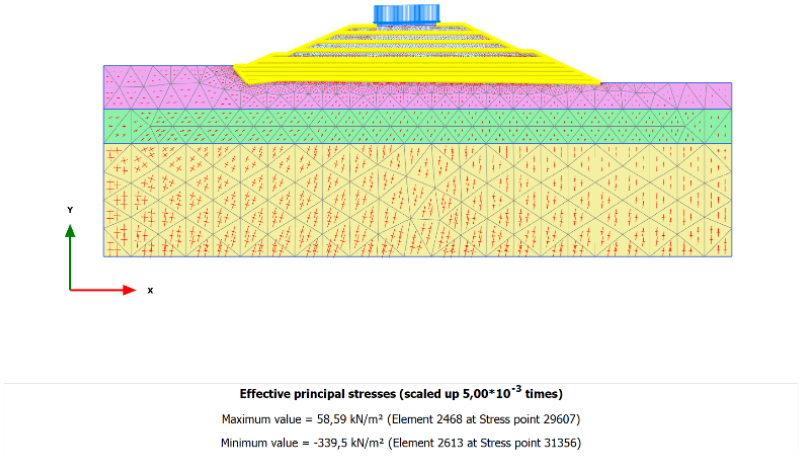


**Figure 5. 51 Effective Stress of Existing Embankment with Angle Of 25º By Adding Road Structure and Earthquake Load Using Geotextile**

Based on the PLAXIS V20 analysis, the type of the slope failure is rotation failure. The analysis result for existing embankment with angle of 25º by adding the road structure load on PLAXIS V20 shows the factor of safety is 2.702. While the

analysis result for existing embankment with angle of 25º by adding the road structure load and earthquake load on PLAXIS V20 shows the factor of safety is 1.402. Potential failure area on the existing embankment with angle of 25º by the road structure load and earthquake load using geotextile can be seen on Figure 5.52 and Figure 5.53.

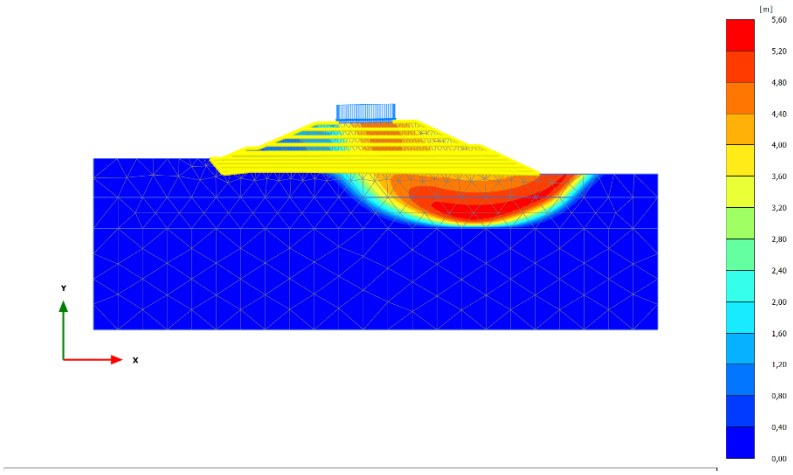


**Figure 5. 52 Potential Failure Area on Existing Embankment with Angle Of 25º By Road Structure Load Using Geotextile**

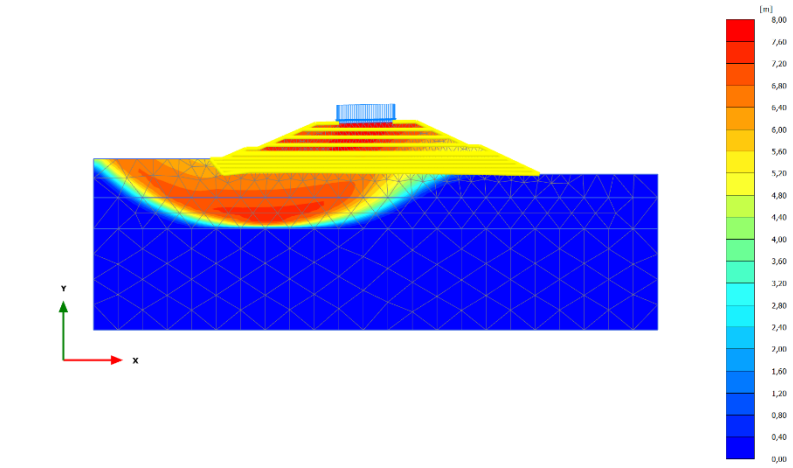


**Figure 5. 53 Potential Failure Area on Existing Embankment with Angle of 25º By Road Structure and Earthquake Load Using Geotextile**

The analysis using PLAXIS indicated a total consolidation settlement of 0.1813 meter for the existing embankment phase 3 with angle of 25º after a 365-day consolidation period. Consolidation settlement of existing embankment post-construction with angle of 25º can be seen on Figure 5.54.

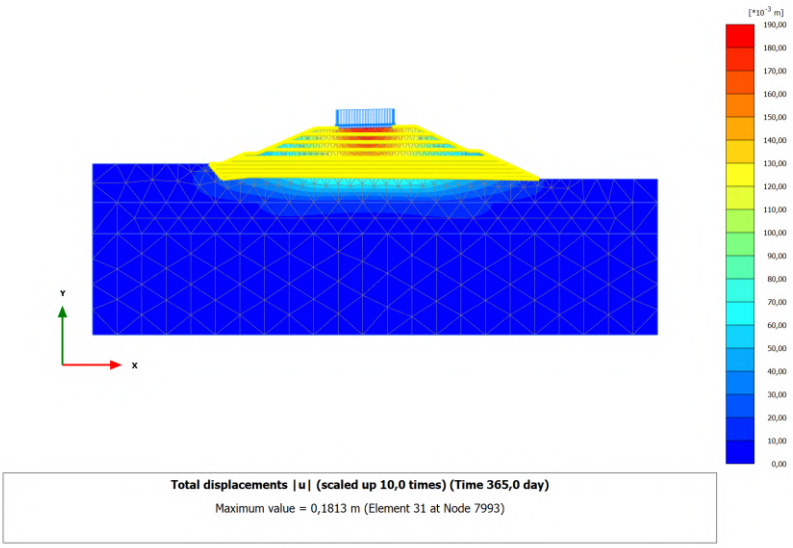


**Figure 5. 54 Consolidation Settlement of Reinforced Existing Embankment Post-Construction with Angle Of 25º**

Based on the embankment stability analysis for existing embankment with internal friction angle of 25˚, factor of safety on embankment with geotextile reinforcement under pavement load is still relatively safe with value more than 1.5 as planned previously. While added with both pavement and earthquake loads, the minimum factor of safety based on SNI 8460:2017 of 1.1 could be obtained. Therefore, smaller value of internal friction angle of 20˚ is created to provide a better alternative.

## 5.7 Discussion

Embankment stability analysis research is meant to find the value of embankment factor of safety. The embankment stability analysis is conducted using PLAXIS V20 based on Finite Element Method under the condition of existing embankment and alternative embankment that has been determined before. Then, the analysis is conducted in two conditions, with and without geotextile reinforcement. Embankment stability analysis is based on construction and post-construction phases. Parameter used for the analysis includes uniformly distributed load of the road structure, traffic load, and earthquake load that refers to earthquake zone map of Indonesia.

### 5.7.1 Factor of safety

Slope stability is an extremely critical aspects in terms of slope structure to resist any external forces that will result in failure. The stability of slope is measured by Factor of Safety. The value is taken based on SNI 8460:2017 about the requirement of geotechnical engineering. The factor of safety for slope structure is no less than 1.25 under normal condition when loaded only with pavement and traffic load. While under the earthquake load, the factor of safety must be or no less than 1.1.

1. Construction phase

   During this phase, the slope condition is still in undrained condition, where stability is not yet achieved due to adjustments of specific gravity of the soil due to the immediate loading. For construction phase, the factor of safety is affected solely by the embankment phase, and for the top layer of the embankment added with pavement and earthquake loads. The factor of safety recapitulation for construction phase can be seen on Table 5.10.

**Table 5. 10 Factor of Safety Recapitulation for Construction Phase**

| Data | Phase 1 | Phase 2 | Phase 3 | |
|---|---|---|---|---|
| | | | Pavement Load | Pavement and Earthquake Loads |
| Existing Embankment of 25$^{o}$ | 3.479 | 2.234 | 1.444 | 1.048 |
| Existing Embankment of 25$^{o}$ Using Geotextile | 5.247 | 3.659 | 2.984 | 1.473 |
| Embankment of 20$^{o}$ | 3.861 | 2.393 | 1.598 | 1.077 |
| Embankment of 20$^{o}$ Using Geotextile | 5.705 | 4.102 | 3.307 | 1.509 |

To better understand regarding the trend of safety factor due to the loading of each variation, the bar chart is presented on Figure 5.55.

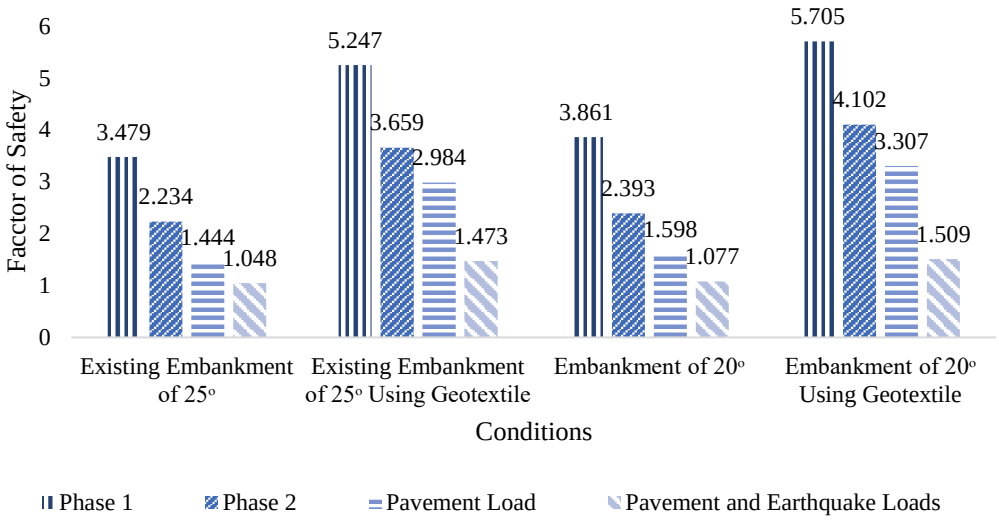


**Figure 5. 55 Safety Factor for Construction Phase**

The factor of safety of each phase indicates a decreasing trend in its value. As the embankment height increase in each phase, the load on embankment also increased.

While analysis on smaller angle resulting a factor of safety value that meets the requirement in SNI 8460:2017. As the smaller angle produce smaller shear stresses. Therefore, the slope is safer compare to the existing angle with bigger value.

Based on the analysis result, the application of geotextile can increase the factor of safety of each phase, both existing embankment, as well as alternative embankment. The shear capacity also increseas as the result of geotextile installation.

2. Post-construction

   On this phase, the slope condition is in drained condition because the stability of pore water pressure is already achieved. The factor of safety recapitulation for post-construction can be seen on Table 5.11.

**Table 5. 11 Factor of Safety Recapitulation for Post-Construction**

| Data | Road Structure Load | Road Structure and Earthquake Load |
|---|---|---|
| Existing Embankment of 25° | 1.211 | collapse |
| Existing Embankment of 25° Using Geotextile | 2.702 | 1.402 |
| Embankment of 20° | 1.343 | collapse |
| Embankment of 20° Using Geotextile | 2.944 | 1.483 |

To better understand regarding the trend of safety factor due to the loading of each variation, the bar chart is presented on Figure 5.56.

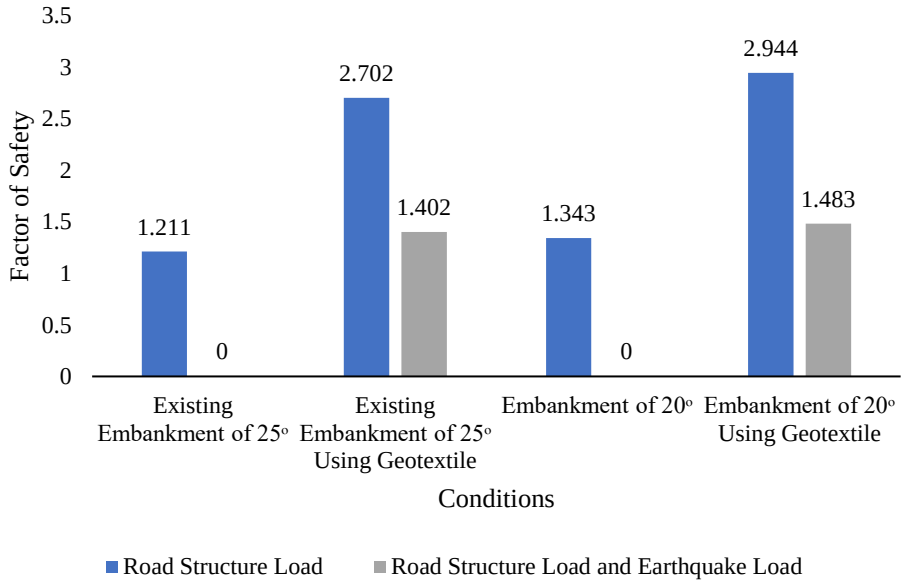


**Figure 5. 56 Safety Factor for Post-construction Phase**

The safety factor on post-construction phase has smaller value compares to the one during construction phase. Because the working load of embankment during this phase is bigger.

Based on the analysis result, the application of geotextile can increase the factor of safety of each phase, both existing embankment, as well as alternative embankment. The shear capacity also increseas as the result of geotextile installation.

### 5.7.2 Consolidation Settlement

The settlement and stability of soil embankment related to each other. Uneven settlement can result in instability on embankment slope. Settlement occurs due to the working load on soil, both from the self-weight load and additional load from the upper structure. The recapitulation of settlement can be seen in Table 5.12.

**Table 5. 12 Recapitulation of Consolidation Settlement**

| Consolidation Settlement | Construction Phase | Post-Construction |
|---|---|---|
| Existing Embankment of 25° | 0.1405 m | 0.1905 m |
| Existing Embankment of 25° Using Geotextile | 0.1378 m | 0.1813 m |
| Embankment of 20° | 0.1364 m | 0.1845 m |
| Embankment of 20° Using Geotextile | 0.1345 m | 0.1764 m |

To better understand regarding the trend of safety factor due to the loading of each variation, the bar chart is presented on Figure 5.57.

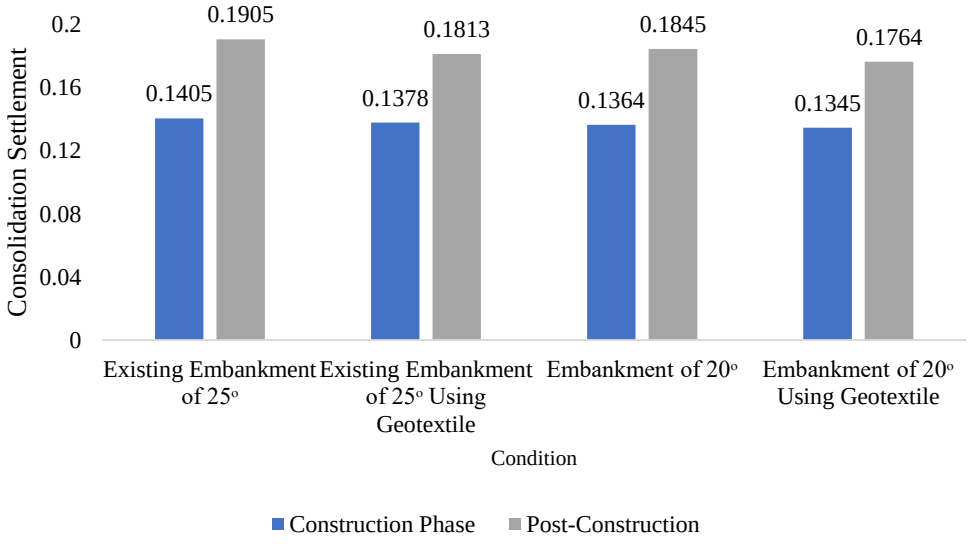


**Figure 5. 57 Consolidation Settlement**

Slope gradient can affect the settlement occured on the slope embankment. The smaller the slope angle, the smaller settlement will occur. This is because the distribution of load working on the lower part of the slope is smaller compare to the gradient of the slope itself.

As has been mentioned before, settlement occurs due to the load working on soil. Therefore, the bigger the load working above the embankment structure, the bigger the settlement will be.

# CHAPTER VI
# CONCLUSION AND SUGGESTION

## 6.1 Conclusion

Based on the analysis and discussion of embankment stability, there are some points that can be drawn as the conclusion. They are:

1. The safety factor analysis of existing slope with internal angle of 25° without reinforcement by using PLAXIS V20 based on finite element method for the construction phase is 1.211, as for the post construction is collapse.
2. The safety factor analysis of reinforced existing slope with internal angle of 25° by using PLAXIS V20 based on finite element method for the construction phase is 2.702, as for the post construction is 1.402.
3. The consolidation settlement of existing slope with internal angle of 25° by using PLAXIS V20 based on finite element method for the construction phase is 0.1405, as for the post construction is 0.1095. While the reinforced existing slope with internal angle of 25° for the construction phase is 0.1378, as for the post construction is 0.1813.
4. The safety factor analysis of alternative internal angle of 20° without reinforcement by using PLAXIS V20 based on finite element method for the construction phase is 1.343, as for the post construction is collapse.
5. The safety factor analysis of reinforced alternative internal angle of 20° by using PLAXIS V20 based on finite element method for the construction phase is 2.944, as for the post construction is 1.483.
6. The consolidation settlement of alternative internal angle of 20° by using the finite element method for PLAXIS V20 based on construction phase is 0.1364, as for the post construction is 0.1845. While the reinforced existing slope with internal angle of 20° for the construction phase is 0.1345, as for the post construction is 0.1764.

## 6.2 Suggestion

There are some suggestions that the writer would like to give to obtain a better result on future research regarding pile foundation design.

1. The application of replacement method is suggested as initial action to reinforce the existing soil. Therefore, the need of additional reinforcement is set to minimum amount.
2. The comprehensive research on the reinforcement type for embankment used to get the most suitable type for the existing condition.
3. The addition of budget plan and time analysis calculations to help the determination of the most effective and efficient embankment reinforcement.

# References


Afdhal, T. (2023). *Analisis Stabilitas Timbunan Lereng Jalan Dengan Perkuatan Geotekstil Menggunakan Program Geoslope 2018 (Studi Kasus: Proyek Jalan Tawang - Ngalang Segmen IV Sta. 7+750 Gunungkidul D.I. Yogyakarta)*.

Arsy, A. A., & Artati, H. K. (2018). Analisis Stabilitas Timbunan Pada Konstruksi Badan Jalan Dengan Perkuatan Geotekstil Menggunakan Metode Fellenius. *Jurnal Teknik Sipil Dan Lingkungan*.

Badan Standardisasi Nasional. (2017). Persyaratan Perancangan Geoteknik. *Standar Nasional Indonesia*, *8460*, 1–323.

Bowles, J. E. (1996). Foundation Analysis and Design. In *Civil Engineering Materials*.

Budhu, M. (2010). *Soil Mechanics and Foundations*.

Budiasto, A., & Purwanto, E. (2018). *Analisis stabilitas timbunan badan jalan dengan perkuatan geotekstil menggunakan program PLAXIS*.

Das, B. M. (1995). Mekanika Tanah Jilid 1(Prinsip-prinsip Rekayasa Geoteknik. *Penerbit Erlangga*, 1–300.

Hardiyatmo. (1992). Mekanika Tanah II. *Gadjah Mada University Press*.

Hardiyatmo, H. C. (2002). Mekanika Tanah I. *Gadjah Mada University Press*.

Isadono, N. S. (2020). *Analisis Stabilitas Timbunan Tanah Menggunakan Perkuatan Geotextile Dengan Program PLAXIS 8.2 Serta Metode Fellenius*. *2*, 1–165.

Marga, D. B. (2017). *Modul Pelatihan Geosintetik*. *1*.

Maulida, A. R. (2023). *Analisis Stabilitas Lereng Timbunan Jalan Dengan Perkuatan Geotekstil Menggunakan Metode Elemen Hingga (Stability Analysis Of Slope Road Embankment With Geotextile Reinforcement Using The Finite Element Method)*.

Panguriseng, D. (2018). *Dasar-Dasar Mekanika Tanah* (Issue January).

Rasdi, R. F. K. (2021). *Analisis Stabilitas Timbunan Tanah Menggunakan Perkuatan Geotekstil Dengan Program PLAXIS 8.2 (Studi Kasus Di Jalan Tol*

*Balikpapan-Samarinda) (Analisys Of Slope Stability Using Geotextil Reinforcement With PLAXIS 8.2)*. *2*, 1–165.

SNI. (2019). *Penerapan Standar Nasional Indonesia*.

Soepandi. 1995. Pengertian Lereng Adalah suatu permukaan tanah yang miring dan membentuk sudut tertentu terhadap suatu bidang horisontal dan tidak terlindungi. Jakarta.

Sukirman, S. (2010). Perencanaan Tebal Struktur Perkerasan Lentur. In *Nova Bandung*.

Suryolelono, K. B. (1993). Teknik fondasi bagian I : fondasi telapak dan dinding penahan tanah. Yogyakarta: NAFIRI.

# Appendix

**Appendix 1 Cross Section of STA 5+325**

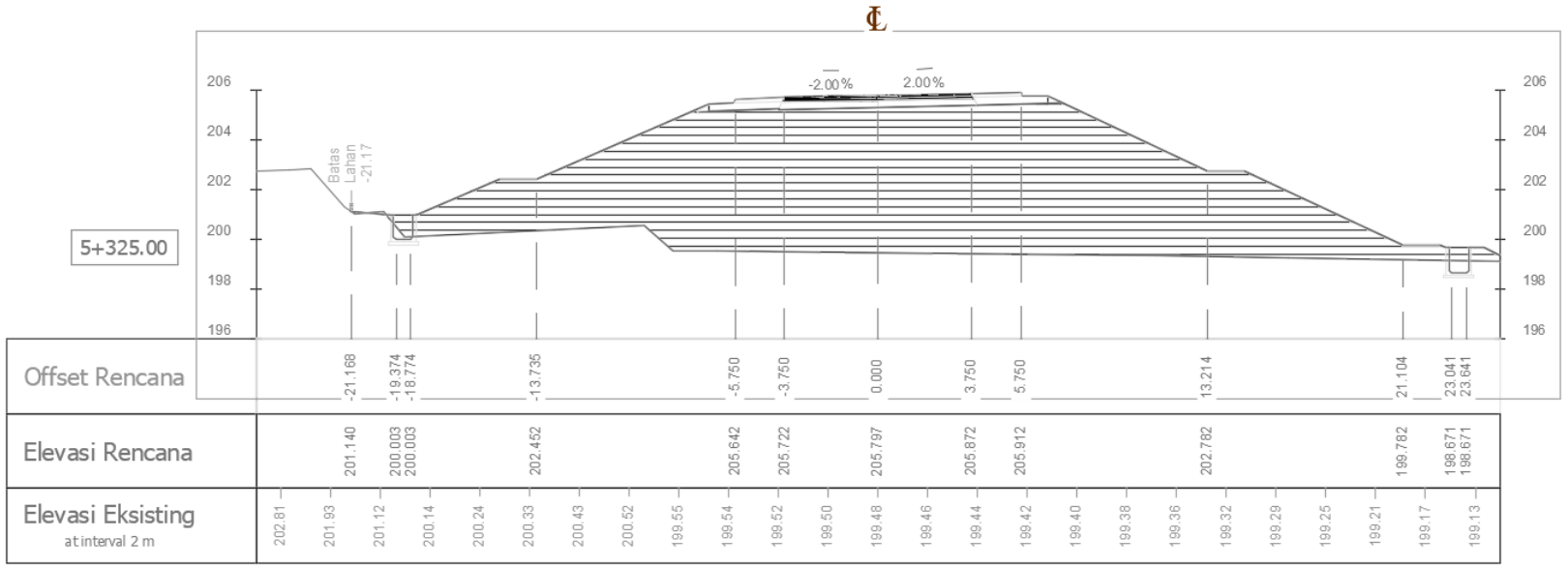

# Appendix 2 SPT Value

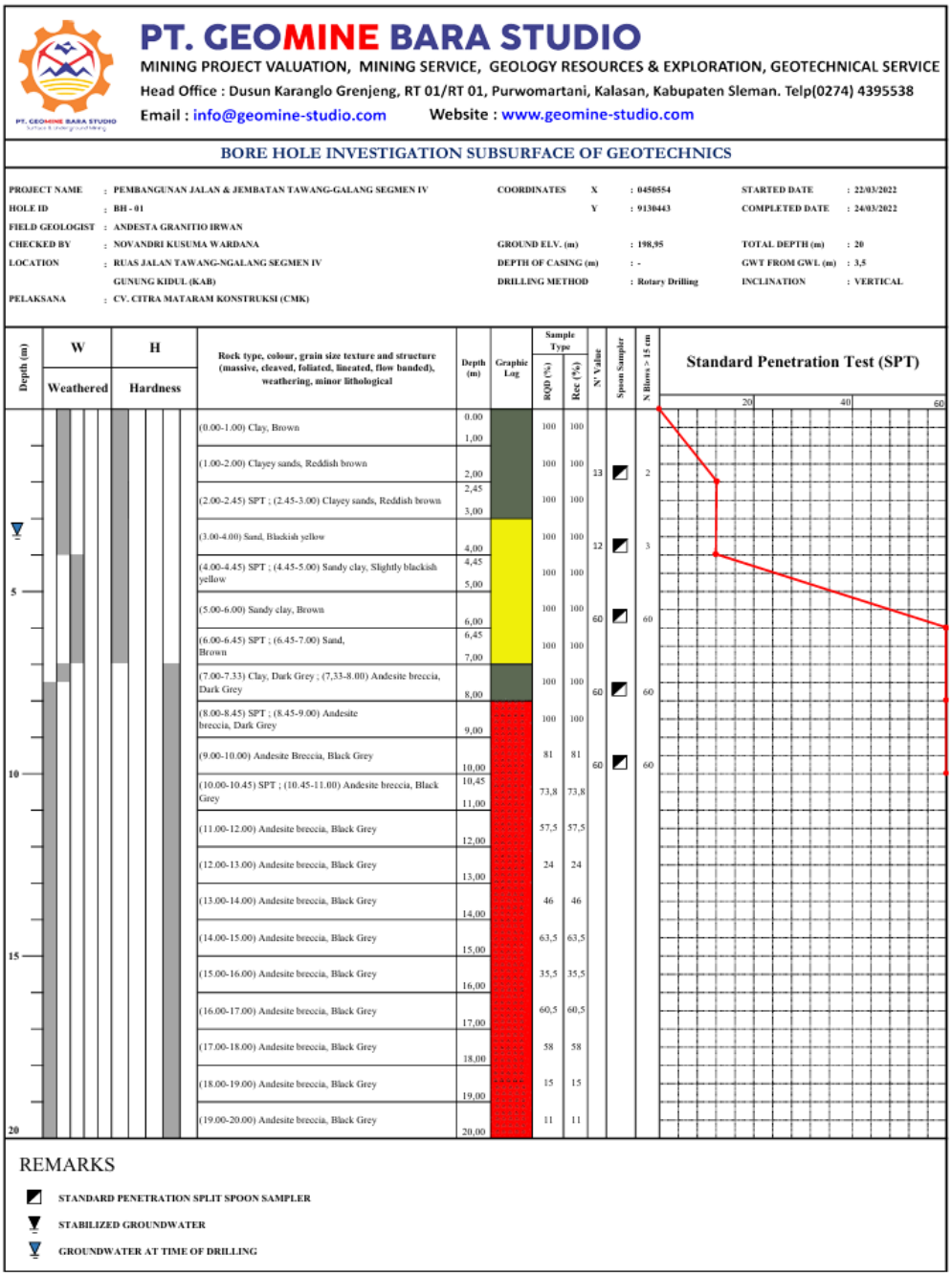

**PT. GEOMINE BARA STUDIO**

MINING PROJECT VALUATION, MINING SERVICE, GEOLOGY RESOURCES & EXPLORATION, GEOTECHNICAL SERVICE

Head Office : Dusun Karanglo Grenjeng, RT 01/RT 01, Purwomartani, Kalasan, Kabupaten Sleman. Telp(0274) 4395538

Email : info@geomine-studio.com Website : www.geomine-studio.com

**BORE HOLE INVESTIGATION SUBSURFACE OF GEOTECHNICS**

| | | | | | |
|---|---|---|---|---|---|
| PROJECT NAME | : PEMBANGUNAN JALAN & JEMBATAN TAWANG-GALANG SEGMEN IV | COORDINATES | X : 0450554 | STARTED DATE | : 22/03/2022 |
| HOLE ID | : BH - 01 | | Y : 9130443 | COMPLETED DATE | : 24/03/2022 |
| FIELD GEOLOGIST | : ANDESTA GRANITIO IRWAN | | | | |
| CHECKED BY | : NOVANDRI KUSUMA WARDANA | GROUND ELV. (m) | : 198,95 | TOTAL DEPTH (m) | : 20 |
| LOCATION | : RUAS JALAN TAWANG-NGALANG SEGMEN IV GUNUNG KIDUL (KAB) | DEPTH OF CASING (m) | : - | GWT FROM GWL (m) | : 3,5 |
| | | DRILLING METHOD | : Rotary Drilling | INCLINATION | : VERTICAL |
| PELAKSANA | : CV. CITRA MATARAM KONSTRUKSI (CMK) | | | | |

| Depth (m) | W Weathered | H Hardness | Rock type, colour, grain size texture and structure (massive, cleaved, foliated, lineated, flow banded), weathering, minor lithological | Depth (m) | Graphic Log | Sample Type | RQD (%) | Rec (%) | N' Value | Spoon Sampler | N Blows > 15 cm | Standard Penetration Test (SPT) |
|---|---|---|---|---|---|---|---|---|---|---|---|---|
| | | | (0.00-1.00) Clay, Brown | 0.00<br>1,00 | | | 100 | 100 | | | | |
| | | | (1.00-2.00) Clayey sands, Reddish brown | 2,00 | | | 100 | 100 | 13 | ◪ | 2 | |
| | | | (2.00-2.45) SPT ; (2.45-3.00) Clayey sands, Reddish brown | 2,45<br>3,00 | | | 100 | 100 | | | | |
| | | | (3.00-4.00) Sand, Blackish yellow | 4,00 | | | 100 | 100 | 12 | ◪ | 3 | |
| | | | (4.00-4.45) SPT ; (4.45-5.00) Sandy clay, Slightly blackish yellow | 4,45<br>5,00 | | | 100 | 100 | | | | |
| | | | (5.00-6.00) Sandy clay, Brown | 6,00 | | | 100 | 100 | 60 | ◪ | 60 | |
| | | | (6.00-6.45) SPT ; (6.45-7.00) Sand, Brown | 6,45<br>7,00 | | | 100 | 100 | | | | |
| | | | (7.00-7.33) Clay, Dark Grey ; (7,33-8.00) Andesite breccia, Dark Grey | 8,00 | | | 100 | 100 | 60 | ◪ | 60 | |
| | | | (8.00-8.45) SPT ; (8.45-9.00) Andesite breccia, Dark Grey | 9,00 | | | 100 | 100 | | | | |
| | | | (9.00-10.00) Andesite Breccia, Black Grey | 10,00 | | | 81 | 81 | 60 | ◪ | 60 | |
| | | | (10.00-10.45) SPT ; (10.45-11.00) Andesite breccia, Black Grey | 10,45<br>11,00 | | | 73,8 | 73,8 | | | | |
| | | | (11.00-12.00) Andesite breccia, Black Grey | 12,00 | | | 57,5 | 57,5 | | | | |
| | | | (12.00-13.00) Andesite breccia, Black Grey | 13,00 | | | 24 | 24 | | | | |
| | | | (13.00-14.00) Andesite breccia, Black Grey | 14,00 | | | 46 | 46 | | | | |
| | | | (14.00-15.00) Andesite breccia, Black Grey | 15,00 | | | 63,5 | 63,5 | | | | |
| | | | (15.00-16.00) Andesite breccia, Black Grey | 16,00 | | | 35,5 | 35,5 | | | | |
| | | | (16.00-17.00) Andesite breccia, Black Grey | 17,00 | | | 60,5 | 60,5 | | | | |
| | | | (17.00-18.00) Andesite breccia, Black Grey | 18,00 | | | 58 | 58 | | | | |
| | | | (18.00-19.00) Andesite breccia, Black Grey | 19,00 | | | 15 | 15 | | | | |
| | | | (19.00-20.00) Andesite breccia, Black Grey | 20,00 | | | 11 | 11 | | | | |

Standard Penetration Test (SPT): 20, 40, 60; depths 5, 10, 15, 20

REMARKS

◪ STANDARD PENETRATION SPLIT SPOON SAMPLER

▼ STABILIZED GROUNDWATER

▼ GROUNDWATER AT TIME OF DRILLING

# Appendix 3 Recapitulation of Laboratory Result

LABORATORIUM MEKANIKA TANAH
JURUSAN TEKNIK SIPIL
FTSP - UII
Gedung 04 Moh Natsir
Kampus Terpadu Universitas Islam Indonesia
Jl. Kaliurang KM 14,4 Yogyakarta 55584
T. (0274) 898444 ext. 3224
F. (0274) 895330
W. ftsp.uii.ac.id

No : 022/Kalab. MT/01/Lab.MT/V/2022
Lampiran : 1 bendel
Hal : Hasil Uji Sampel

Kepada Yth;
Pimpinan
PT Geomin Bara Studio
di
Tempat

Dengan ini kami sampaikan Hasil Uji Sampel Tanah untuk Pekerjaan : Proyek Pembangunan Jalan Segmen IV Tawang-Ngalang, sebagai berikut

| No | Parameter Uji | Satuan | Hasil Uji | | | | | | | | | | | | | |
|---|---|---|---|---|---|---|---|---|---|---|---|---|---|---|---|---|
| A. Soil Properties | | | : D01 GT/TW/08 BH 01 | : D04 GT/TW/07 BH 04 | : D04 GT/TW/03 BH 04 | : D04 GT/TW/02 BH 04 | : D01 GT/TW/15 BH 01 | : D01 GT/TW/04 BH 01 | : D01 GT/TW/01 BH 03 | : D01 GT/TW/02 BH 01 | : D01 GT/TW/09 BH 01 | : D01 GT/TW/09 BH 02 | : D01 GT/TW/06 BH 01 | : D01 GT/TW/03 BH 03 | : D01 GT/TW/10 BH 02 | : D01 GT/TW/01 BH 01 |
| Soil Properties | Kadar air *(Natural Water Content, w)* | % | 51.997 | 4.470 | 32.238 | 32.238 | 2.810 | 30.797 | 36.679 | 4.470 | 17.996 | 9.957 | 30.797 | 49.765 | 13.476 | 25.536 |
| | Berat Jenis Tanah *(Specific Gravity of Soil, Gs)* | | 2.601 | 2.594 | 2.559 | 2.594 | 2.724 | 2.672 | 2.599 | 2.601 | 2.675 | 2.558 | 2.631 | 2.724 | 2.538 | 2.724 |
| | Berat volume tanah basah ($\gamma_b$) | gr/cm$^3$ | 1.668 | 2.180 | 1.628 | 1.652 | 2.289 | 1.651 | 1.698 | 1.620 | 2.023 | 2.101 | 1.815 | 2.104 | 1.916 | 1.668 |
| | Berat volume tanah kering ($\gamma_d$) | gr/cm$^3$ | 1.097 | 2.087 | 1.231 | 1.249 | 2.226 | 1.262 | 1.242 | 1.551 | 1.714 | 1.911 | 1.388 | 1.405 | 1.689 | 1.328 |
| | Angka pori, e | | 1.371 | 0.243 | 1.078 | 1.077 | 0.224 | 1.117 | 1.092 | 0.678 | 0.560 | 0.339 | 0.896 | 0.939 | 0.503 | 1.051 |
| | Porositas, n | % | 57.83 | 19.53 | 51.88 | 51.85 | 18.28 | 52.76 | 52.20 | 40.40 | 35.90 | 25.30 | 47.25 | 48.42 | 33.47 | 51.24 |
| | Derajad kejenuhan | % | 98.65 | 47.76 | 76.51 | 77.66 | 34.23 | 73.68 | 87.30 | 17.16 | 85.95 | 75.21 | 90.44 | 144.41 | 68.00 | 66.20 |
| Grain size analysis | Kandungan Kriki *(Gravel part )* | % | 0.00 | | 42.57 | 0.00 | | 0.00 | 0.00 | 0.00 | | | 0.00 | 0.00 | | 0.00 |
| | Kandungan Pasir *(Sand part )* | % | 23.78 | | 39.90 | 52.17 | | 39.27 | 16.63 | 46.23 | | | 29.22 | 33.95 | | 48.45 |
| | Kandungan Lanau *(Silt part )* | % | 57.53 | | 17.53 | 38.64 | | 51.59 | 74.38 | 42.68 | | | 59.70 | 57.05 | | 33.80 |
| | Kandungan Lempung *(Clay part )* | % | 18.69 | | 0.00 | 9.20 | | 9.15 | 8.98 | 11.08 | | | 11.08 | 9.00 | | 17.75 |
| | D10 (mm) | mm | - | | 0.0282 | 0.0023 | | 0.0023 | 0.0026 | 0.0016 | | | 0.0013 | 0.0026 | | - |
| | D30 (mm) | mm | 0.0077 | | 0.0047 | 0.0184 | | 0.0059 | 0.0087 | 0.0068 | | | 0.0100 | 0.0546 | | 0.0546 |
| | D60 (mm) | mm | 0.0405 | | 0.0346 | 0.0639 | | 0.0320 | 0.0397 | 0.0259 | | | 0.0500 | 0.0626 | | 0.0626 |
| | Uniformity Coefficient, Cu | | - | | 1.2266 | 27.8059 | | 13.7998 | 15.1484 | 15.7241 | | | 39.9034 | 23.8492 | | - |
| | cc | | - | | 0.0224 | 2.2989 | | 0.4739 | 0.7233 | 1.0767 | | | 1.5852 | 18.1700 | | - |
| Engineering Properties | q ult (UCS), | kg/cm$^2$ | 0.27 | 166.47 | 1.42 | 2.22 | 168.39 | 0.52 | 0.31 | 0.18 | 174.71 | 193.51 | 0.28 | 0.87 | 206.18 | 4.85 |
| | Friction angle (Triaxial test UU), $\phi$ | ° | 10.75 | | 24.53 | 14.58 | | 16.48 | 33.53 | 15.41 | | | 5.51 | 22.28 | | 9.39 |
| | Cohesion, c (Triaxial test UU) | kg/cm$^2$ | 0.19 | | 0.53 | 0.15 | | 0.01 | 0.34 | 0.11 | | | 0.20 | 0.48 | | 0.24 |
| | Koef. Permeabilitas, k (constan head permeameter) | cm/det | - | 2.14E-08 | - | - | 3.06E-08 | - | - | - | 2.23E-08 | 2.02E-08 | - | - | 1.57E-08 | - |
| | Koef. Permeabilitas, k (falling head permeameter) | cm/det | 3.23E-04 | - | 4.49E-05 | 4.82E-04 | | 5.51E-04 | 1.71E-05 | 3.13E-04 | | - | 2.54E-05 | 3.77E-05 | - | 9.74E-05 |

Atas kepercayaan dan kerjasamanya disampaikan terimakasih

Yogyakarta, 7 Mei 2022

Muhammad Iqbal A., ST., M.Eng
Kepala Laboratorium

## Appendix 4 Geotextile Specification

# UnggulTex

**POLYPROPYLENE WOVEN GEOTEXTILES**

## TECHNICAL SPESIFICATIONS

| PROPERTIES | UNIT | TEST METHOD | UW - 150 | UW - 200 | UW - 250 |
|---|---|---|---|---|---|
| **Physical Properties** | | | | | |
| Mass | $g/m^2$ | ASTM D 5261-92 | 150 | 200 | 250 |
| Thickness | mm | ASTM D 5199-91 | 0.5 | 0.6 | 0.7 |
| Colour | - | - | Black | Black | Black |
| **Mechanical Properties** | | | | | |
| Strip Tensile Strength (Wrab/Weft) | kN/m | ASTM D 4595-94 | 37/35 | 42/39 | 52/52 |
| Elongation at Max. Load (Wrab/Weft) | % | ASTM D 4595-94 | 19/18 | 20/20 | 20/20 |
| Grap Tensile Strength (Wrab/Weft) | N | ASTM D 4632-91 | 1210/1200 | 1600/1600 | 1750/1750 |
| Elongation at Max. Load (Wrab/Weft) | % | ASTM D 4632-91 | 14/13 | 22/22 | 22/22 |
| Trapezoidal Tear Strength (Wrab/Weft) | N | ASTM D 4533-91 | 615/615 | 700/700 | 800/800 |
| **Hydraulic Properties** | | | | | |
| Pore Size $O_{95}$ | µm | ASTM D 4751-95 | 320 | 275 | 250 |
| Water Permeability | $l/m^2/sec$ | 100 mm water head | 28 | 16 | 7.5 |
| **Environmental Properties** | | | | | |
| Effect of soil Alkalinity | - | - | nil | nil | nil |
| Effect of soil Acidity | - | - | nil | nil | nil |
| Effect of Bacteria | - | - | nil | nil | nil |
| Effect of U.V. Light | - | - | Stabilized | Stabilized | Stabilized |
| **Packaging** | | | | | |
| Roll Length | m | - | 150 - 200 | 150 - 200 | 150 - 200 |
| Roll Width | m | - | 3 - 4 | 3 - 4 | 3 - 4 |
| Roll Area | $m^2$ | - | 640 - 760 | 640 - 760 | 640 - 760 |
| Roll Diameter (Approx) | m | - | 0.4 - 0.5 | 0.4 - 0.5 | 0.4 - 0.5 |
| Roll Weight (Approx) | kg | - | 96 - 114 | 128 - 152 | 160 - 190 |

All information, illustration and specification are based on the latest product information available at the time of printing.
The right is reserved to make changes at any time without notice.

GEOSISTEM CERTIFICATE NO. JKT 6013866 CERTIFICATE NO. JKT 6016676

## Appendix 5 Deformed Mesh of Alternative Internal Angle Of 20° For Phase 1 Without Reinforcement Due to Embankment Load

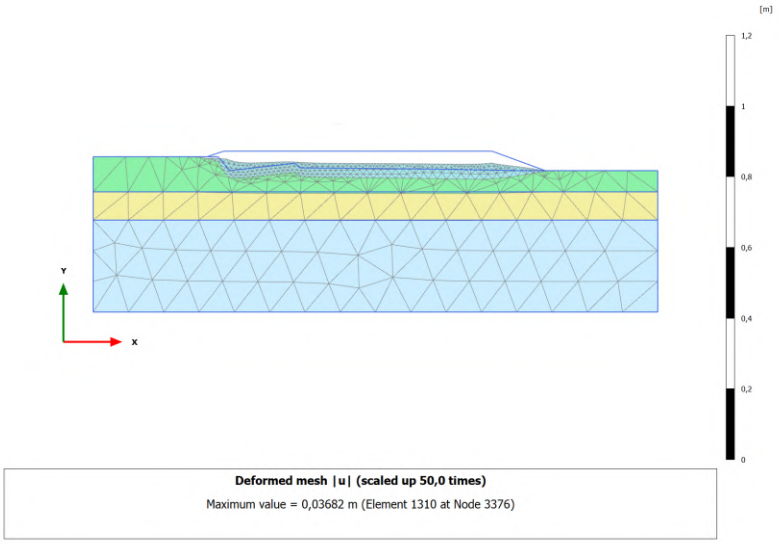


## Appendix 6 Displacement Value of Alternative Internal Angle Of 20° For Phase 1 Without Reinforcement Due to Embankment Load

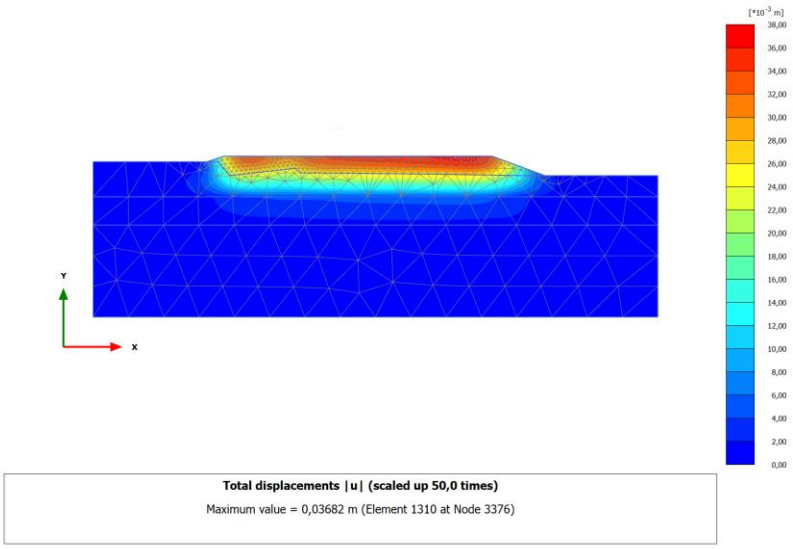

## Appendix 7 Effective Stress of Alternative Internal Angle Of 20° Phase 1 Without Reinforcement Due to Embankment Load

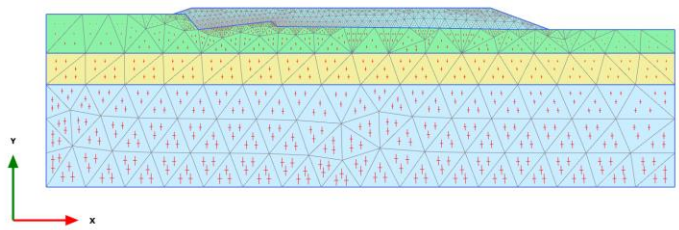


**Effective principal stresses (scaled up $5{,}00*10^{-3}$ times)**

Maximum value = $1{,}776*10^{-15}$ kN/m² (Element 1393 at Stress point 16705)

Minimum value = -280,6 kN/m² (Element 1638 at Stress point 19653)

## Appendix 8 Potential Failure Area on Alternative Internal Angle Of 20° Phase 1 Without Reinforcement Due to Embankment Load

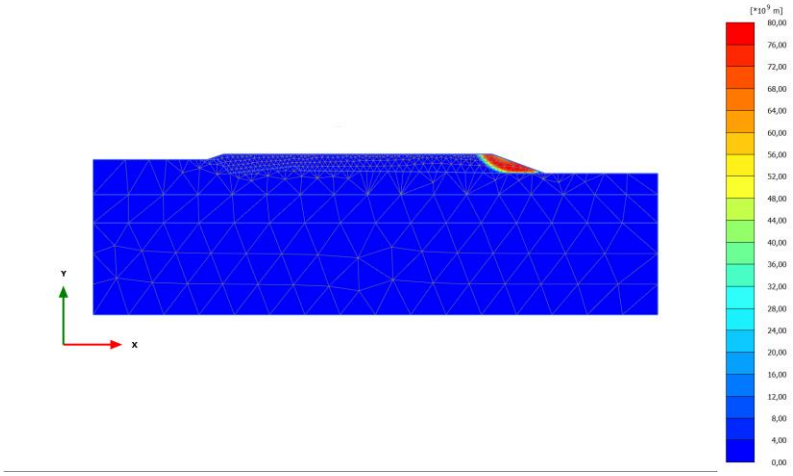

## Appendix 9 Deformed Mesh of Alternative Internal Angle Of 20° For Phase 2 Without Reinforcement Due to Embankment Load

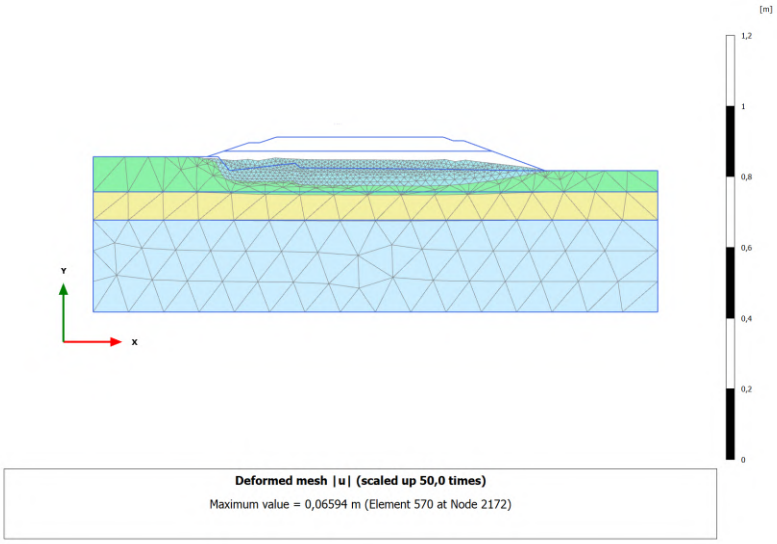


## Appendix 10 Displacement Value of The Alternative Internal Angle Of 20° For Phase 2 Without Reinforcement Due to Embankment Load

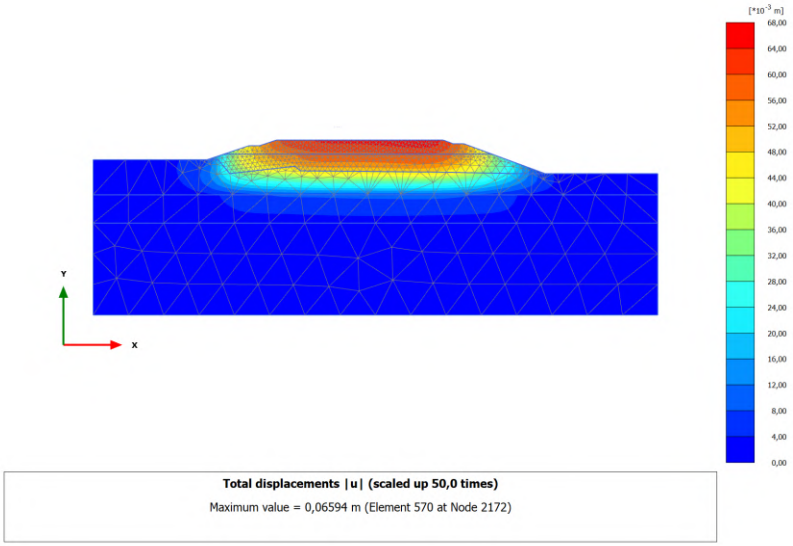

## Appendix 11 Effective Stress of Alternative Internal Angle Of 20° Phase 2 Without Reinforcement Due to Embankment Load

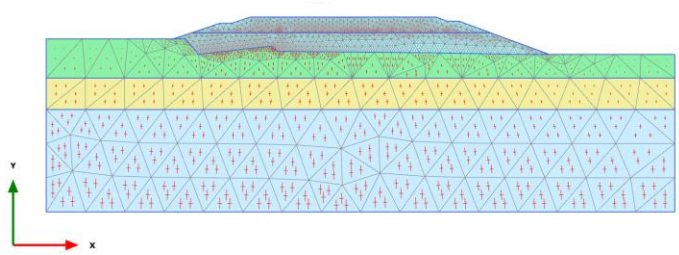


**Effective principal stresses (scaled up $5{,}00*10^{-3}$ times)**

Maximum value = $5{,}773*10^{-15}$ kN/m² (Element 1315 at Stress point 15771)

Minimum value = -298,3 kN/m² (Element 1638 at Stress point 19653)

## Appendix 12 Potential Failure Area on Alternative Internal Angle Of 20° Phase 2 Without Reinforcement Due to Embankment Load

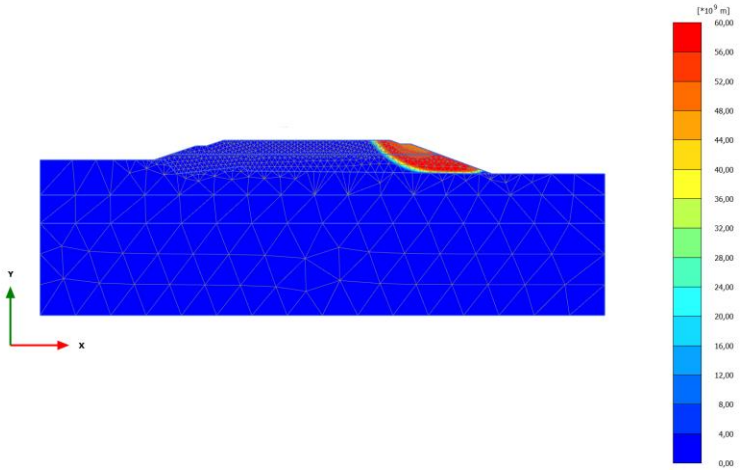

## Appendix 13 Deformed Mesh of Alternative Internal Angle Of 20° For Phase 3 Without Reinforcement by Adding Pavement Load

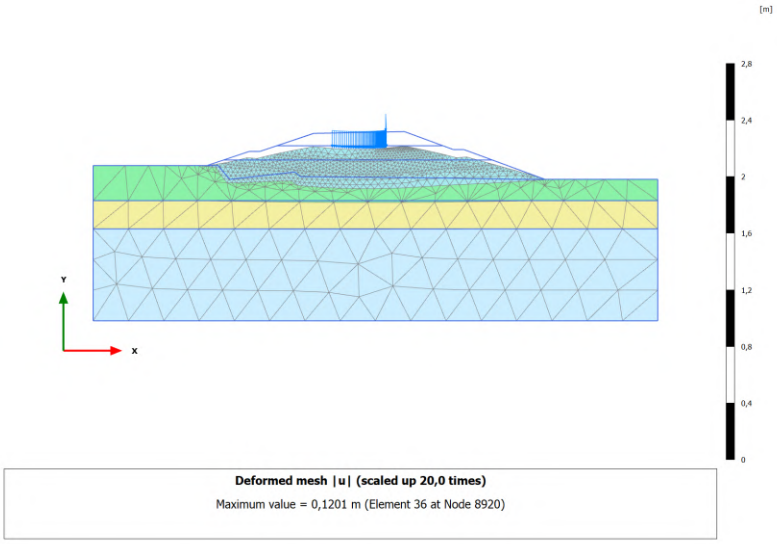


## Appendix 14 Deformed Mesh of Alternative Internal Angle Of 20° For Phase 3 Without Reinforcement by Adding Pavement and Earthquake Load

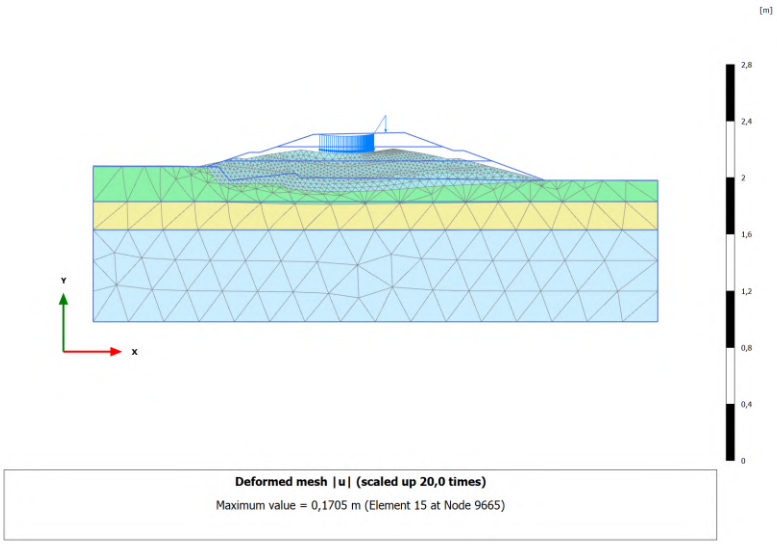

**Appendix 15 Displacement Value of The Alternative Internal Angle Of 20° For Phase 3 Without Reinforcement by Adding Pavement Load**

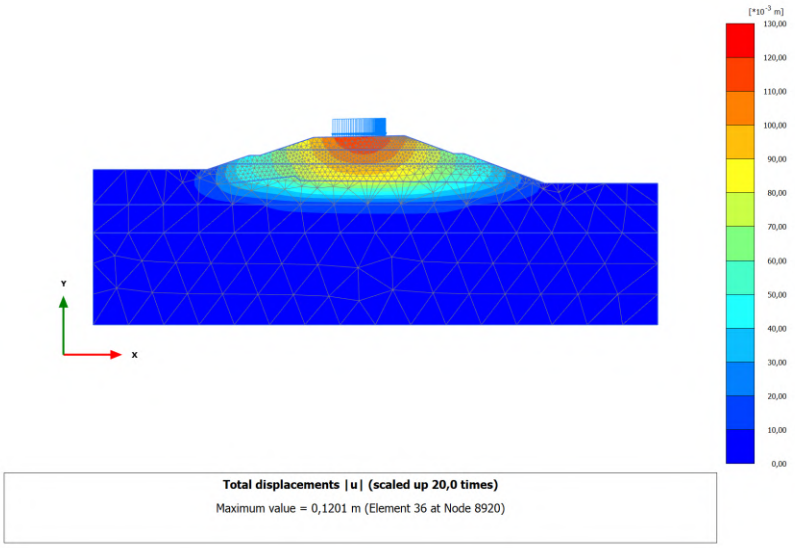


**Appendix 16 Displacement Value of The Alternative Internal Angle Of 20° For Phase 3 Without Reinforcement by Adding Pavement and Earthquake Load**

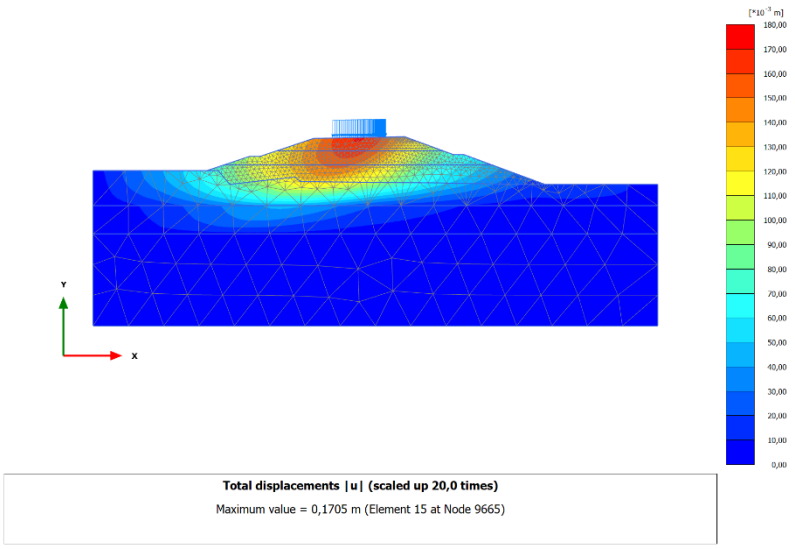

## Appendix 17 Effective Stress of Alternative Internal Angle Of 20° Phase 3 Without Reinforcement by Adding Pavement Load

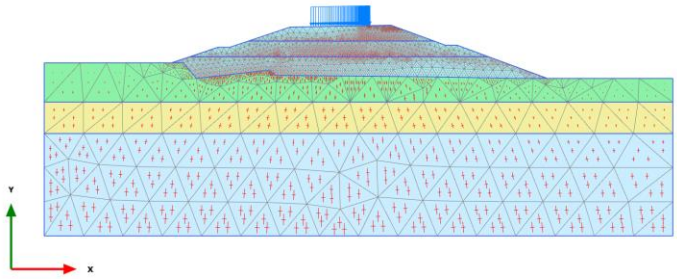


**Effective principal stresses (scaled up $5{,}00*10^{-3}$ times)**

Maximum value = $0{,}01243*10^{-12}$ kN/m² (Element 785 at Stress point 9420)

Minimum value = -307,4 kN/m² (Element 1638 at Stress point 19653)

## Appendix 18 Effective Stress of Alternative Internal Angle Of 20° Phase 3 Without Reinforcement by Adding Pavement and Earthquake Load

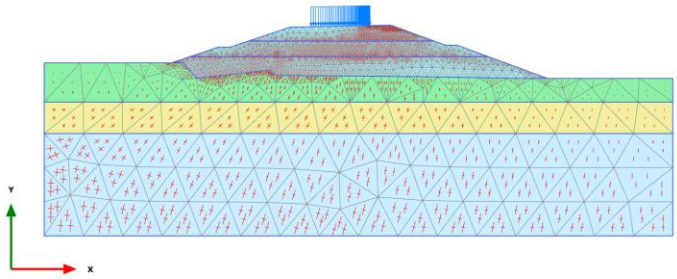


**Effective principal stresses (scaled up $5{,}00*10^{-3}$ times)**

Maximum value = 60,47 kN/m² (Element 1715 at Stress point 20570)

Minimum value = -333,9 kN/m² (Element 1714 at Stress point 20558)

**Appendix 19 Potential Failure Area on Alternative Internal Angle Of 20° Phase 3 Without Reinforcement by Adding Pavement Load**

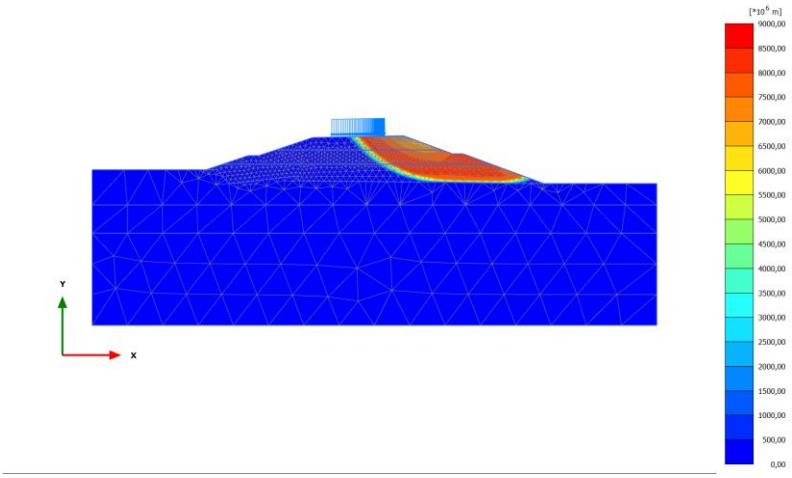


**Appendix 20 Potential Failure Area on Alternative Internal Angle Of 20° Phase 3 Without Reinforcement by Adding Pavement and Earthquake Load**

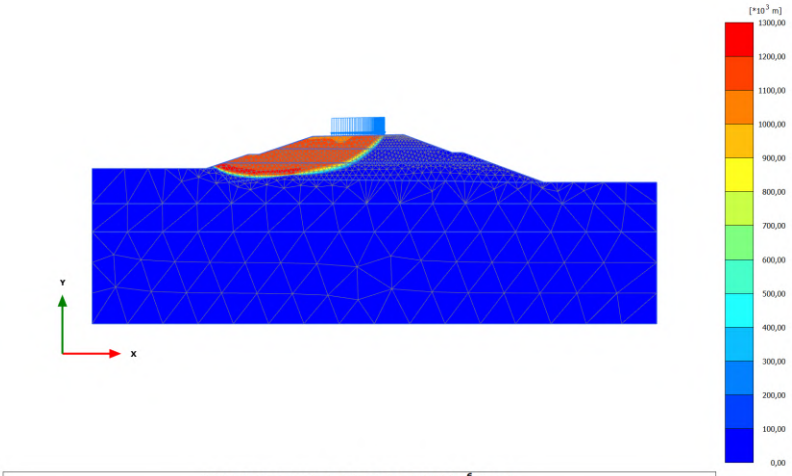

**Appendix 21 Consolidation Settlement of Alternative Internal Angle Of 20° Phase 3 For Construction Phase**

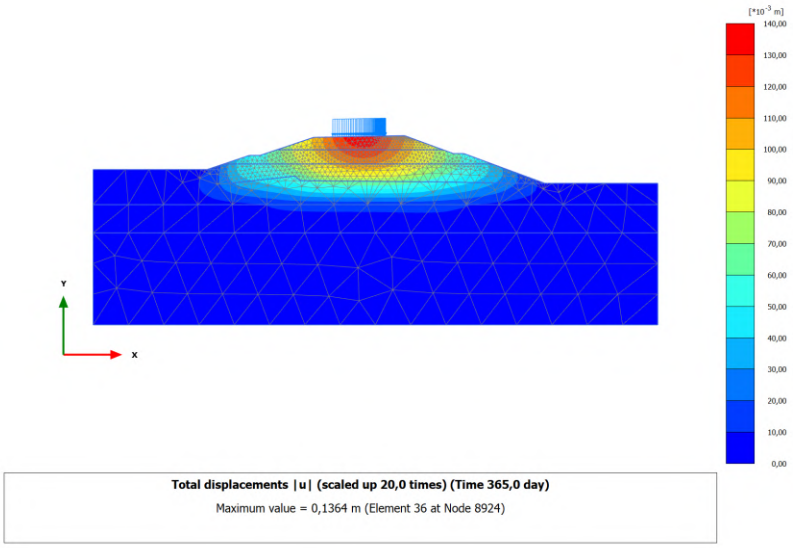


**Appendix 22 Deformed Mesh for On Alternative Internal Angle Of 20° By Adding Road Structure Load Without Reinforcement**

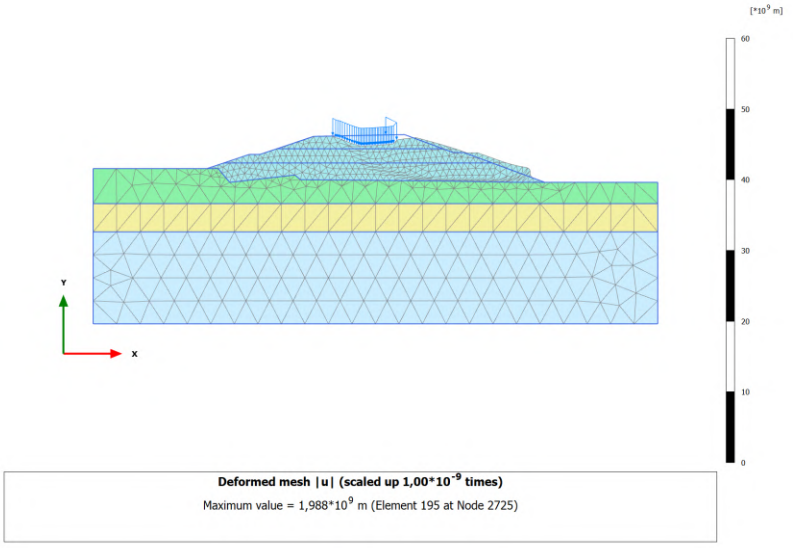

## Appendix 23 Displacement Value of The Alternative Internal Angle Of 20° By Adding Road Structure Load Without Reinforcement

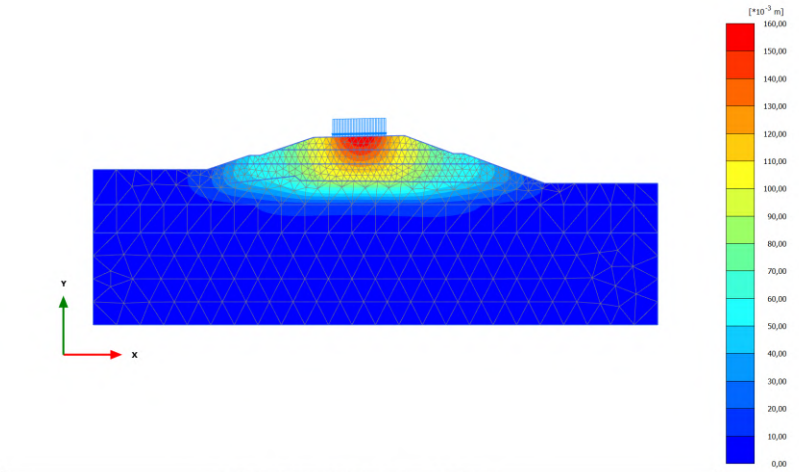


## Appendix 24 Effective Stress of Alternative Internal Angle Of 20° By Adding Road Structure Load Without Reinforcement

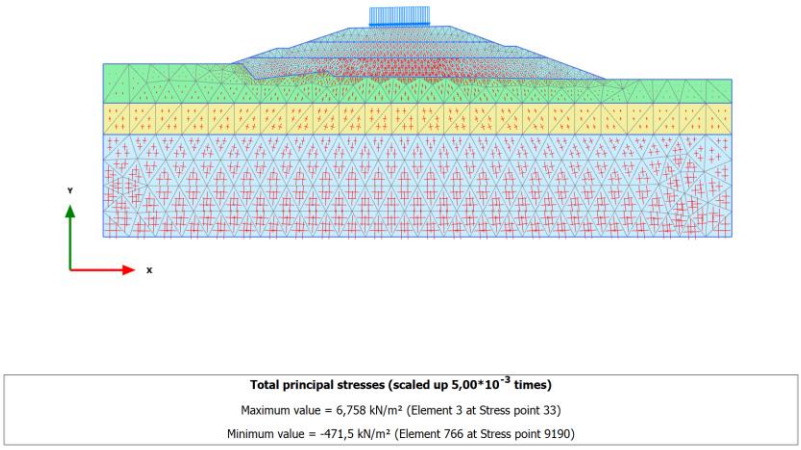

**Appendix 25 Potential Failure Area on The Alternative Internal Angle Of 20° By Road Structure Load Without Reinforcement**

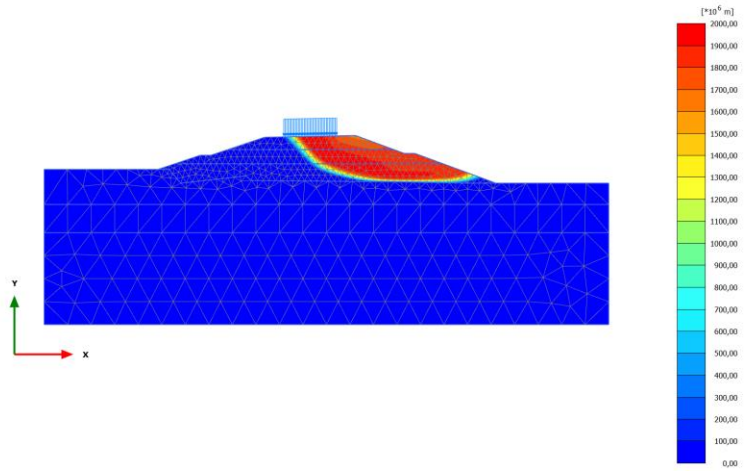


**Appendix 26 Consolidation Settlement of Alternative Internal Angle Of 20° For Post-Construction**

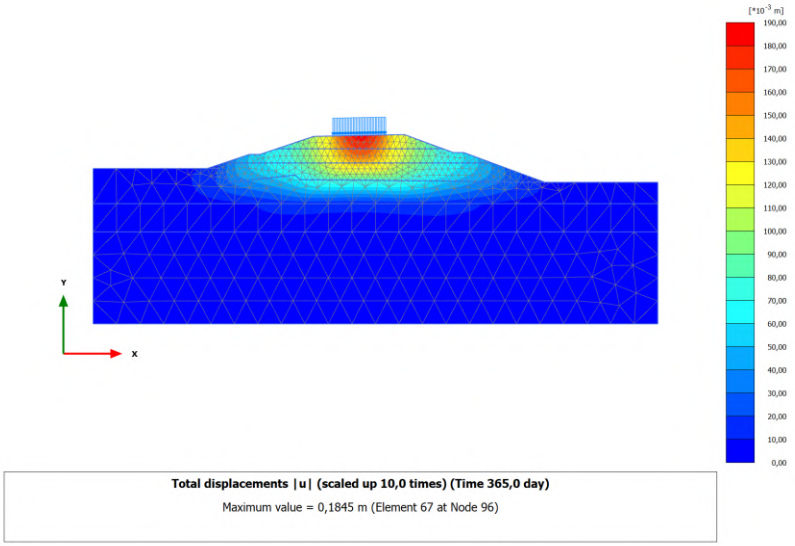

**Appendix 27 Deformed Mesh of Reinforced Alternative Internal Angle Of 20° For Phase 1 Using Geotextile Due to Embankment Load**

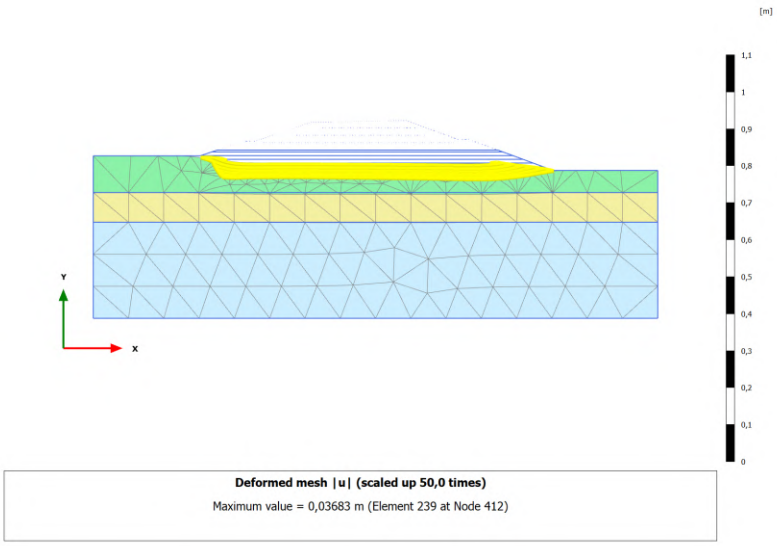


**Appendix 28 Displacement Value of The Reinforced Alternative Internal Angle Of 20° For Phase 1 Using Geotextile Due to Embankment Load**

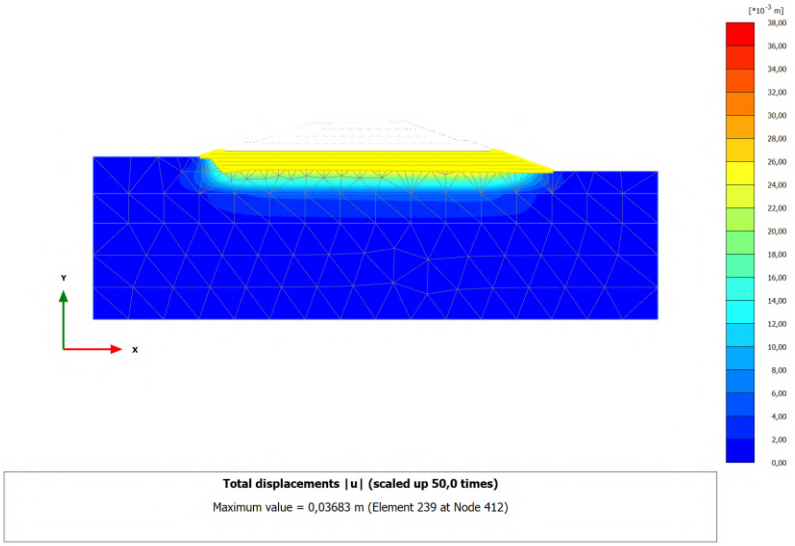

**Appendix 29 Effective Stress of Reinforced Alternative Internal Angle Of 20° Phase 1 Using Geotextile Due to Embankment Load**

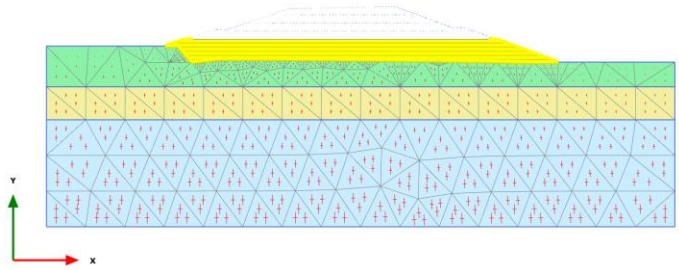


**Effective principal stresses (scaled up $5{,}00*10^{-3}$ times)**

Maximum value = $1{,}110*10^{-15}$ kN/m² (Element 398 at Stress point 4773)

Minimum value = -280,0 kN/m² (Element 754 at Stress point 9045)

**Appendix 30 Potential Failure Area on Reinforced Alternative Internal Angle Of 20° Phase 1 Using Geotextile Due to Embankment Load**

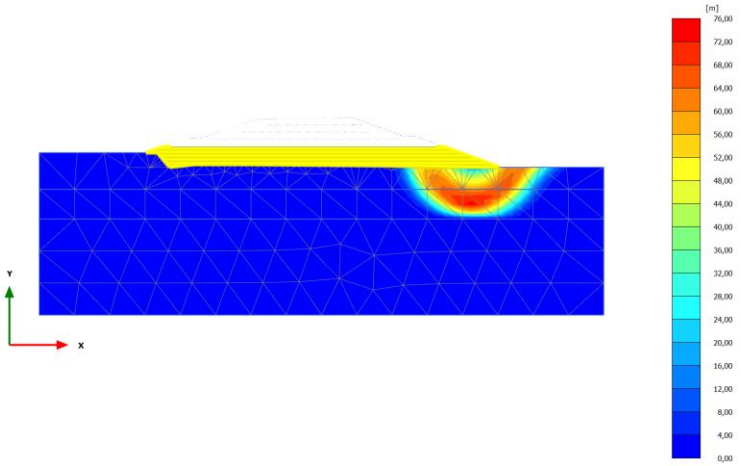

## Appendix 31 Deformed Mesh of Reinforced Alternative Internal Angle Of 20° For Phase 2 Using Geotextile Due to Embankment Load

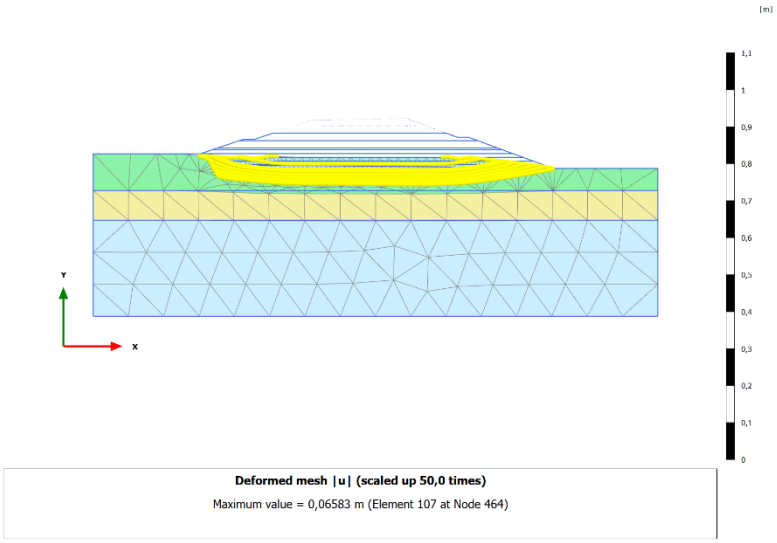


## Appendix 32 Displacement Value of The Reinforced Alternative Internal Angle Of 20° For Phase 2 Using Geotextile Due to Embankment Load

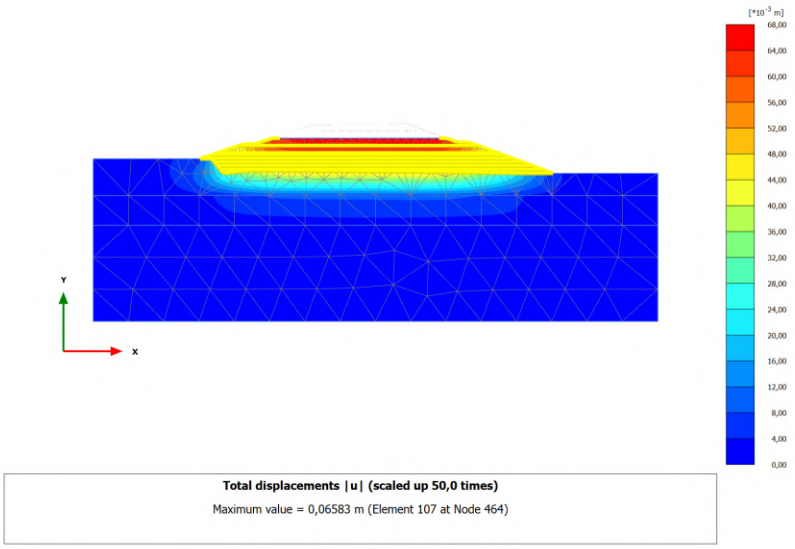

**Appendix 33 Effective Stress of Reinforced Alternative Internal Angle Of 20° Phase 2 Using Geotextile Due to Embankment Load**

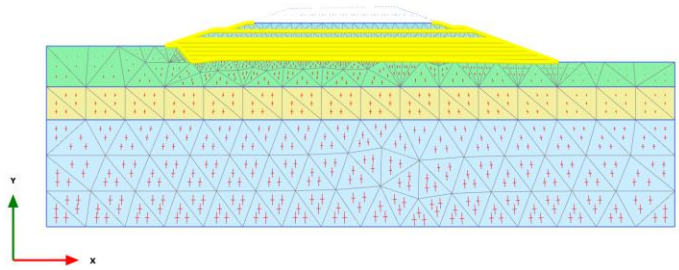


**Effective principal stresses (scaled up $5{,}00*10^{-3}$ times)**

Maximum value = $3{,}997*10^{-15}$ kN/m² (Element 284 at Stress point 3400)

Minimum value = -297,5 kN/m² (Element 756 at Stress point 9069)

**Appendix 34 Potential Failure Area on Reinforced Alternative Internal Angle Of 20° Phase 2 Using Geotextile Due to Embankment Load**

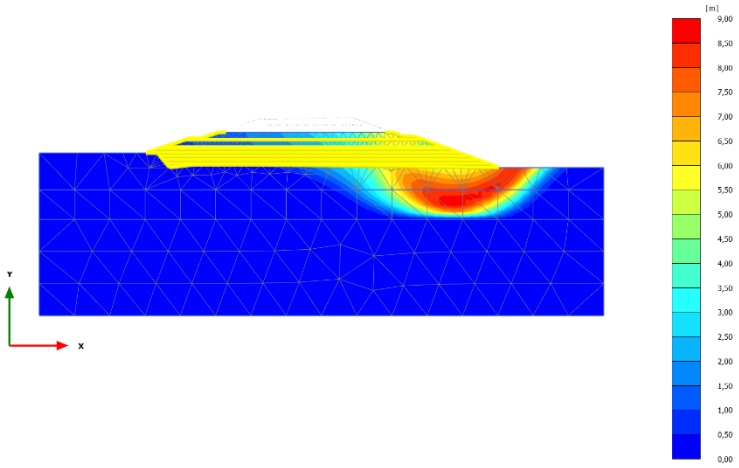

**Appendix 35 Deformed Mesh of Reinforced Alternative Internal Angle Of 20° For Phase 3 Using Geotextile by Adding Pavement Load**

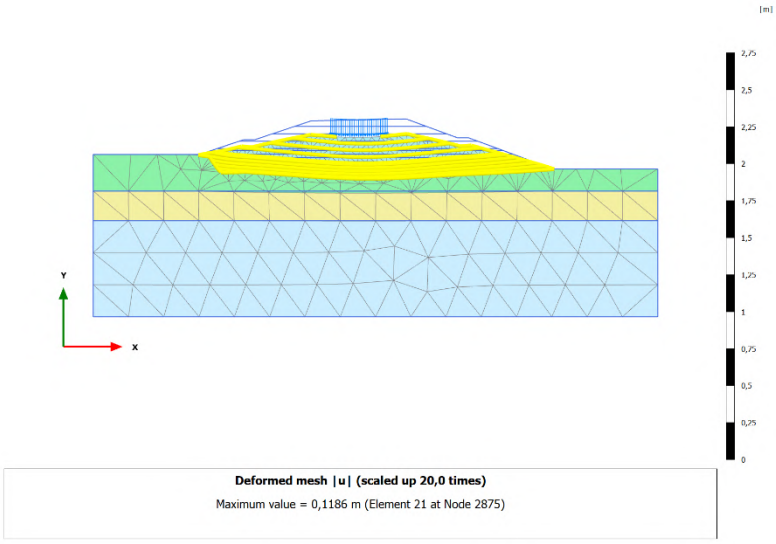


**Appendix 36 Deformed Mesh of Reinforced Alternative Internal Angle Of 20° For Phase 3 Using Geotextile by Adding Pavement and Earthquake Loads**

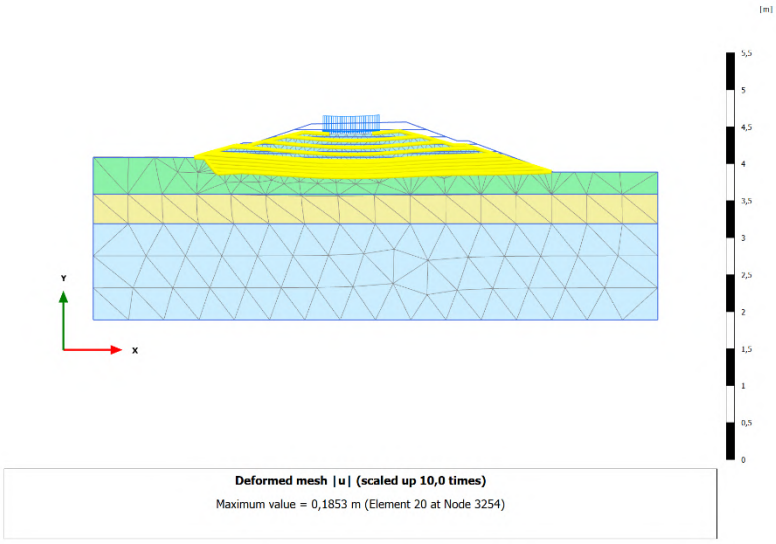

**Appendix 37 Displacement Value of Reinforced Alternative Internal Angle Of 20° For Phase 3 Using Geotextile by Adding Pavement Load**

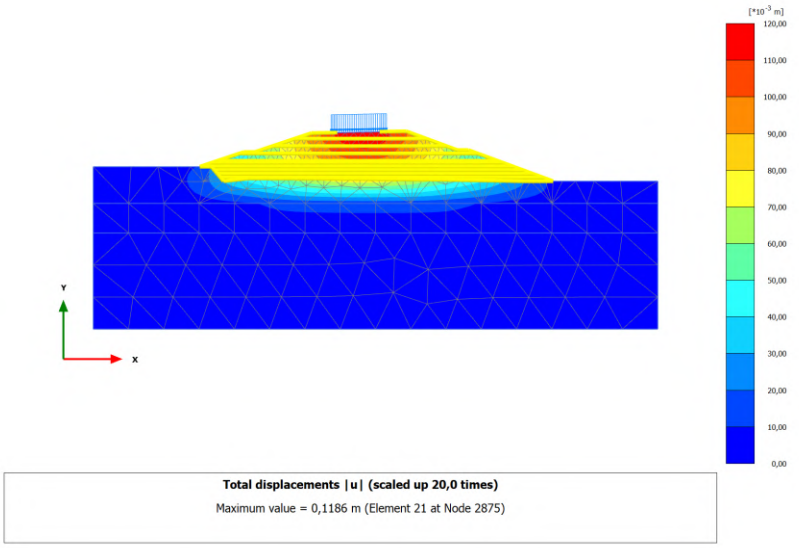


**Appendix 38 Displacement Value of Reinforced Alternative Internal Angle Of 20° For Phase 3 Using Geotextile by Adding Pavement And Earthquake Loads**

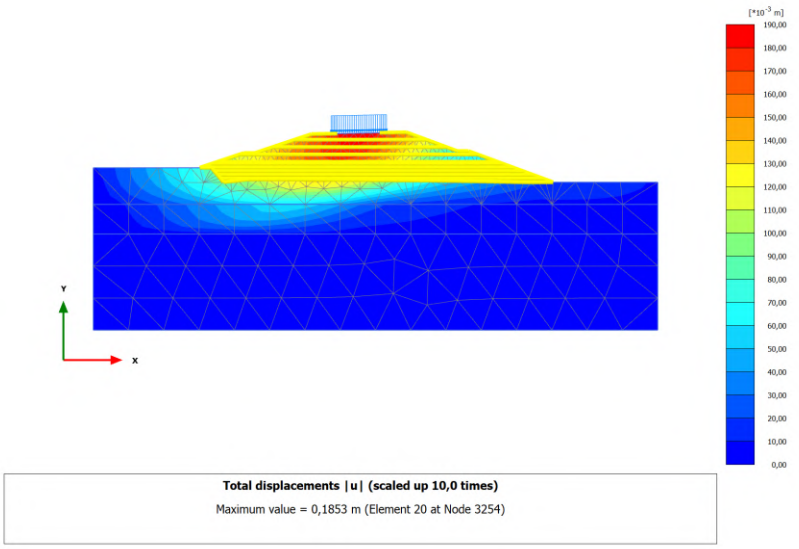

## Appendix 39 Effective Stress of Reinforced Alternative Internal Angle Of 20° Phase 3 Using Geotextile by Adding Pavement Load

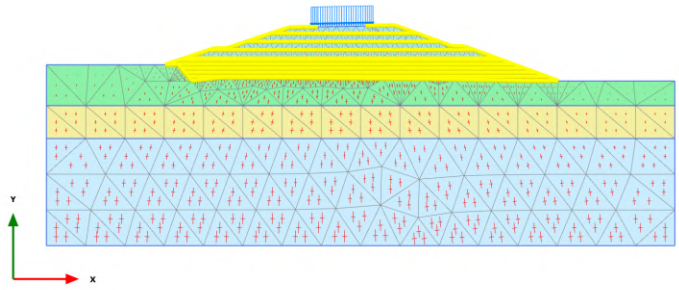


**Effective principal stresses (scaled up $5{,}00*10^{-3}$ times)**

Maximum value = $0{,}01243*10^{-12}$ kN/m² (Element 340 at Stress point 4078)

Minimum value = -306,9 kN/m² (Element 756 at Stress point 9069)

## Appendix 40 Effective Stress of Reinforced Alternative Internal Angle Of 20° Phase 3 Using Geotextile by Adding Pavement And Earthquake Loads

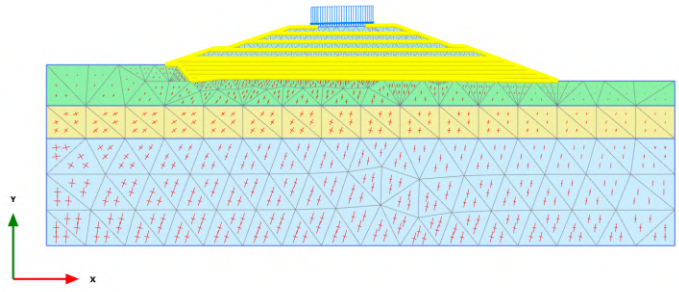


**Effective principal stresses (scaled up $5{,}00*10^{-3}$ times)**

Maximum value = 72,04 kN/m² (Element 834 at Stress point 9998)

Minimum value = -340,2 kN/m² (Element 836 at Stress point 10022)

**Appendix 41 Potential Failure Area on Reinforced Alternative Internal Angle of 20° For Phase 3 Using Geotextile by Adding Pavement Load**

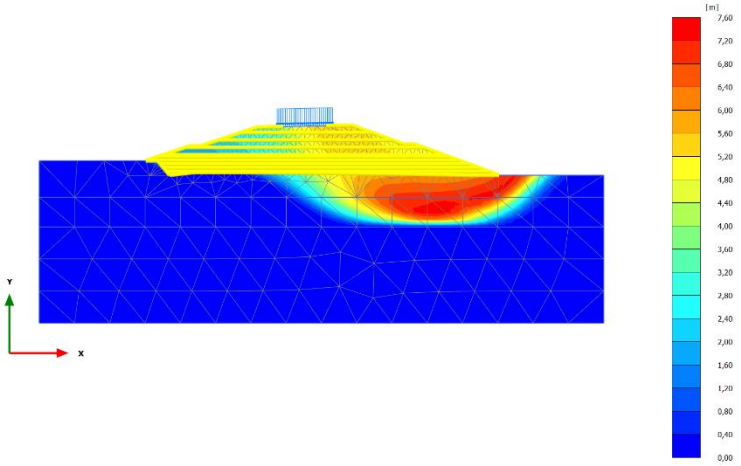


**Appendix 42 Potential Failure Area on Reinforced Alternative Internal Angle Of 20° For Phase 3 Using Geotextile by Adding Pavement and Earthquake Loads**

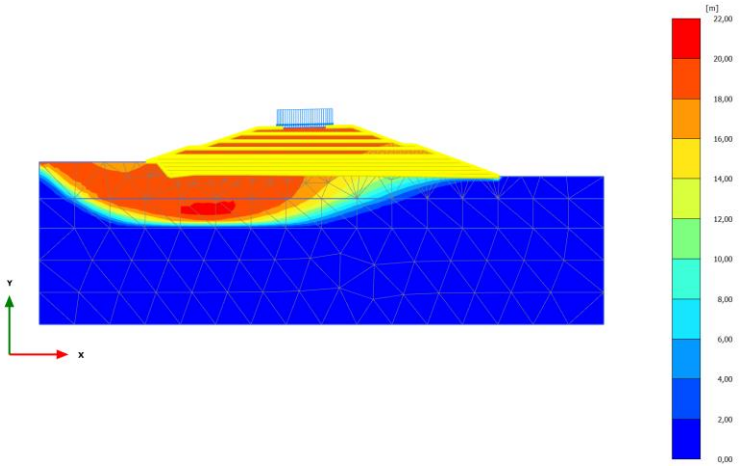

## Appendix 43 Consolidation Settlement on Reinforced Alternative Internal Angle Of 20° For Construction Phase

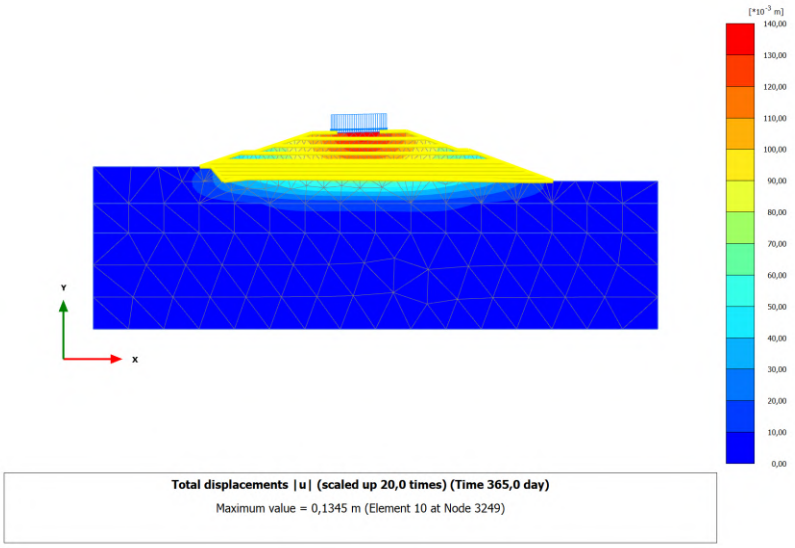


## Appendix 44 Deformed Mesh for Reinforced Alternative Angle Of 20º By Adding Road Structure Load Using Reinforcement

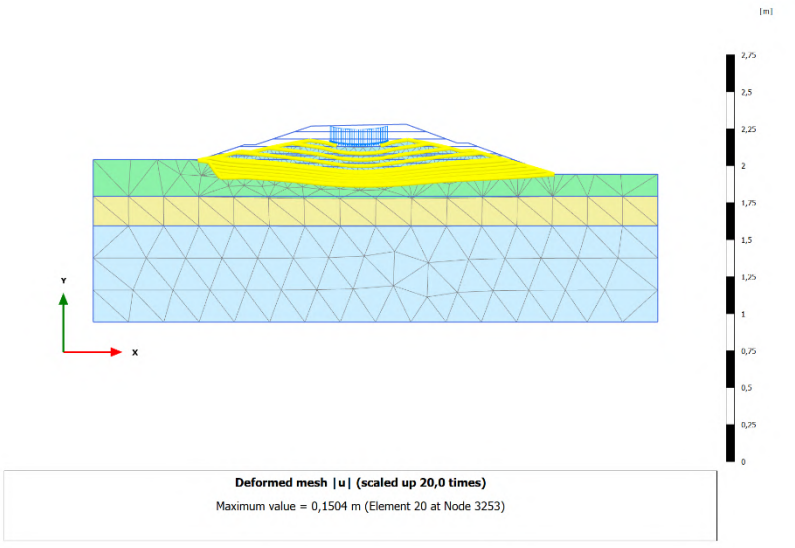

**Appendix 45 Deformed Mesh for The Reinforced Alternative Angle Of 20º By Adding Road Structure and Earthquake Loads Using Reinforcement**

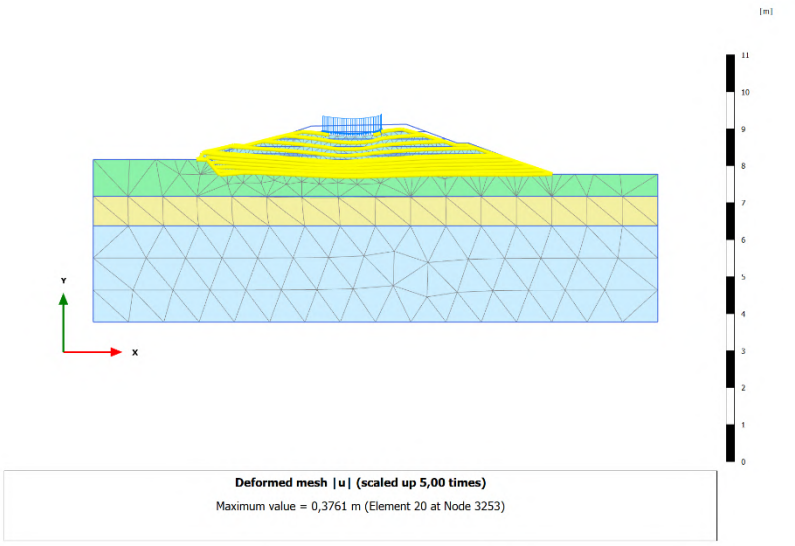


**Appendix 46 Displacement Value of Reinforced Alternative Internal Angle of 20° Using Geotextile by Adding Road Structure Load**

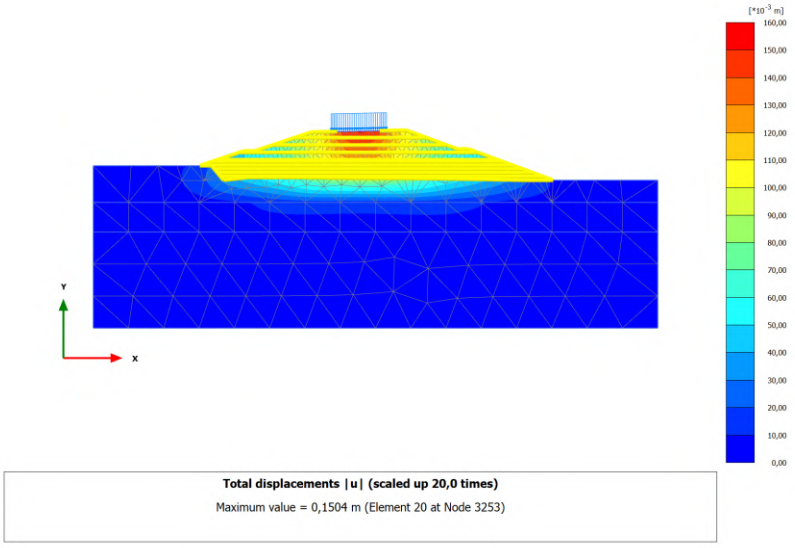

**Appendix 47 Displacement Value of Reinforced Alternative Internal Angle Of 20° Using Geotextile by Adding Road Structure and Earthquake Loads**

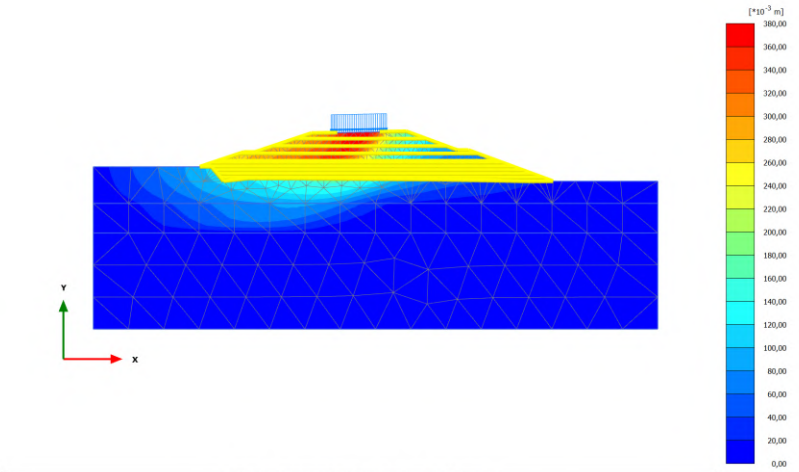


**Appendix 48 Effective Stress of Reinforced Alternative Internal Angle Of 20° By Adding Road Structure Load Using Geotextile**

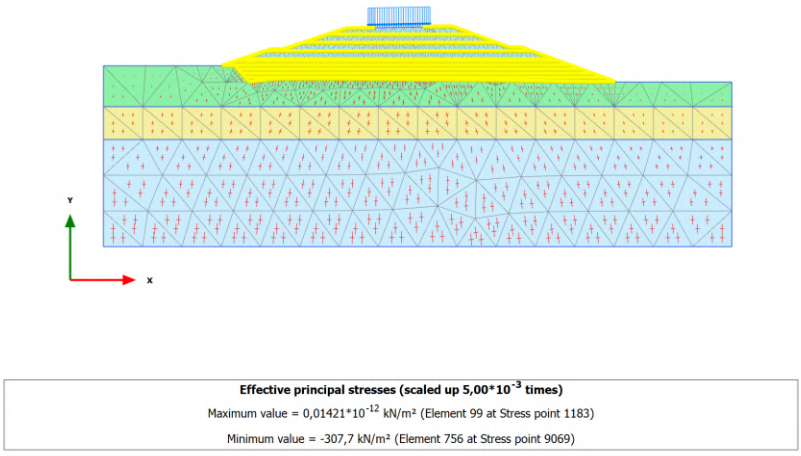

**Appendix 49 Effective Stress of Reinforced Alternative Internal Angle Of 20° By Adding Road Structure and Earthquake Loads Using Geotextile**

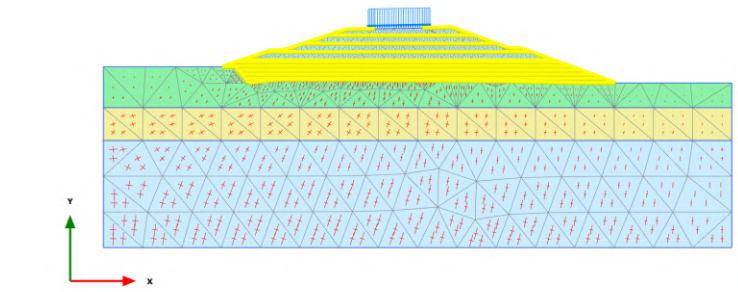


**Effective principal stresses (scaled up 5,00*10$^{-3}$ times)**

Maximum value = 70,64 kN/m² (Element 834 at Stress point 9998)

Minimum value = -338,9 kN/m² (Element 836 at Stress point 10022)

**Appendix 50 Potential Failure Area on The Reinforced Alternative Internal Angle Of 20° By Road Structure Load Using Geotextile**

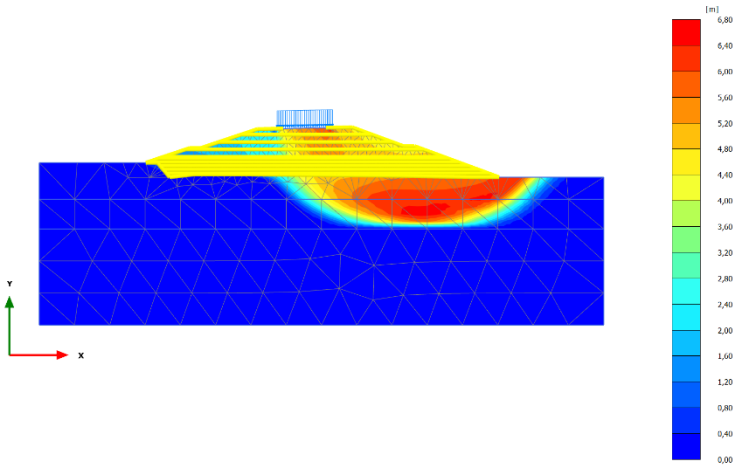

**Appendix 51 Potential Failure Area on The Reinforced Alternative Internal Angle Of 20° By Road Structure and Earthquake Loads Using Geotextile**

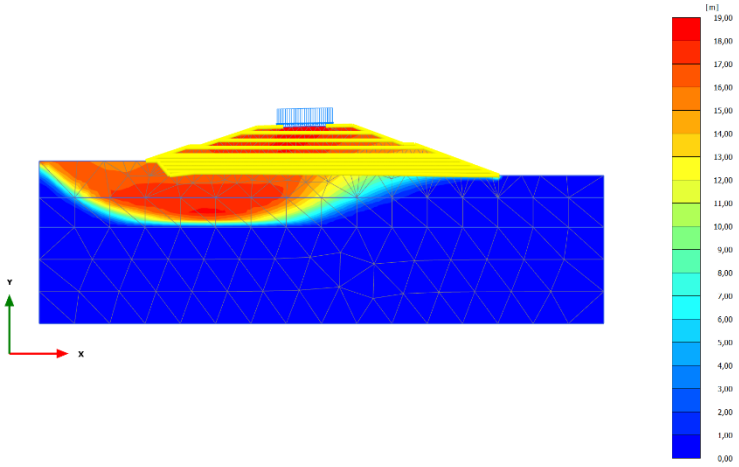

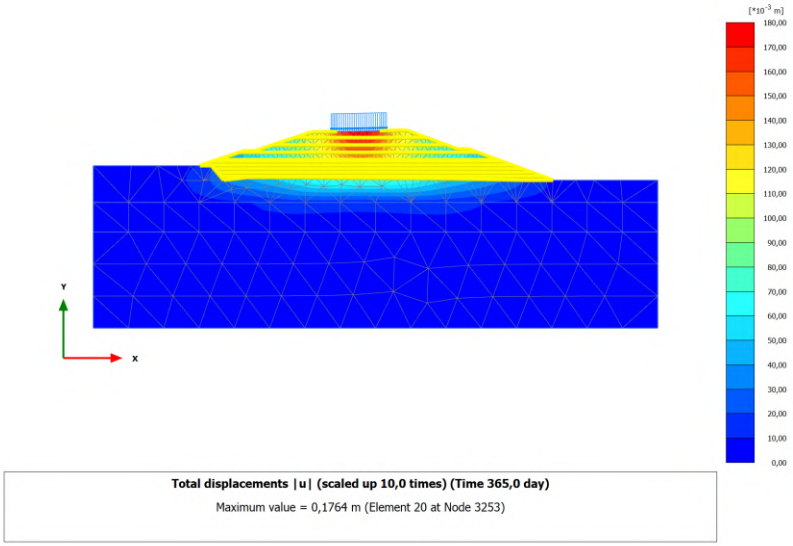
**Appendix 52 Consolidation Settlement of Reinforced Alternative Internal Angle Of 20° Using Geotextile for Post-Construction**